



UNIVERSIDADE DE BRASÍLIA – UnB
INSTITUTO DE GEOCIÊNCIAS – IG

DISSERTAÇÃO DE MESTRADO

N° 425

**PROVENIÊNCIA SEDIMENTAR DOS SEDIMENTOS JURÁSSICOS E
CRETÁCEOS DA BACIA DE AREQUIPA – TARAPACÁ (SUL DO PERU):
IMPLICAÇÕES PALEOGEOGRÁFICAS E GEODINÂMICAS.**

ÁREA DE CONCENTRAÇÃO: GEOLOGIA REGIONAL

Aluno: César Anthony Chávez Machaca.

Orientador: Prof. Dr. Elton Luiz Dantas.

Brasília/DF
2019



UNIVERSIDADE DE BRASÍLIA – UnB
INSTITUTO DE GEOCIÊNCIAS – IG

**PROVENIÊNCIA SEDIMENTAR DOS SEDIMENTOS JURÁSSICOS E
CRETÁCEOS DA BACIA DE AREQUIPA – TARAPACÁ (SUL DO PERU):
IMPLICAÇÕES PALEOGEOGRÁFICAS E GEODINÂMICAS.**

César Anthony Chávez Machaca

DISSERTAÇÃO DE MESTRADO
Nº425

Orientador: Prof. Dr. Elton Luiz Dantas (IG/UnB).

Co-orientadores: Prof. Dr. Carlos A. Tello Sáenz (UNESP).

Prof. Dr. Martin Roddaz (IG/UnB)

Prof. Dr. Roberto Ventura Santos (IG/UnB)

Comissão Examinadora:

Profa. Dra. Natalia Houser (IG/UnB)

Prof. Dr. João Marinho de Moraes Neto (Petrobras)

Prof. Dr. Elton Luiz Dantas (IG/UnB)

Brasília-DF
2019

-Para minha linda mãe Alina, graças a você, sou o que sou.

-Para minha irmã Anhely, meu motor e motivo.

-Aos meus avós Catalina e Antolin, sempre me empurrando para ir em frente.

AGRADECIMENTOS:

- Primeiramente agradeço a Deus por me abençoar em todos os momentos de fraqueza, mostrando-me o caminho certo para continuar.
- Gostaria de agradecer ao Prof. Elton Dantas, que me apoiou em todos os momentos para o ponto culminante da presente dissertação.
- Obrigado ao prof. Dr. Carlos Tello Sáenz por depositar sua confiança em mim, para a realização deste projeto.
- Aos professores Dr. Matin Roddaz, Dr. Roberto Ventura, por todas as sugestões e contribuições para a presente dissertação.
- À instituição CAPES pela bolsa de mestrado concedido.
- Aos professores Msc. Pedro Figueroa, Msc. Juan Carlos Grande, Msc. Pablo Meza pelas palavras de força nesta luta.
- A la Dra. Miriam Mamani y al Dr. Aldo Alván por su apoyo constante en las sugerencias para la realización del presente trabajo.
- A meus amigos, Ju! Bola! Alan!, Christian! pelas grandes noites no laboratório de Geocronología da Universidade de Brasília.
- E a todos aqueles amigos que me ajudaram na etapa de campo, Miguel!, Javier (Chateto)! Jordy, Virgilio! Passarillo! Fredo!, Wichou!, Judith! Kike! Rafo!, y muchas otras personas en el anonimato, muchas gracias por todo su apoyo.

RESUMO

Durante a ruptura do Gondwana, os processos de extensão permitiram a formação de bacias sedimentares em diversos ambientes tectônicos. Existem estudos limitados sobre o reconhecimento destes. Este estudo trata da origem sedimentar das rochas mesozoicas do intervalo Jurássico - Cretáceo depositadas na bacia Arequipa, com base em análises Nd-Sr em rocha total e idades U-Pb em zircões detriticos, como ferramentas para reconhecer o ambiente tectônico da bacia de Arequipa - Tarapacá no sul do Peru. Os resultados mostram que os arenitos do Jurássico inferior possuem populações significativas de fontes com idades Grenville - Sunsás (1.3 – 0.9 Ga) e idades neoproterozoicas (0.7 a 0.5 Ga) com valores de $\xi_{Nd(0)}$ pouco irregulares que variam entre -12,0 -7,5 com um fracção de $^{87}Sr/^{86}Sr$ entre 0.70796 - 0.7318, sugerindo como fonte potencial a cordilheira oriental. Na sequência Jurássica superior (Titoniano), idades obtidas principalmente são paleo-neoproterozóicas (2,0 - 0,5 Ga) com valores de $\xi_{Nd(0)}$ entre -9,0 e -7,28 e razões $^{87}Sr/^{86}Sr$ entre 0,7145 - 0,72158, cuja assinatura isotópica $\xi_{Nd(0)}$ é afetado pelas rochas intrusivas do Permo-Triássico, baseados nas idades que sugerem uma fonte potencial do escudo brasileiro. Durante o Eocretáceo , os resultados foram principalmente de idades do Neoproterozóico (0,7 a 0,5 Ga) com valores de $\xi_{Nd(0)}$ entre -11,9 e -7,01 e as razões $^{87}Sr/^{86}Sr$ entre 0,70760 - 0,71343; esses padrões sugerem uma origem da Cordilheira Oriental e durante o Cretáceo superior, e também idades do arco magnético Jurássico (<200 Ma) e idades do Paleo-Neoproterozoicos (2,0-0,5 Ga). O valor de $\xi_{Nd(0)} = -5,35$ e razões $^{87}Sr/^{86}Sr = 0,70786$ sugerem que os sedimentos foram afetados pela assinatura arco. Isto sugere a associação de uma fonte oriental (Cordilheira Oriental) e uma fonte ocidental (Cordilheira da Costa). As potenciais fontes para os sedimentos do Jurássico e do Cretáceo Inferior são da cordilheira oriental e do escudo brasileiro, possivelmente sugerindo uma paleodrenagem do leste para o oeste. Assim, com base nos resultados de U-Pb em zircões detriticos e as análises de Sr-Nd, descartamos como uma potencial fonte os sedimentos do arco vulcânico Jurássico, mostrando que as distribuições de idades U-Pb são preferencialmente mais antigas, sugestivas com um ambiente do tipo rifte.

ABSTRACT

During the break-up of Gondwana, extension processes allowed the formation of sedimentary basins in different tectonic environments. There are limited studies on the recognition of these settings. We studied the sedimentary provenience of Mesozoic rocks of the Jurassic - Cretaceous interval deposited in the Arequipa basin, based on isotopic compositions of Sr-Nd in total rock and U-Pb ages of detrital zircons, to recognize the tectonic environment of the Basin of southern of Peru. The results showed: The sandstones of middle - upper Jurassic have important populations of sources with Greenville - Sunsas ages (0.9 - 1.3 Ga), as well as Neoproterozoic ages (0.5 - 0.7 Ga). The values of $\xi_{\text{Nd}}(0)$ are a little irregular, ranging from -12.0 to -7.5 with a ratio of $^{87}\text{Sr}/^{86}\text{Sr}$ ratio between 0.70796 to 0.7318, suggesting a potential source to the eastern mountain range. In the Upper Jurassic sequence (Titonian), ages were mainly Paleo-Neoproterozoic (2.0 - 0.5 Ga) with $\xi_{\text{Nd}}(0)$ values between -9.0 and -7.28 and the $^{87}\text{Sr}/^{86}\text{Sr}$ ratios between 0.7145 to 0.72158; we interpret that the ξ_{Nd} isotopic signature was affected by Perm-Triassic intrusive rocks, and the ages suggest the Brazilian shield as a potential source. During the lower Cretaceous ages were mainly Neoproterozoic (0.5 - 0.7 Ga) with values of $\xi_{\text{Nd}}(0)$ between -11.9 and -7.01 and $^{87}\text{Sr}/^{86}\text{Sr}$ ratios between 0.70760 to 0.71343; these patterns suggest a source from the Eastern Cordillera, and during the Upper Cretaceous, Paleo-Neoproterozoic ages (2.0 - 0.5 Ga), and Jurassic arc ages (<200 Ma) were found. The value of the $\xi_{\text{Nd}}(0) = -5.35$ and the ratios of $^{87}\text{Sr}/^{86}\text{Sr} = 0.70786$, show a signature affected by arc sediments. This suggests both an eastern source (Eastern Cordillera) and western source (Coastal Cordillera). Potential sources for the Jurassic and Lower Cretaceous sediments are found in the eastern cordillera and the Brazilian shield, possibly suggesting a paleo-drainage from the East to the West. In this way, based on the results of U-Pb in detrital zircons and the results of Sr-Nd, we discard the Jurassic volcanic arc as a potential source, with the U-Pb age distributions being preferably of older ages, suggesting with those of a rift-type environment.

RESUMEN

Durante la ruptura de Gondwana, procesos de extensión permitieron la formación de cuencas sedimentarias en diversos ambientes tectónicos. Existen estudios limitados sobre el reconocimiento de estos. Nosotros estudiamos la proveniencia sedimentaria de las rocas mesozoicas del intervalo Jurásico – Cretácico depositadas en la cuenca de Arequipa basados en composiciones isotópicas de Sr-Nd en roca total y edades U-Pb de zircones detríticos, para reconocer el ambiente tectónico de la Cuenca del sur del Perú. Los resultados mostraron: Las areniscas del Jurásico inferior - superior poseen poblaciones importantes de fuentes con edades Greenville – Sunsas (1.3 – 0.9 Ga), así como edades Neoproterozoicas (0.7 – 0.5 Ga). Los valores de $\xi_{\text{Nd}}(0)$ son un poco irregulares varian de -12.0 a -7.5 con una razón de $^{87}\text{Sr}/^{86}\text{Sr}$ entre 0.70796 to 0.7318, que sugieren como potencial fuente a la cordillera oriental. En el Jurásico Superior (Titoniano), se obtuvieron edades principalmente Paleo-Neoproterozoicas (2.0 – 0.5 Ga) con valores de $\xi_{\text{Nd}}(0)$ entre -9.0 y -7.28 y las razones de $^{87}\text{Sr}/^{86}\text{Sr}$ entre 0.7145 to 0.72158; interpretamos que la firma isotópica del eNd se ve afectada por rocas intrusivas Permo-Triásicas, y que las edades sugieren como potencial fuente al escudo Brasileño. Durante el cretácico inferior se encontraron edades principalmente Neoproterozoicas (0.7 – 0.5 Ga) con valores de $\xi_{\text{Nd}}(0)$ entre -11.9 y -7.01 y las razones de $^{87}\text{Sr}/^{86}\text{Sr}$ entre 0.70760 – 0.71343; estos patrones sugieren a una fuente de Cordillera Oriental y durante el Cretácico superior se encontraron edades Paleo-Neoproterozoicas (2.0 – 0.5 Ga), así como, edades de arco Jurásico (<200 Ma). El valor del $\xi_{\text{Nd}}(0) = -5.35$ y las razones de $^{87}\text{Sr}/^{86}\text{Sr} = 0.70786$, que muestra una firma isotópica afectada por sedimentos provenientes del arco. Esto sugiere asociarlo una fuente oriental (Cordillera Oriental) y una fuente occidental (Cordillera de la Costa). Las potenciales fuentes para el Jurásico y Cretácico inferior, se encuentran en desarrollados en cordillera oriental y el escudo brasileño lo que sugiere posiblemente un paleo-drenaje del Este para el Oeste. De esta forma basados en los resultados de U-Pb en zircones detríticos y los resultados de Sr-Nd, descartan como potencial fuente al arco volcánico Jurásico, siendo las distribuciones de edades U-Pb preferentemente de edades antiguas, coincidentes con los de un ambiente tipo rift.

SUMARIO

RESUMO	5
ABSTRACT	6
RESUMEN.....	7
SUMARIO	8
LISTA DE FIGURAS	10
LISTA DE TABELAS	11
<i>CAPÍTULO I</i>	12
1.INTRODUÇÃO	12
1.1 PROBLEMA CIENTÍFICO	15
1.2 OBJETIVOS GERAIS	15
1.3 OBJETIVOS ESPECÍFICOS	15
1.4 ESTRUTURA DA DISSERTAÇÃO	15
<i>CAPÍTULO II</i>	17
2. AR CABOUÇO GEOLOGICO REGIONAL	17
2. A CORDILHEIRA DOS ANDES.....	17
2.1 ANDES SEPTENTRIONAIS (12°N – 4°S)	17
2.2 ANDES CENTRAIS (5°S-35°S)	17
3. CONTEXTO GEOLOGICO DOS ANDES CENTRAIS NA PARTE SUL DO PERU	20
4. A CONTEXTUALIZAÇÃO DA BACIA DE AREQUIPA TARAPACÁ	21
5. ALGUMAS CARACTERÍSTICAS DAS POSSÍVEIS FONTES:.....	23
5.1 ROCAS INTRUSIVAS PERMIANAS - TRIÁSSICAS.....	23
5.2 ARCO MAGMÁTICO JURÁSICO.....	24
<i>CAPÍTULO III</i>	27
AMOSTRAGEM E MÉTODOS.....	27
3.1 AMOSTRAGEM	27
3.2 PREPARAÇÃO DE AMOSTRA.....	27
3.3 POR QUE O MINERAL ZIRÇÃO?	30
3.4 ISÓTOPOS DE Sm-Nd.....	31
3.5 ISÓTOPOS DE U-Pb.....	31
<i>CAPITULO IV</i>	34
ARTIGO:.....	34
WAS THE AREQUIPA BASIN DEPOSITED IN BACK-ARC BASIN CONTEXT? REVEALED USING U-PB AGES ON DETRITAL ZIRCON AND Sr-Nd ISOTOPES.....	34

ABSTRACT	35
4.1 INTRODUCTION.....	35
4.2 Geological Setting:.....	37
4.2.1 Stratigraphy of the Arequipa Basin.....	37
4.2.2 Potential Sources.....	39
4.3 SAMPLING AND ANALITICAL METHODS	40
4.3.1 Sm – Nd isotopes.....	40
4.3.2 U-Pb isotopes	41
4.4 RESULTS	42
5. DISCUSIONS	43
5.1. Interpretation of provenance	43
5.2. TECTONIC SETTING	46
6. CONCLUSIONS.....	47
7. REFERENCES.....	62
5. CONCLUSÃO:.....	73
REFERÊNCIAS BIBLIOGRÁFICAS	77
ANEXOS.....	87

LISTA DE FIGURAS

Figure 1: Localização da area de estudo (no retângulo vermelho) na região Arequipa, no sul do Peru. E sua localização em relação às bacias mesozoicas de Sul-America....	14
Figure 2. A cadeia dos Andes, e as principais caraterísticas (descritas no texto). In azul a extensão da bacia de Arequipa - Tarapacá.....	19
Figure 3. Principais elementos morfoestruturais nos Andes Centrais ao Sul do Perú. Em vermelho a localização atual do área de estudo (Modificado Armijo et al., 2015). AM: Embasamento de Arequipa.....	21
Figure 4: Afloramentos mesozoicos no sul do Peru (azul claro). Em negro as principais falhas regionais. O arco volcanico do jurásico (vermelho escuro). As vulcânicas estão restritas a Cordilheira da Costa (Vermelho oscuro). As rochas mesozóicas estavam restritas à Cordilheira Oriental até a alta estrutural de Abancay-Totos-Paras (ao Norte da bacia). Em vermelhão para estudar área.	23
Figure 5: Fotografias de campo	29
Figure 6: Perfil estratigráfico das rochas sedimentarias Jurássicas e Cretáceas da bacia de Arequipa e o controle de amostras segundo a posição estratigráfica e o tipo de análise que foi feito.....	33

LISTA DE TABELAS

Table 1 Sm, Nd, Sr values of sedimentary units, and coordinates of localization.	49
Table 2: U-Pb percentages ages, by known orogenic event. Based on Reimann et al (2010), Chew et al, (2007), Hurtado et al (2018).	52
Table 3: Summary of U-Pb data, localization and major pekas.	53

ANEXO

Tabela 1:Sumário dos dados de LA-ICPMS da amostra ARE304	88
Tabela 2:Sumário dos dados de LA-ICPMS da amostra ARE312	92
Tabela 3:Sumário dos dados de LA-ICPMS da amostra ARE305	96
Tabela 4:Sumário dos dados de LA-ICPMS da amostra ARE306	99
Tabela 5:Sumário dos dados de LA-ICPMS da amostra ARE-14.....	101
Tabela 6:Sumário dos dados de LA-ICPMS da amostra ARE-367.....	104
Tabela 7:Sumário dos dados de LA-ICPMS da amostra ARE-16	107
Tabela 8:Sumário dos dados de LA-ICPMS da amostra ARE-17	110
Tabela 9:Sumário dos dados de LA-ICPMS da amostra ARE-339.....	112
Tabela 10:Sumário dos dados de LA-ICPMS da amostra ARE332	117

CAPÍTULO I

1. INTRODUÇÃO

A Cordilheira dos Andes é dividida em três segmentos: os Andes do Norte (Ao norte dos 5° de latitude Sul), os Andes Centrais (maior segmento) e os Andes do Sul (Sempere et al., 2002), trata-se de um complexo sistema orogénico formado por processos de subducção que começaram ~530Ma (Cawood et al., 2005), evidenciados por um intenso magmatismo no Ordoviciano e terminando no começo do Devoniano (Chew et al., 2007), com um processo de quiescência magmática até o Pensilvaniano. O Permiano foi um período de conformação do Gondwana, onde a acumulação de calor no Triássico que levou ao período de geração de riftes no Oeste do Gondwana em ausência de processos de subdução (por exemplo: o rifte grupo Mitu; Spikings et al., 2016). O fechamento do rifte do Mitu é o reflexo do começo da subducção oblíqua, produzida pela subducção da placa oceânica Phoenix sob a placa Continental Sul-Americana, processo conhecido como o começo o “Ciclo Andino” (Romeuf et al., 1995; Boekhout et al., 2013; Haschke et al., 2006; Aleman & Ramos, 2000, Oliveros et al., 2006).

Este período da subducção é marcado por grandes processos distensionais, gerados pelos processos de *roll-back* negativo (Ramos & Mpodozis., 1989), que deram origem à bacias mesozoicas sincrônicas, desenvolvidas na borda oeste do Gondwana. Estas bacias foram: Bacia Neuquén (Argentina), Bacia Austral (Chile e Argentina), Bacia Maracaibo e Bacia Oriental (Venezuela), Bacia de Arequipa (Perú), Bacia Tarapacá (Chile).

A bacia mesozoica do Arequipa - Tarapacá (Perú - Chile) faz parte de um conjunto de bacias que se desenvolveram no Mesozoico (Fig 1); esta bacia desenvolveu-se entre os paralelos 14°S – 26°S, limitada ao leste pelas rochas paleozoicas da Cordilheira Oriental, e a Oeste pelo arco vulcânico do Chocolate. A bacia tem uma forma alongada preferencialmente na direção Norte-Sul (Fig 1).

A bacia de Arequipa possui aproximadamente ~4.4 km de espessura, formada de sedimentos jurássicos e cretáceos. Os sedimentos jurássicos estão compostos pelo Grupo Yura (Formações Socosani, Puente, Cachios, Labra e Gramadal), e os sedimentos cretáceos pelas formações Hualhuani, Murco, Arcurquina e Chilcane.

A paleogeografia inicial da bacia na área de Arequipa, no sul do Peru (Fig 1), foi estabelecida por Vicente (1981), Vicente et al., 1982. Seguido por León (1981), Chávez (1981), Acosta et al. (2010), e Trinidad (2017), e sugere que os sedimentos são provenientes da parte ocidental da própria bacia em concomitância com o arco vulcânico Chocolate, estabelecendo deste modo uma proveniência sedimentar principalmente do arco vulcânico, definindo assim um contexto de *back-arc* (Vicente et al., 2006).

Os dados de U-Pb em zircões detriticos e dados isotópicos de Sm-Nd e $^{87}\text{Sr}/^{86}\text{Sr}$ em rocha total, apresentados nesta dissertação, são os primeiros dados inéditos para estabelecer a proveniência sedimentar e a redefinição do contexto geodinâmico da bacia de Arequipa – Tarapacá no sul do Perú.

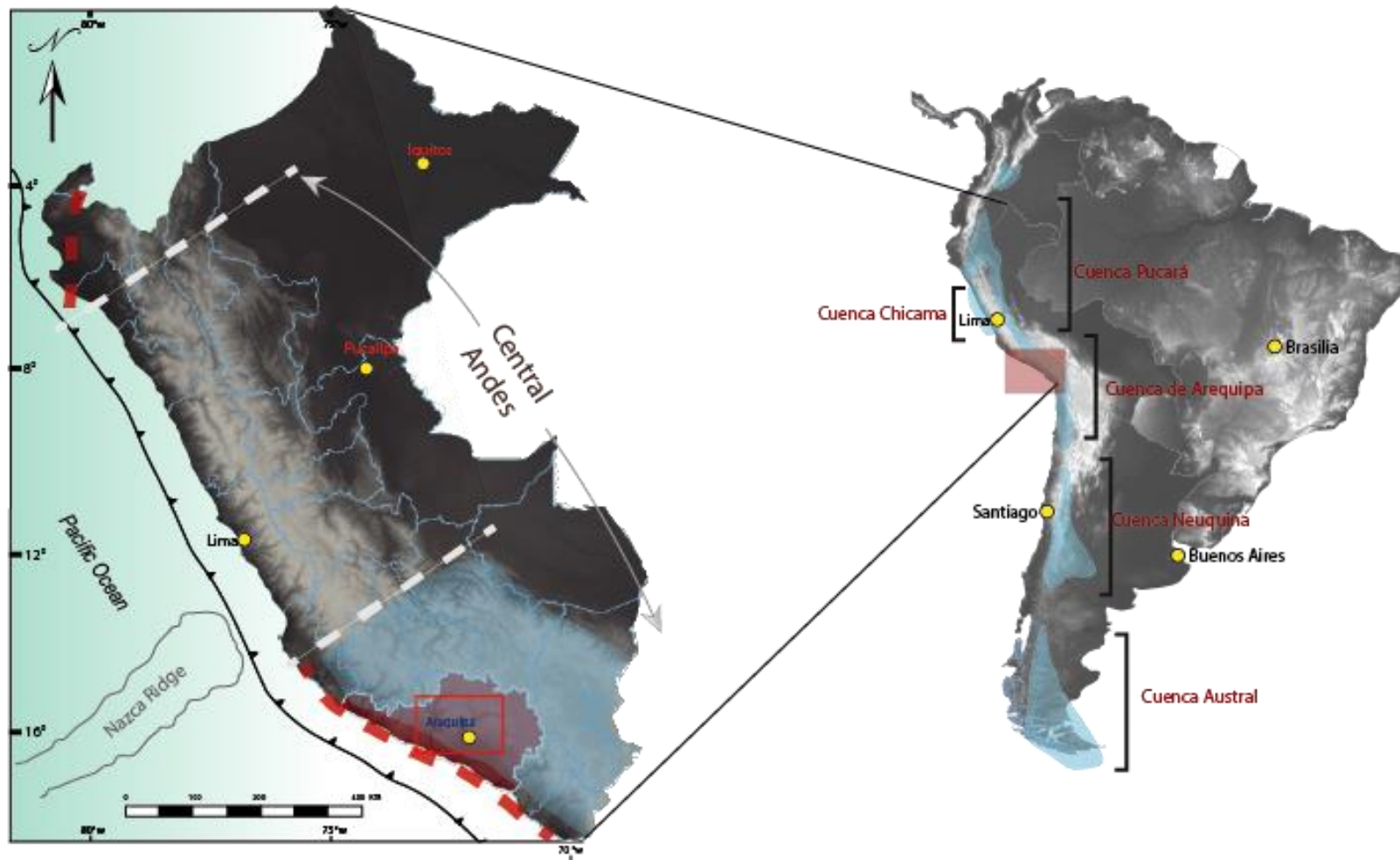


Figure 1: Localização da área de estudo (no retângulo vermelho) na região de Arequipa, no sul do Peru. E sua localização em relação às bacias mesozoicas de América do Sul.

1.1 PROBLEMA CIENTÍFICO

- Demonstrar o contexto tectônico da bacia de Arequipa – Tarapacá, se desenvolveu em um contexto de *back-arc* ou em um contexto do tipo rift, a partir das aplicações da metodologia baseada em geocronologia U-Pb sobre zircões detriticos (proveniência sedimentar) e análises isotópicas de Sm-Nd e $^{87}\text{Sr}/^{86}\text{Sr}$.

1.2 OBJETIVOS GERAIS

- Caracterização do ambiente tectônico de deposição da bacia Arequipa – Tarapacá.

1.3 OBJETIVOS ESPECÍFICOS

- Estabelecer as potenciais fontes de aporte sedimentar para o preenchimento da bacia.
- Estabelecer os processos geodinâmicos que afetaram a bacia.
- Estabelecer uma paleogeografia do Jurássico entre os paralelos 14° - 26° de latitude sul dos Andes Centrais.

1.4 ESTRUTURA DA DISSERTAÇÃO

A presente dissertação está estruturada com base em uma extensa revisão bibliográfica, cujo objetivo é a compreensão dos Andes Centrais.

- **O capítulo I** refere-se à introdução da dissertação, em que é estabelecida a problemática, e os objetivos gerais e específicos da dissertação, e quais são os pontos importantes para a compreensão do corpo do texto.
- **O capítulo II** comprehende um esboço geral da tectônica dos Andes, principais orogenias associadas aos processos magmáticos e de sedimentação que aconteceram na borda oeste de Gondwana Ocidental e uma introdução a arcabouço geológico da bacia.
- **O capítulo III** descreve o controle de amostra para a amostragem, a metodologia utilizada para a preparação das amostras e os métodos isotópicos que serão utilizados.
- **O capítulo IV** apresenta o artigo realizado no presente mestrado, ***WAS THE AREQUIPA BASIN DEPOSITED IN BACK-ARC BASIN CONTEXT?***

REVEALED USING U-PB AGES ON DETRITAL ZIRCON AND SR, ND ISOTOPES.

- O capítulo VI apresenta as principais conclusões e as novas conjecturas para a pesquisa científica nesta área.

CAPÍTULO II

2. ARCABOUÇO GEOLOGICO REGIONAL

2. A CORDILHEIRA DOS ANDES.

A cordilheira dos Andes, é um dos maiores sistemas orogênicos ativos (aproximadamente 8000 km de extensão) e também um dos mais complexos desenvolvidos entre a subducção da crosta oceânica da placa de Nazca sob a crosta continental da plataforma Sul Americana (Fig.2, Jaillard et al., 2000; Ramos, 2009).

A margem ocidental da América do Sul é um mosaico de domínios crustais pré-cambrianos e paleozoicos, com características distintas que controlaram algumas das deformações andinas, tais como o bloco Arequipa – Antofalla, o bloco Paracas, os Amotapes, entre outros (Ramos, 2008; 2009; 2018; Cawood, 2005; Chew et al., 2007; Romero et al., 2013; Spikings et al., 2016).

De acordo com as variações latitudinais da espessura da crosta e largura das cadeias, este sistema montanhoso foi dividido (Jaillard et al., 2000; Sempere et al., 2002), em três domínios morfoestruturais principais (Fig.2): *i*) Andes setentrionais, *ii*) Andes centrais e *iii*) Andes meridionais.

2.1 ANDES SETENTRIONAIS (12°N – 4°S)

Os Andes setentrionais compreendem as regiões dos Andes entre a Venezuela e a deflexão de Huancabamba, ao norte do Perú (Mégard, 1987). São áreas complexas que possuem três cadeias de montanhas: a cordilheira Ocidental, que está composta de rochas ígneas de afinidade oceânica (e.g. no golfo de Guayaquil, McCourt et al., 1984), dominadas por uma deformação colisional transpressiva, que foram acretadas no Neocretáceo (Spikings et al., 2015; Chew et al., 2008); a cordilheira central, que está composta de rochas ígneas jurássicas - cretáceas que intrudiram o embasamento (estas rochas ígneas possuem tanto origem continental como origem oceânica; Aspden & McCourt, 1986); a cordilheira oriental, que possui rochas metassedimentares paleozoicas e mesoproterozoicas em áreas localizadas, este embasamento está coberto por sedimentos fanerozoicos, onde tem-se registro de um ambiente de extensão no

Mesozoico e compressão no Cenozoico (Horton et al., 2010). As rochas paleozoicas desta área têm registrado o evento magmático do Arco Famatiniano (Rapela et al., 1998; Horton et al., 2010; Ramos, 2018).

No Jurássico predominou um ambiente de extensão, com o desenvolvimento de um ambiente rifte e posterior geração de crosta oceânica (Horton et al., 2010); é possível que a configuração da atual da Cordilheira Ocidental e Central, pode ter se alterado como consequência da acreção no Cenozoico.

2.2 ANDES CENTRAIS (5°S-35°S)

A cordilheira Oriental é composta por rochas paleozoicas metamorfizadas. Estas rochas depositaram-se no começo da separação entre o leste de Laurentia e a parte oeste do Gondwana (Cawood et al., 2012; Chew et al., 2008). Estas rochas da cordilheira Oriental possuem registro magmático do ciclo orogênico Gondwanide (Mišković et al., 2009) que é característico desta zona. A cordilheira Ocidental é composta por rochas sedimentares mesozoicas, rochas plutônicas registradas no Jurásico e Cretácico (Mukasa, 1986; Demouy et al., 2012; Polliand et al., 2005; Boekhout et al., 2013, 2015), que atualmente encontram-se afetadas por vulcanismo recente (Mamani et al., 2010). No Peru central registra-se o desenvolvimento de um *sag termal*, durante o Triássico, que gerou a bacia de Pucará (Rosas et al., 2007); este processo também poderia ser correlacionado ao desenvolvimento de folhelhos e carbonatos no Altiplano conhecidos como a unidade de Calcáreos do Grupo Lagunillas, de idade Sinemuriano (Portugal 1942, Jaillard, 1994). Onde possuem as mesmas idades, sedimentos calcários de estas idades são encontrados na parte leste da Bolívia. Esta extensa plataforma carbonática esteve ativa até o Toarciano (Rosas et al., 2007).

Durante o Neojurássico, no segmento oeste do Peru central, desenvolveu-se o Grupo Chicama, grupo está formado por sedimentos jurássicos e cretáceos. Os sedimentos Jurássicos estão conformados pela Formação Simbal (Jaillar & Jacay, 1989), caracterizada por folhelhos marinhos, cuja idade foi determinada por amonites de idade titoniano (Jaillard & Jacay, 1989). Sobreposta-se o Grupo Chicama, de idade Jurássico – Cretáceo, formada pelas Formações Punta Moreno, Sapotal (de idade Jurássica), e pela Formação Tinajones, de idade berriasiense (Jaillar & Jacay, 1989; Jacay, 1992). A estes sedimentos sobreposta-se em uma descontinuidade erosiva o Grupo Goyllarisquisga, de idade Albiano -Aptiano.

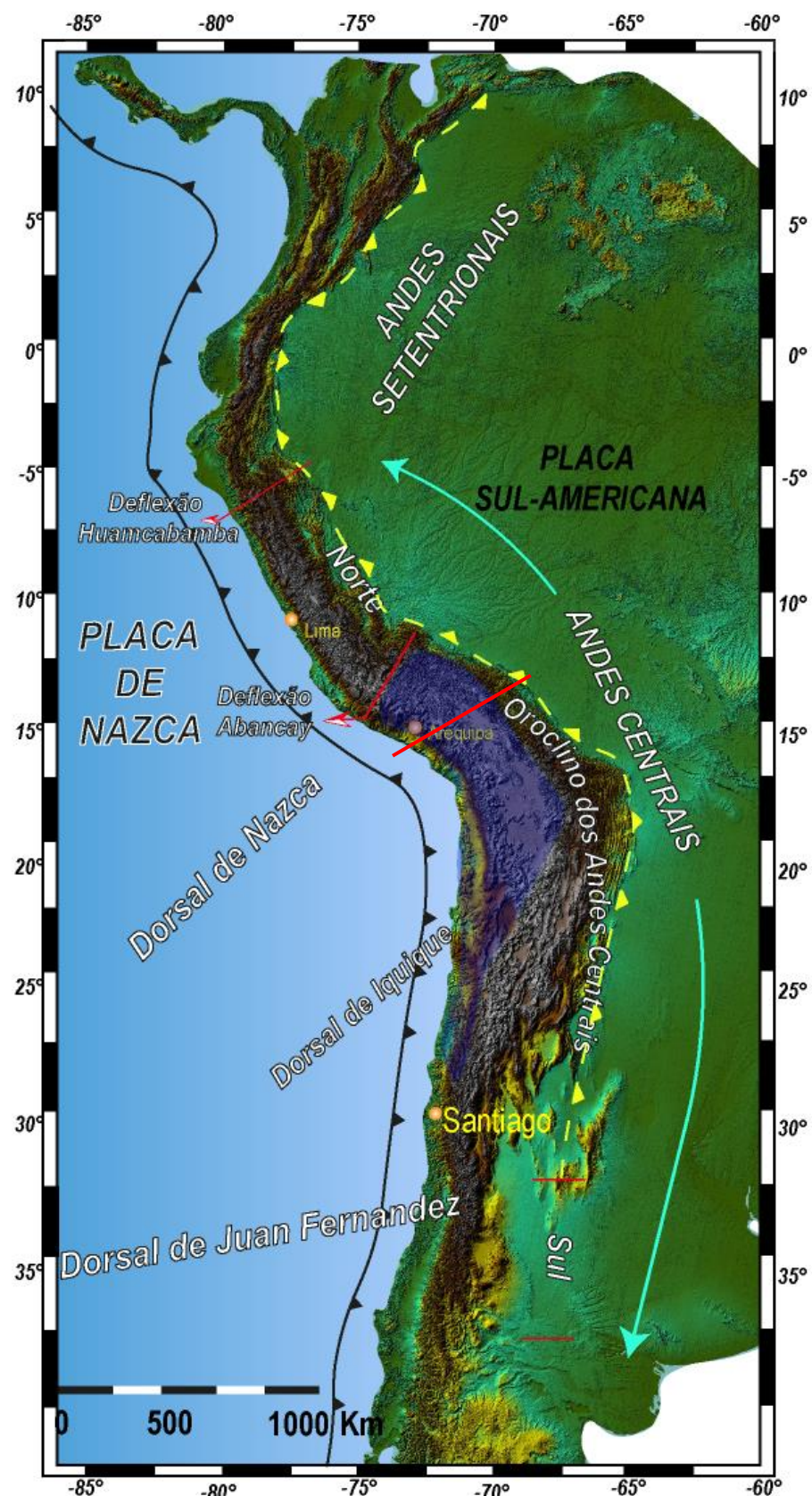


Figure 2. A cadeia dos Andes, e as principais características (descritas no texto). Em azul a extensão da bacia de Arequipa - Tarapacá.

3. CONTEXTO GEOLÓGICO DOS ANDES CENTRAIS NA PARTE SUL DO PERU

Os Andes Centrais na parte sul do Perú, são compostos pela Cordilheira da Costa, a Depressão Central, Cordilheira Ocidental, Altiplano e Cordilheira Oriental, Zona Sub-andina e Amazônia.

- i) A Cordilheira da Costa encontra-se formada pelo embasamento Arequipa (Casquet et al., 2010; Fernandez-Lopez et al., 2014; Loewy et al., 2004), e sedimentos paleozoicos do Grupo Yamayo (Boekhout et al., 2013; Sempere et al., 2012), rochas vulcânicas e vulcano-sedimentares de idade jurássica da Formação Chocolate (Boekhout et al., 2013; Boekhout et al., 2012; Jacay & Sempere, 2004), assim como depósitos cenozoicos da Formação Camaná (Alván and von Eynatten, 2014), as quais aumentam em espessura para oeste, em direção a Cordilheira da Costa (Cobbing et al., 1977; Bellido e Narváez, 1960). A cordilheira da Costa possui um alto estrutural formado pelo embasamento Arequipa, o qual separa a Bacia de Camana da Bacia Moquegua (Alván and von Eynatten, 2014; Decou et al., 2013). Este alto estrutural encontra-se afetado pelos eventos magmáticos do Ordoviciano associados ao evento magnético do Famatiniano (Cobbing et al., 1977; Loewy et al., 2004; Chew et al., 2008, Ramos et al., 2008, 2018). A bacia Moquegua se depositou entre a porção Cordilheira da Costa e a Cordilheira Ocidental, sendo composta de rochas cenozoicas (Boekhout et al., 2012; Decou et al., 2013); esta bacia começou a formar-se no Eoceno, quando a Cordilheira da Costa começou a ser exumada (Decou et al., 2013).
- ii) A Cordilheira Ocidental encontra-se conformada pelo batólito da Caldera (Demouy et al., 2012) e rochas sedimentares mesozoicas que são cobertos pelo arco magnético atual (Mamani et al., 2010). O batólito da Caldera possui rochas de idades jurássicas e cretáceas, as quais intruem o embasamento de Arequipa (Boekhout et al. 2013; Demouy et al. 2012). As rochas sedimentares desta área foram usadas para se-estabelecer a estratigrafia regional do Mesozoico no sul do Peru (Portugal, 1974, Benavides, 1962, Vicente et al., 1981; Sempere et al., 2002, Alvan et al., 2018).

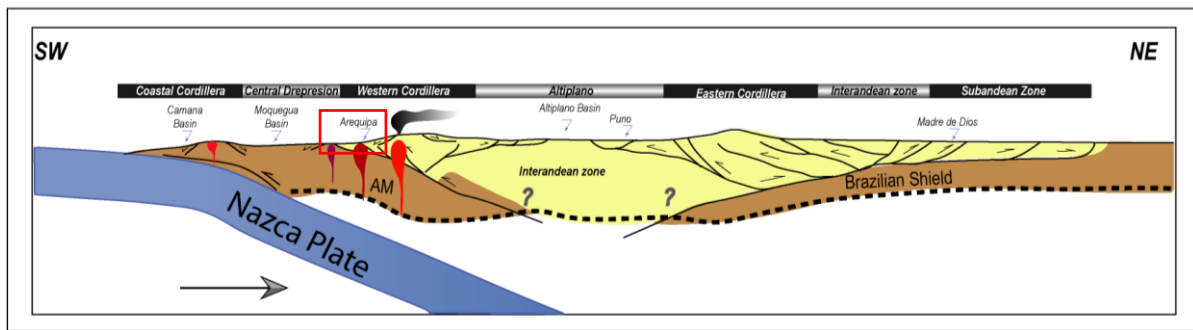


Figure 3. Principais elementos morfoestruturais nos Andes Centrais ao Sul do Perú. Em vermelho a localização atual da área de estudo (Modificado de Armijo et al., 2015). AM: Embasamento de Arequipa.

- iii) O Altiplano é uma superfície alto-andina, sub-horizontal, que se encontra localizada entre a cordilheira Ocidental e cordilheira Oriental, sendo constituído por sedimentos paleozoicos - jurássicos e cretáceos que possuem o registro da proto-cordilheira oriental (Jaillard e Santander, 1992; Jaillard et al., 2000; Reimann et al., 2010; Perez & Horton, 2014, Perez et al., 2016).
- iv) A cordilheira Oriental é composta por sedimentos paleozoicos e corpos intrusivos de idade Permiano ao Triássico, associados à orogenia Gondwanide (Miscovic et al., 2009). Neste segmento desenvolveu-se o rifte do Grupo Mitu (Perez & Horton, 2014; Spikings et al., 2016; Perez et al., 2016) dominado por rochas vulcânicas e vulcano-clásticas que se produziram entre 245-220 Ma (Spikings et al., 2016); as rochas paleozoicas deste segmento, como o Grupo Copacabana são rocha mãe para diversos depósitos de hidrocarbonetos (McGrober et al., 2015, Baby et al., 2018).
- v) A zona sub-andina composta de rochas paleozoicas e cretáceas; há dúvidas sobre a ocorrência de sedimentos jurássicos nesta área (Baby et al., 2018), isto poderia ser devido a não deposição ou à erosão das rochas sedimentares.

4. A CONTEXTUALIZAÇÃO DA BACIA DE AREQUIPA - TARAPACÁ

A bacia de Arequipa-Tarapacá desenvolveu-se em um contexto extensional associado à quebra de Gondwana (Jaillard et al., 2000; Ramos et al., 2009). Estes eventos extensionais, conjugados a processos de *roll-back* (Ramos & Mpodozis, 1989), geraram bacias em toda a borda oeste do Gondwana (Vicente, 2006; Oliveros et al., 2012; Martinez et al., 2017), entre elas a Bacia de Arequipa-Tarapacá.

A bacia de Arequipa-Tarapacá desenvolveu-se entre os paralelos 13 ° S - 26 ° de latitude Sul na borda oeste do Gondwana (Naipauer et al., 2015). Esta bacia no sul do Peru estava limitada ao oeste pelo Arco Magmático Jurásico (Fm. Chocolate; Jenks, 1948); ao leste limita-se pelas rochas paleozoicas da Cordilheira Oriental (Jaillar, 1994, 2004; Perello & Carlotto, 2003), ao Norte pelo alto estrutural de Abancay-Totos-Paras (Carlotto et al., 2009; Fernandes-Lopez et al., 2015; Alvan et al., 2018), ao Sul pelo Alto de Norte Chico (Vicente et al., 2006; Oliveros et al., 2012; Naipauer et al., 2015). A estratigrafia foi inicialmente proposta por Jenks, 1948 e Vicente, 1981, adotada rapidamente para o sul do Peru (Jaillar, 1992).

As rochas mesozoicas da bacia Arequipa foram inicialmente definidas pelos trabalhos iniciais de Jenks (1948) e Benavides (1962), os quais determinaram a Formação Yura, a qual estava definida por 5 membros iniciais (Membro Puente, Cachios, Labra, Gramadal e Hualhuani); posteriormente, pela extensão regional destas rochas, foram elevadas à categoria de formações (Vargas, 1970, León 1981, Vicente, 1981, Vicente et al., 1982). Por outro lado, Sempere et al. (2002) adicionou uma base às formações Chocolate e Socosani, e ao topo as formações Murco e Arcurquina, deste modo estabelecendo que os sedimentos da bacia Arequipa são formados pelas rochas jurássicas e cretáceas, chegando à espessura de ~ 4.4 km de empilhamento sedimentar. Recentemente os trabalhos de Alvan et al., (2018) apoiam o conceito planteado por Sempere et al., (2002). No presente trabalho propõe-se que a Formação Chilcane, seja adicionada na série cretácea como parte de um possível estagio “termal-sag” da Formação Arcurquina.

A Formação Chocolate na área de Arequipa é caracterizada por sequências vulcânicas e vulcano-clásticas, estas são sobre-postas por uma camada de cinza vulcânica com idade de 186 ± 1 Ma (U-Pb, Boekhout et al., 2013). Na área de Pampa Estique, Tacna, a Formação Chocolate (= Fm Junerata; Wilson & García, 1962) recobre sedimentos do Grupo Yamayo (sedimentos paleozoicos); nesta área a Formação Chocolate tem idade de $215,85 \pm 0,82$ (Boekhout et al. al., 2013), que é considerada como o início dos processos de subducção e com estes o início do “Ciclo Andino”. O último registro da atividade vulcânica foi identificado em Chala, onde se obteve idades de 132 Ma (Boekhout et al., 2013). Sequências vulcânicas e vulcanoclásticas, como as formações Rio Gran, Chala e Guaneros, foram consideradas como outra série; no entanto, foram interpretadas como acumulações relativas a um ambiente de subducção (Romeuf et al.,

1995). No entanto eles estão dentro do intervalo de atividade do arco planteada por Boekhout et al., (2013), quer dizer estas rochas vulcanoclásticas, poderiam se depositar em uma bacia de *back-arc* ou perto do arco vulcânico concomitante (Sempere et al., 2002). As grandes acumulações de sedimentos e rochas vulcânicas (>3000m) na área da costa, dão ideia da forte subsidência nesta área.

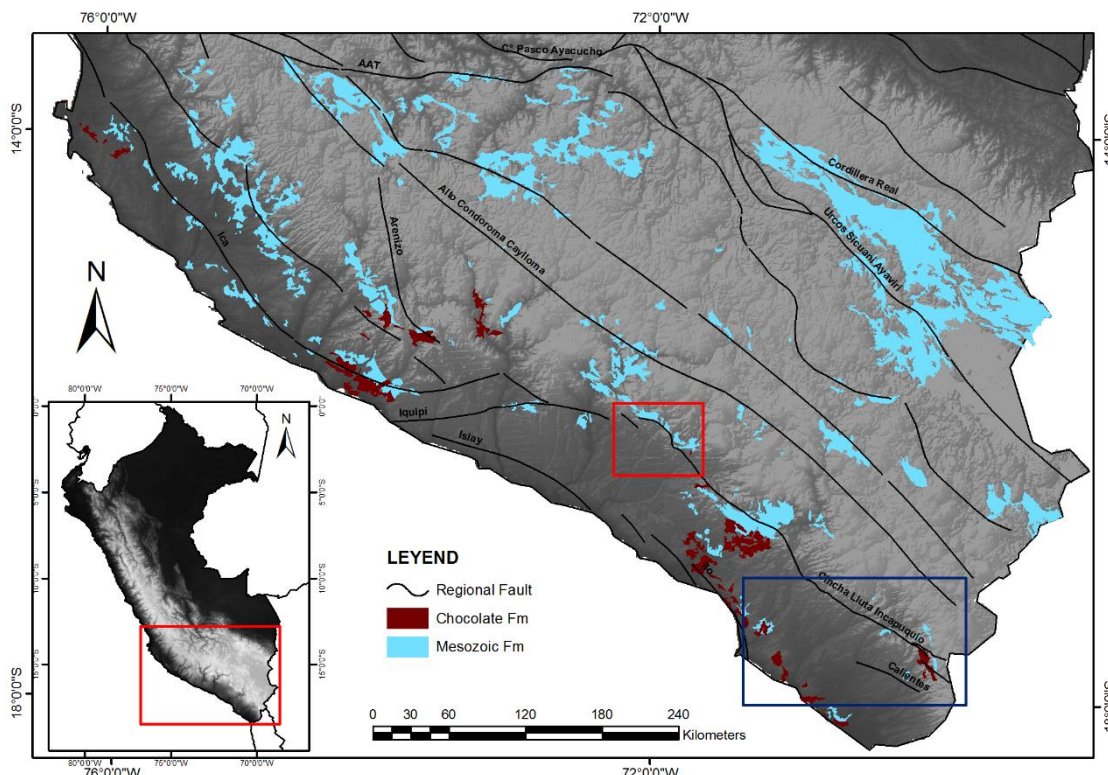


Figure 4: Afloramentos mesozóicos no sul do Peru (azul claro). Linhas pretas representam as principais falhas regionais. O arco vulcânico do Jurásico (vermelho escuro). As vulcânicas estão restritas a Cordilheira da Costa (Vermelho escuro). As rochas mesozóicas estavam restritas à Cordilheira Oriental até o alto estrutural de Abancay-Totos-Paras (ao Norte da bacia). O quadro em vermelho representa nossa área de estudo.

5. ALGUMAS CARACTERÍSTICAS DAS POSSÍVEIS FONTES

5.1 ROCHAS INTRUSIVAS PERMIANAS - TRIÁSICAS

As rochas intrusivas do Triássico estão expostas em uma faixa paralela aos afloramentos do Grupo Mitu, sendo mais volumosas ao longo da Cordilheira de Carabaya. Possuem uma movimentação de ~ 130 km até a Cordilheira Andahuaylas, onde perdem volume até deixarem de existir para o norte, à altura do paralelo 10 ° S (Spikings et al., 2016).

As rochas jurássicas aparecem restritas ao trend NE-NW do território peruano, não havendo manifestações das mesmas na porção central do país, talvez por terem sido erodidas devido à alta taxa de subducção da placa (Stern et al., 2012). Na Cordilheira Oriental também há ocorrência de rochas de idade jurássica, intrusivas e extrusivas, como no caso do Complexo Allincapac (Cordillera de Carabaya), que possui idades U-Pb (195 ± 11 Ma e 184 ± 4 Ma), obtidas em Nefelina Sienito (Miscovic et al. al., 2009), rocha peralcalina, tipicamente formada a partir da descompressão do manto superficial em um ambiente de *back-arc* (Miscovic et al., 2009; Reitsma, 2012).

Há um granito alcalino com idade U-Pb em zircão de $304,3 \pm 0,1$ Ma (Reitsma, 2012) em contato erosivo com as camadas superiores do Grupo Mitu, que podem pertencer à Formação Huambutío ou à Formação Huancané (Spikings et al., 2016).

5.2 ARCO MAGMÁTICO JURÁSSICO

O arco magmático jurássico desenvolveu-se na margem oeste do Gondwana, durante o início da subducção que originou o chamado “Ciclo Andino”, iniciado aproximadamente a 216 Ma (Boekhout et al., 2013; Oliveros et al., 2006, 2012; Jaillard et al., 1990, Romeuf et al., 1995, Ramos & Mpodozis et al., 1989). O arco magmático manifestou-se pela subducção entre a placa oceânica Phoenix sob a placa continental Sul-Americana. Este arco magmático é reconhecido na Colômbia e no Equador como a Formação Misahualli/Colán (Romeuf et al., 1995); são derrames vulcânicos de composição basáltico-andesítica de afinidade cálcio-alcalina, em alguns casos com depósitos de queda, os quais possuem composição riolítica. Estes depósitos vulcânicos encontram-se afetados pela intrusão de plútões jurássicos (e.g. Batólito de Zamora, Abitagua, La Florida, Spikings et al., 2015). O Arco magmático Jurássico dos Andes do norte encontra-se na atual cordilheira Real e na frente Sub Andino. A diferença desta, nos Andes do Norte é que a subducção foi perpendicular, o que provocou a acreção dos terrenos na borda de Gondwana (e.g. Amotapes). No entanto nos Andes Centrais foi oblíqua, afetando desta forma a formação das bacias (e.g. Casma, Arequipa-Tarapacá), possivelmente com movimento sinistral (Romeuf et al., 1995, Chen et al 2013, Ramos & Mpodozis et al., 1989, Jaillard, 1990). No segmento peruano (parte central) não está exposto o arco jurássico, possivelmente esteja erodido pela subducção, pois só aflora de novo a partir do paralelo 14° de latitude Sul e é continuo até o sul de Chile. No sul do

Perú toma o nome da Formação Chocolate (como também Rio Grande e Chala, Romeuf et al., 1995). No Chile ele é conhecido como a Formação La Negra (Garcia, 1967; Oliveros et al., 2002, 2006; 2012), correlativa com a Formação Punta del Cobre (Oliveros et al., 2018). Estes arcos vulcânicos têm afinidade cálcio-alcalina, com altos teores de Zr (ppm) na composição geoquímica, o que os diferencia dos Andes do Norte (Romeuf et al., 1995).

2.3. POTENCIAS FONTES

CORDILLHEIRA DA COSTA

- i) O embasamento Arequipa é formado por rochas metamórficas alóctones cuja colisão com o Cráton Amazônico aconteceu a 1.0 Ga (Loewy et al., 2004, Casquet et al., 2010). O embasamento Arequipa possui três idades características: idades ordovicianas (0.45 Ga), idades Grenvillianas (0.9-1.0 Ga) e idades Paleoproterozoicas (2.0 - 1.8 Ga). Estas idades são características também das rochas paleozoicas que estão presentes na cordilheira da Costa (Reimman et al., 2010).
- ii) As idades Ordovicianas reportadas por Loewy *et al.*, (2004), Chew *et al.*, (2007), Romero *et al.*, (2013), são referentes ao Arco Famatiniano (Ramos, 2018). O magmatismo Ordoviciano desenvolveu-se entre 467-477 Ma, e que também foram reportadas nas ilhas Hormigas de Afuera, no Macizo del Marañón, no entanto, no Macizo de Arequipa que são similares. O arco magnético Famatiniano é um magmatismo que vai desde a Patagonia (Argentina) até os Andes do Norte (Venezuela), deste modo foi levado desde um evento a escala local até um evento em escala continental (Ramos & Mpodozis et al., 1989; Ramos, 2018).

CORDILHEIRA ORIENTAL

- i) A cordilheira oriental é constituída por rochas paleozoicas com duas idades características, 0.7 - 0.5Ga e 1.3 - 0.9Ga (Chew et al., 2007; 2008). Por outro lado, um tipo de idade que só ocorre na cordilheira Oriental são as rochas permo-triásicas, que estão relacionadas à Orogenia Gondwanide (Miscovic

et al., 2009; Reitsma, 2012; Boekhout et al., 2018). Chew *et al.*, (2007), sustentam que as idades neoproterozoicas provêm de um arco magmático que se encontra coberto pelos sedimentos paleozoicos da atual cordilheira Oriental.

CAPÍTULO III

AMOSTRAGEM E MÉTODOS

3.1 AMOSTRAGEM

O objetivo dos trabalhos de campo foi obter amostras das rochas sedimentares mesozoicas que constituem a bacia de Arequipa no intervalo Jurássico–Cretáceo, ao longo do perfil típico, na margem direita do Rio Yura (Vicente, 1981; Benavides, 1962),

O método de controle de amostragem adotado foi a coleta da base e do topo de cada formação, totalizando 10 amostras, para metodologia U-Pb, (Fig. 6), com o propósito de identificar as possíveis mudanças de fontes para cada formação. Foram coletadas 42 amostras para análise de isótopos de Sm-Nd e Sr/Sr que foram coletadas ao longo de todo o perfil estratigráfico da secção tipo.

As amostras foram coletadas nos seguintes perfis:

- A) Ao longo do perfil do Rio Yura para a Fm. Puente e paleo-canais da Fm. Cachios.
- B) Ao longo do vale Cachios para as formações Cachios e Labra.
- C) Sobre a rodovia Yura-Cincha para as Fm. Gramadal e Fm. Hualhuani.
- D) Rodovia Yura-Huanca para as Formações Murco, Arcurquina e Chilcane.

3.2 PREPARAÇÃO DE AMOSTRA

As primeiras amostras: ARE 14; ARE 16; ARE 17 foram preparadas na Universidade Estadual Paulista “Julio Mesquita Filho” – Presidente Prudente, São Paulo, na Faculdade de Física, Química e Biologia (DFQB), no Laboratório de Geocronologia do grupo de pesquisa DETRAN, segundo o procedimento de separação do mineral zircão estabelecido por Resende, 2011 (Fig. 6).

O segundo agrupamento de amostras ARE304-ARE339 foi processado no Instituto Geológico Minero e Metalúrgico (INGEMMET), nos laboratórios de Geologia Regional, segundo os procedimentos internos estabelecidos para a separação de zircão (Alvan & Trinidad, 2016).

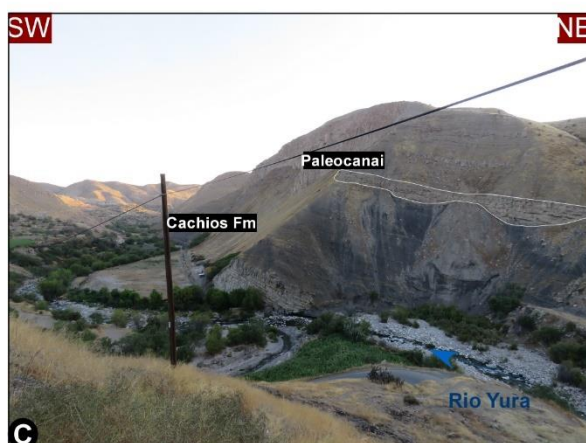




Figure 5: Fotografias dos afloramentos A) Contato entre as Formações Sosani e a Formação Puente. C) Contato transicional entre as formações Puente e Cachios. C) Paleocanal dentro da Formação Cachios. D) Paleocanal superior da Formação Cachios. E) Contato entre as formações Cachios e Labra F) Formação Gramadal sobre a Formação Labra G) Contato entre as formações Gramadal e Hualhuani H) A Formação Chilcane dentro da Formação Arcurquina I) A Formação Cachios e pequenos paleocanais. J) Contato entre as formações Cachios e Labra. K) Contato erosional entre as formações Chocolate e Sosani. L) Secção típica da Formação Puente.

Em ambos os laboratórios foi utilizado o método de separação de zircão por líquido denso, e a montagem do zircão foi feita no Laboratório de Geocronologia da

Universidade de Brasília (UnB), para posterior polimento, imageamento e análise dos grãos de zircão detriticos.

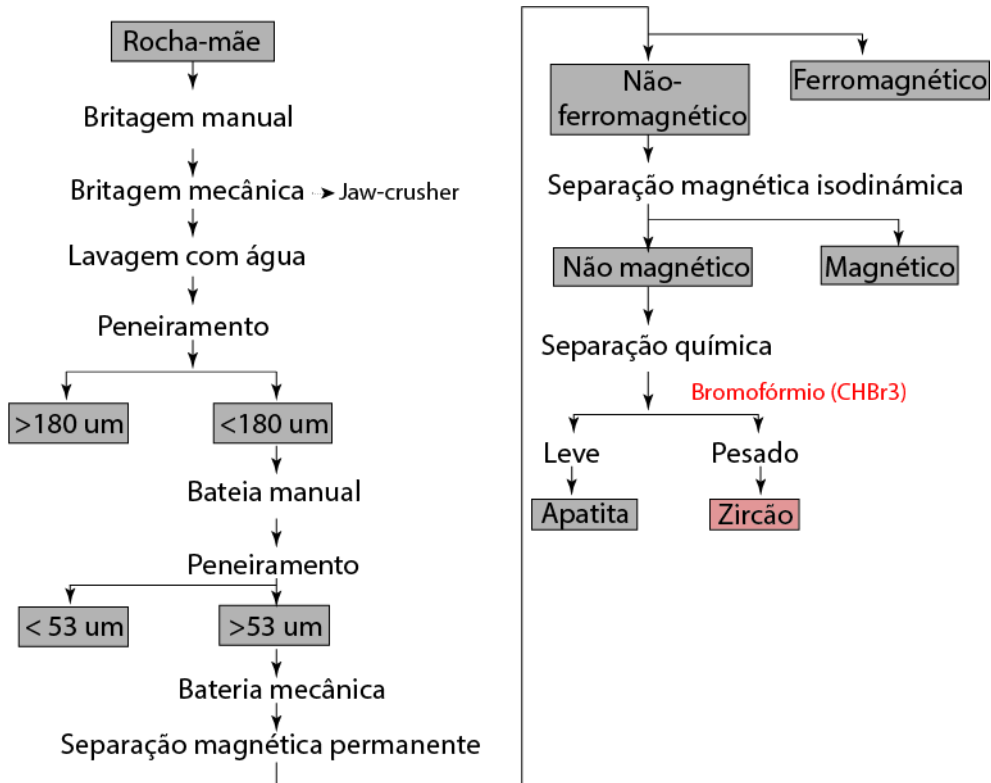


Figure 6: Fluxograma de preparação de amostra no laboratório DETRAN da UNESP. (Resende, 2011).

As amostras ARE 304 e ARE339 foram preparadas no Instituto Geológico Minero Metalúrgico – INGEMMET, no departamento de Geologia Regional, mediante o uso de líquido denso (politungstato de sódio), com o protocolo estabelecido no Instituto Minero e Metalurgico.

As amostras para análises de Sm-Nd e Sr-Sr foram preparadas no Laboratório de Geocronologia da Universidade de Brasília (UnB), mediante os protocolos estabelecidos para preparação mecânica do laboratório.

3.3 POR QUE O MINERAL ZIRCÃO?

O zircão é um mineral resistente ao processo físico de ablação e intemperismo químico (Cawood & Nemchin, 2000; Cawood et al., 2012). Os cristais de zircão podem indicar a idade de cristalização deles. O estudo das populações de zircões detriticos em rochas

sedimentares levam em consideração as assinaturas das idades das rochas fontes em uma província distributiva. Cada província distributiva possui diferentes padrões de zircões detriticos (Cawood & Nemchin, 2000), o que é importante para distinção de bacias, morfologias e proporções de diferentes grãos minerais.

3.4 ISÓTOPOS DE Sm-Nd

As análises isotópicas de Sm-Nd seguiram o método descrito por Gioia e Pimentel (2000) e foram realizadas no Laboratório de Geocronologia da Universidade de Brasília. Após passar pelo moinho de anéis ~ 50 mg de cada amostra foram misturados com ^{149}Sm - ^{150}Nd spike solution e dissolvidos em beckers Savillex. A extração de Sm e Nd da amostra (rocha total) seguiu as técnicas convencionais de cromatografia de troca de catiões, com colunas de Teflon contendo resina LN-Spec (HDEHP – *diethylhexil phosphoric acid supported on PTFE powder*). Os resultados isotópicos foram obtidos pelo *multicollector TRITON thermal ionization mass spectrometer multicollector* (TIMS) em modo estático.

As incertezas das relações Sm/Nd e $^{143}\text{Nd}/^{144}\text{Nd}$ foram melhores do que $\pm 0,1\%$ (2 Standard Error) e $\pm 0,0015\%$ (1σ), respectivamente, de acordo com as análises repetidas dos padrões internacionais BHVO-1. As razões $^{143}\text{Nd}/^{144}\text{Nd}$ foram normalizadas para $^{146}\text{Nd}/^{144}\text{Nd}$ 0.7219. A constante de decaimento utilizada foi (λ) 6.54×10^{-12} . As idades modelos T_{DM} foram calculadas usando o modelo de DePaolo et al., 1981.

3.5 ISÓTOPOS DE U-Pb

As análises isotópicas de U-Pb foram realizadas em cristais de zircões usando o *Thermo-Fisher Neptune* HR-MC-ICP-MS acoplado com um sistema de laser Nd:YAG UP213 New Wave, também no Laboratório de Geocronologia da Universidade de Brasília. As análises foram realizadas seguindo o método de Albarède et al. (2004), sendo o zircão GJ-1 (Jackson et al., 2004) o padrão para quantificar o fraccionamento ICP-MS. Dois a quatro cristais desconhecidos de zircão foram analisados entre as análises do padrão GJ-1. As massas quantificadas foram ^{238}U , ^{207}U , ^{206}U , ^{204}U e ^{202}U . O tempo de integração foi de 1 s e o tempo de ablação de 40 s. Utilizou-se um spot de 30 μm , com laser a 10 Hz e 2-3 J/cm². As relações $^{206}\text{Pb}/^{207}\text{Pb}$ e $^{206}\text{Pb}/^{238}\text{U}$ foram corrigidas pelo tempo. Para zircões menores (< 50 μm), o fraccionamento $^{206}\text{Pb}/^{238}\text{U}$

induzido pelo laser (*single-spot*) foi corrigido pelo método de regressão linear (Košler et al., 2002). Os dados brutos foram processados e reduzidos (e.g., Chronus; Oliveira, 2016) usando a planilha Excel descrita por Bühn et al., (2009). Durante a aquisição, o padrão 91500 (Jackson et al., 2004) também foi analisado como padrão externo.

O ^{204}Pb comum foi monitorado utilizando as massas de ^{202}Hg e ($^{204}\text{Hg} + ^{204}\text{Pb}$). Correções do Pb comum não foram realizadas devido a sinais muito baixos para ^{204}Pb (<30 cps) e altas razões $^{206}\text{Pb}/^{204}\text{Pb}$. Os erros relatados são propagados por adição quadrática [$(2\text{SD}^2 + 2\text{SE}^2)/2$] ($\text{SD} = \text{standard deviation}$; $\text{SE} = \text{standard error}$) de reproducibilidade externa e “precisão interna” (*within-run precision*). A reproducibilidade externa é representada pelo desvio padrão obtido a partir de análises repetidas ($n = 20$, ~ 1,1% para $^{207}\text{Pb}/^{206}\text{Pb}$ até ~ 2% para $^{206}\text{Pb}/^{238}\text{U}$) do padrão GJ-1 durante as aquisições analíticas, a precisão interna é o erro padrão calculado para cada análise. Os gráficos de densidade de probabilidade e idades foram calculados usando o software Isoplot-3/Ex (Ludwig, 2008).

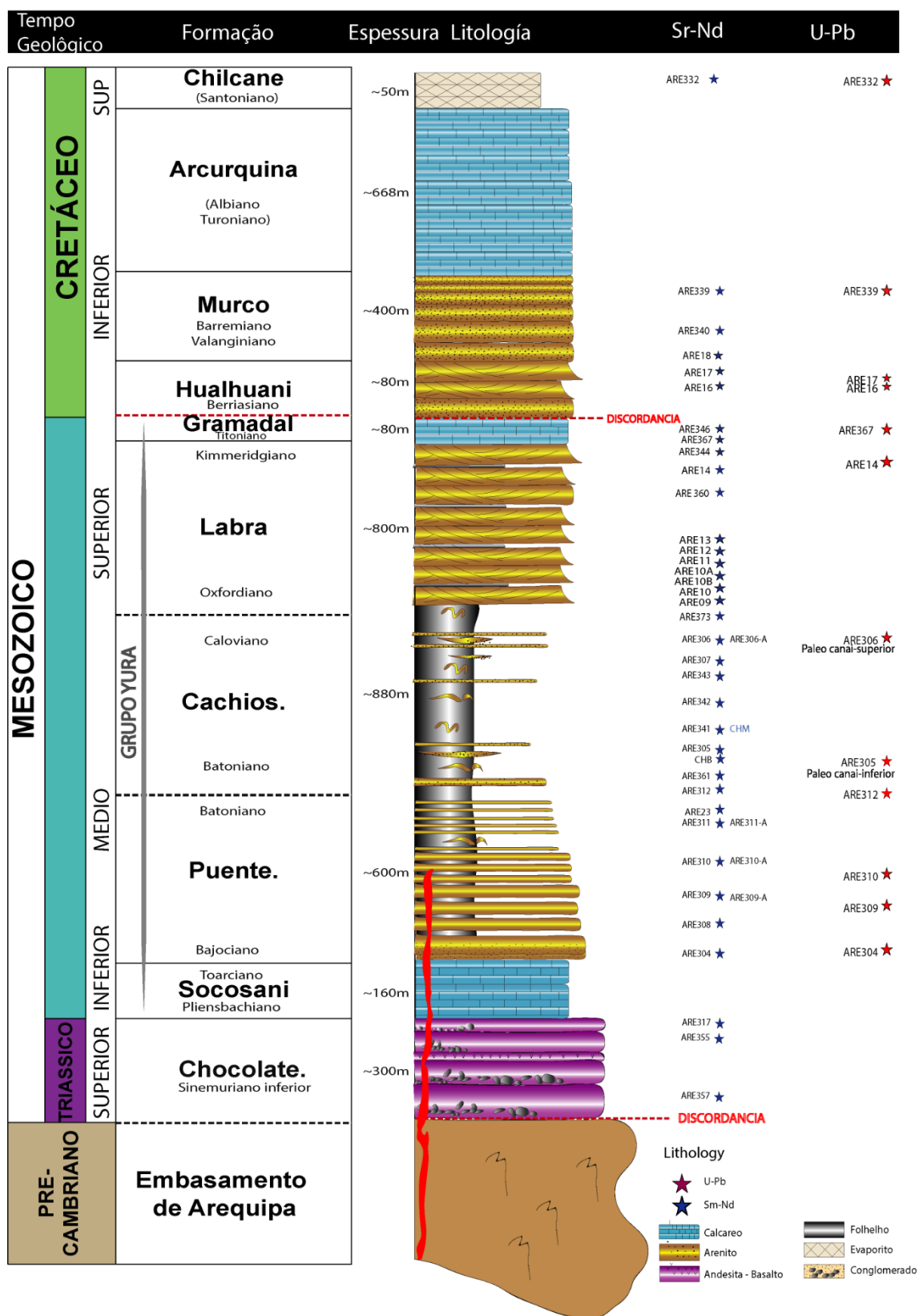


Figure 7: Perfil estratigráfico das rochas sedimentares Jurássicas e Cretáceas da bacia de Arequipa e o controle de amostras segundo a posição estratigráfica e o tipo de análise efetuada.

CAPITULO IV

ARTIGO:

AREQUIPA BASIN WAS DEPOSITED IN BACK-ARC BASIN CONTEXT? REVEALED USING U-Pb AGES ON DETRITAL ZIRCON AND Sr-Nd ISOTOPES.

**Cesar Chavez¹, Elton Luiz Dantas¹, Martín Roddaz^{1,2}, Roberto Ventura Santos¹,
Carlos Tello Sáenz³, Aldo Alván⁴.**

¹Laboratório de Geocronologia, Instituto de Geociências, Universidade de Brasília,
Brasília, DF 70910-000, Brazil.

² Géosciences-Environnement Toulouse, Université de Toulouse; UPS (SVT-OMP);
CNRS; IRD; 14 Avenue Édouard Belin, F-31400 Toulouse, France.

³Laboratorio de Geocronología, Departamento de Física, Química e Biología,
Universidade Estadual Paulista Julio Mesquita de Filho, UNESP, Campus Presidente
Prudente, Brazil.

⁴Instituto Geológico Minero Metalúrgico – INGEMMET , Dirección de Geología
Regional, Av. Canada 1470, San Borja-Lima, Peru.

ABSTRACT

During the break-up of Gondwana, extension processes allowed the formation of sedimentary basins in different tectonic environments. There are limited studies on the recognition of these. We study the sedimentary provenance of Mesozoic rocks from the Jurassic to Cretaceous interval deposited in Arequipa - Tarapacá basin, based on isotopic compositions of Sr-Nd (Wall-rock) and U-Pb ages of detrital zircon, to recognize the tectonic environment of the Arequipa-Tarapacá Basin of the south of Peru. The sandstones of the Lower-Upper Jurassic have important populations of sources with ages Greenville - Sunzas (1.3 - 0.9 Ga), as well as Neoproterozoic ages (0.5 - 0.7 Ga). The values of $\xi_{\text{Nd}}(0)$ are a little irregular ranging from -12.0 to -7.5 with ratios of $^{87}\text{Sr}/^{86}\text{Sr}$ between 0.70796 to 0.7318, suggesting as potential source, the eastern cordillera. In the Upper Jurassic (Titonian), ages were mainly Paleo-Neoproterozoic (0.5 - 2.0) with values of $\xi_{\text{Nd}}(0)$ between -9.0 and -7.28 and the ratios of $^{87}\text{Sr}/^{86}\text{Sr}$ between 0.7145 to 0.72158, we interpret the Nd isotopic signature was affected by Permian – Triassic intrusive rocks, and the distribution ages suggest the Brazilian shield as a potential source. During the lower Cretaceous ages were mainly Neoproterozoic (0.5 - 0.7 Ga) with values of $\xi_{\text{Nd}}(0)$ between -11.9 and -7.01 and the ratios of $^{87}\text{Sr}/^{86}\text{Sr}$ between 0.70760 to 0.71343, these patterns suggest a source of Eastern Cordillera and during the Upper Cretaceous, Paleo-Neoproterozoic ages (2.0 - 0.5 Ga), and Jurassic arc ages (<200 Ma) were found. The value of the $\xi_{\text{Nd}}(0) = -5.35$ and the ratios of $^{87}\text{Sr}/^{86}\text{Sr} = 0.70786$, which shows a signature affected by arc sediments. This suggests associating an eastern source (Cordillera Oriental) and a western source (Cordillera de la Costa). Potential sources for the Jurassic and Lower Cretaceous are found in the eastern cordillera and the Brazilian shield, possibly suggesting a paleo-drainage from the East to the West. In this way, based on the results of U-Pb in detrital zircons and the results of Sr-Nd, they discard as a potential source the Jurassic volcanic arc, with the U-Pb age distributions being preferably of older ages coinciding with a rift type tectonic setting.

4.1 INTRODUCTION

The western margin of South America is considered as a type example of ocean-continent plate convergence that has been the site of almost continuous subduction since at least the Cambrian (Aleman & Ramos, 2000). Intermittent magmatic arcs have been documented to be active since then as a consequence of the subduction of Pacific

oceanic plates beneath South America (Cawood, 2005) so that southern Peru is considered a type locality for long-lived, active continental margin (Boekhout et al., 2013; Chew et al., 2007; Mišković et al., 2009; Mukasa, 1986; Pindell and Tabbutt, 1995). Following the Gonwanide orogeny and during the initiation of Pangea breakup, the Central Andes of Peru and Bolivia experimented several extensional episodes. The oldest extensional episode is recorded by the rift system of the Mitu group which is caused by the collapse of the Gondwanide orogeny (Mégard, 1979, 1984; Carlotto et al., 2008; Spikings et al., 2016). After this Triassic rifting episodes, most of the study suggest that Jurassic and Lower Cretaceous times have essentially been marked by arc and back-arc extension (e.g., Jaillard and Soler, 1996; Ramos and Mpodozis, 1989). However, definitive geological evidences that allow to distinguish between a back-arc and continental rifting settings are scarce.

From a geodynamic point of view, it is important to separate between rifting or aborted rifting and back arc extensional settings because the former is linked to the dynamic of gondwana breakup and hence mantle dynamic (see (Lamotte et al., 2015; Murphy and Nance, 2013; Nance et al., 2014) and references therein) whereas the latter only depends on the age of the subducting oceanic crust and on the dip angle of the subduction slab (Sdrolias and Müller, 2006). One way to tackle this problem is to determine the provenance of the sediments deposited in the basin adjacent to the Jurassic Andean volcanic arc. Sediments deposited in a back arc setting are dominated by U-Pb zircon ages that approximate the depositional age of the samples (Cawood et al., 2012; Stern and Dickinson, 2010) and radiogenic Nd isotopic composition reflecting the dominant contribution from the volcanic arc (McLennan et al., 1993). Sediments deposited in a rift setting have also Nd radiogenic isotopic composition that reflect contribution from the rift related mafic volcanism (McLennan et al., 1993; Hurtado et al., 2018) but typical U-Pb zircon age distribution show lack in component of syn-depositional magmatic activity and are dominated by input from older sources because zircons are mostly absent in rift related mafic volcanism (Cawood et al., 2012; Cawood and Nemchin, 2000).

Unlike other sections of the western South American margin, the Peruvian margin has not been modified by terrane accretion since the onset of subduction (Loewy et al., 2004; Mišković et al., 2009) and hence it has the potential of preserving the original configuration of its adjacent basins since the onset of subduction. The aim of this study

is to determine the provenance of the Jurassic sediments deposited in southern Peruvian Arequipa-Tarapacá basin based on the measurement of ^{41}Sr - ^{87}Nd isotopic composition, 12 samples for U-Pb zircons ages. The provenance results are then used to discuss the paleo tectonic setting of the Arequipa-Tarapacá basin and the geodynamic process that control the Jurassic evolution of the Peruvian margin. mainly preserving original rock relationships, providing the opportunity to construct a chronostratigraphic framework for the evolution of the Jurassic arc system.

4.2 Geological Setting:

4.2.1 Stratigraphy of the Arequipa Basin

The oblique subduction of the Phoenix Oceanic plate beneath the Continental South American plate (Ramos & Mpodozis, 1989, Romeuf et al., 1995, Jaillard et al., 1990, Ramos and Aleman, 2000; Chen et al., 2013), associated to roll-back processes is responsible for generating extension along the western Gondwana margin (Ramos & Mpodozis, 1989) and supposed formation of the back-arc basins in the region (e.g. Arequipa - Tarapacá Basin (Vicente, 2005), Neuquén Basin (Naipauer et al., 2015), Rocas Verdes Basin, Fig 1), located to the east of the Jurassic Magmatic Arc (215 – 132 Ma; Romeuf et al., 1995; Oliveros et al., 2006, 2012; Boekhout et al., 2013,). The Mesozoic Arequipa – Tarapacá basin extent from 13° lat S to 26° lat S (Fig. 1). The basin is limited to the east by the Paleozoic sediments of the Eastern Cordillera (Jaillard, 1994, 2004; Perello et al., 2003; Fig. 1) and to the west, by the Jurassic magmatic arc (Jenks, 1948, Romeouf et al., 1995, Boekhout et a., 2013, 2015). Structural basement inliers define the south and north boundaries, the Norte Chico high (Vicente et al., 2006, Oliveros et al., 2012), and the Alto-Totos-Paras High (Calotto et al., 2009, Fernandez Lopez et al., 2014, Alvan et al., 2018), respectively (Fig 1). The present study area is concentrated in the district of Yura, at ~ 25km NW of the City of Arequipa (Fig. 2), where the strato-type of the Jurassic-Cretaceous series of the Arequipa-Tarapacá Basin have been defined along the Yura River by Jenks, (1946), Benavides (1962) and Vicente (1981).

The stratigraphic record of the Arequipa Basin -Tarapacá in this area is made up of approximately ~ 4.4 km thick of Jurassic – Cretaceous sedimentary rocks represented by the Yura Group, (Fig. 2, 3, Socosani, Puente, Cachios, Labra and Gramadal

formations, Benavides, 1962 Vicente, 1981, Vargas 1968, Sempere et al., 2004) and the Cretaceous sedimentary rocks are part of Hualhuani, Murco, Arcurquina and Chilcane formations (Fig 2, 3. Benavides, 1962, Pamparo & Batty, 1994, Alván et al., 2018).

The Chocolate Formation consists approximately ~900m thick of andesitic lava flows, breccias, volcanosedimentary levels and coral reefs (Fig. 4, Jenks, 1942, 1948; Vargas 1970, Boekhout et al., 2013). This arc outcrop along the Chilean margin and is known as the La Negra arc (García et al., 1947, Oliveros et al., 2006, 2012, Rossel et al., 2013, Martinez et al., 2017), disappears in the central part of Peru, and reappears in northern Peru - Ecuador where it is known as the Misahualli-Colán Arc(Litherland et al., 1994; Romeouf et al., 1995, 1997, Spikings et al., 2015).

The Socosani formation is characterized by platform limestones that define the first transgressive event, overlying in erosional contact the volcanic and volcanosedimentary sequence of the Chocolate Formation (Jenks, 1948). At the base of the Socosani Formation, a volcanic ash dated by U-Pb age at ca 186 Ma was reported (Fig. 4) (Boekhout et al., 2013); Presence of ammonites suggest a Toarcian - Lower Bajocian age (Vicente et al., 1981, 1982; Acosta et al., 2009).

The Puente formation overlays in transitional contact the Socosani formation. This formation, is characterized by ~600m of marine intercalations of shales and sandstone (Fig.4) (Benavides, 1962; Vicente, 1981), dated from the Bajocian to Callovian (Benavides, 1962, Vicente 1981).

The Cachios formation is overlying in transitional contact the Puente formation. It is characterized by ~800 m of marine black shales, at the base and the top is characterized by the paleo-channels (Vicente 1981, Leon, 1981).

The Labra formation is overlying in transitional contact on the Cachios formation. This formation is characterized by ~800m of quartz rich sandstone, shales, and calcareous levels (Leon, 1981, Vicente, 1981).

The Gramadal formation is characterized by ~80 m limestone with occasional sandstone bars. The presence of *Virgatophinctes* sp. (Chávez, 1982) and *Aulacosphictoides* sp. (Batty, 1992), suggest a Tithonian age for this formation (Alvan et al., 2018).

The Hualhuani formation is conform by 70 m of sandstone, with cross lamination, in this formation no macrofauna data were found, their age was defined based on their stratigraphic position (Vicente et al., 1979).

The Murco formation is overlying conformably the Gramadal formation. It is characterized by red shales at its base and coarse sandstones at its top (Benavides, 1962). The Arcurquina formation is made up of 800m of limestones deposited by the Albian-Turonian transgressions (Megard, 1967) . The Chilcane Formation consist of red shales with common evaporites intercalations.

4.2.2 Potential Sources

Potential sources of the Jurassic – Cretaceous sedimentary rocks can be divided in western sources (Coastal Cordillera) and eastern sources (Eastern Cordillera and Brazilian shield, Fig. 3).

The coastal cordillera (Fig. 3), is composed of Arequipa-Antofalla basement, Paleozoic sediments of Yamayo group, Famatinian arc and volcanic and volcano-sedimentary units of Jurassic magmatic arc (Fig. 3). The Arequipa-Antofalla basement have Paleoproterozoic ages between (1.8 - 2.1 Ga), Grenville-Sunsás ages between (1.08 - 0.94 Ga). Its TDM ages range between 2.2 to 1.9 Ga and $\Sigma\text{Nd}(0)$ values between -33.2 to -17.9 (Loewy et al., 2004; Wörner et al., 2000; Casquet et al., 2010). Magmatism Famatinian arc associated with yield ages between 470 – 440 Ma (Loewy et al., 2004; Chew et al., 2007; Wröner et al., 2000) with TDM age 1.8 Ga and $\Sigma\text{Nd}(0)$ value -15.78 (Loewy et al., 2004).

The ages above exposed was recognized in the offshore basement too, this indicate the continuity of these rocks in offshore area to the central Peru (cf. Romero et al., 2013). The sedimentary rocks of Yamayo Group (Bellido and Guevara, 1963; Boekhout et al., 2013) is established as all rocks that overlaying the Arequipa Antofalla Basement by erosional discordance or normal faults and underwent the Chocolate Formation (Boekhout et al., 2013), and using all ages of the Paleozoic rocks have the same peak of the Arequipa-Antofalla Basement (2.1 , 1.8, 0.9 and 0.4 Ga), this indicates that the Paleozoic sedimentary rocks that are outcropping in the Costal Cordillera area, have mainly source from the Arequipa basement (Reimann et al., 2010).

The eastern cordillera is composed by the Marañon complex in Central Peru; in the other hand, Paleozoic and Triassic sedimentary rocks occurs in southern Peru. (Fig 3).

The Marañon Complex is composed by Paleozoic metasedimentary rocks, that are affected by Ordovician, Permian and Triassic intrusions (Cardona et al., 2006; Chew et al., 2007, 2008; Miscovic et al., 2009; Chew et al., 2016). Chew et al., (2007), demonstrate that a lot of rocks in Marañon complex show two principal detrital zircon populations age, 0.5 – 0.7 Ga and 0.9 – 1.2 Ga, where the source of Neoproterozoic ages is possible a magmatic arc that was formed in SW Amazonia border and are buried under Eastern cordillera. This area its possible was possible exhumed at 250 Ma (Chew et al., 2016; Ramos et al., 2018).

To the south, the eastern cordillera is conformed by ~1500m of Paleozoic sedimentary rocks (Reimman et al., 2010), Triassic Mitu rift (Spikings et al., 2016) and Permo-Triassic intrusions (Clark et al., 1900; Kontak et al., 1985; Sempere et al., 2002; Miscovic et al., 2009), and Jurassic volcanic rock Allincapac complex (Miscovic et al., 2009) (Fig 3). This complex is composed of intrusive and extrusive rocks with alkaline-peralkaline affinities of Jurassic age (175 Ma, 156 Ma, K-Ar method, Kontak et al., 1990). According to its composition and isotope signature of Sr(i), it is argued that these rocks come from a mantle source (Kontak et al., 1990). The Ordovician sedimentary rocks of Sandia and Amutara formations (Reimman et al., 2010), have dominant zircon ages of Pampean/Brazilian ages (0.5-0.7, ~45%) and grenvillian ages (0.9-1.2 Ga, ~10%), and Permian magmatism ages (Boekhout et al., 2018), similar to the zircon age distribution of the Marañon Complex.

4.3 SAMPLING AND ANALITICAL METHODS

4.3.1 Sm – Nd isotopes:

Sm–Nd isotopic analyses followed the method described by Gioia and Pimentel (2000) and were carried out at the Geochronology Laboratory of the University of Brasília. Whole-rock powders (~ 50 mg) of 42 representative samples were mixed with ^{149}Sm – ^{150}Nd spike solution and dissolved in Savillex beckers. Sm and Nd extraction of whole-rock samples followed conventional cation exchange chromatography techniques, with Teflon columns containing LN-Spec resin (HDEHP – diethylhexil phosphoric acid

supported on PTFE powder). Sm and Nd samples were loaded on Re evaporation filaments of double filament assemblies, and the isotopic measurements were carried out on a multicollector TRITON thermal ionization mass spectrometer in static mode. Uncertainties of Sm/Nd and $^{143}\text{Nd}/^{144}\text{Nd}$ ratios were better than $\pm 0.1\%$ (2 Standard Error) and $\pm 0.0015\%$ (1σ), respectively, according to repeated analyses of international rock standards BHVO-1. $^{143}\text{Nd}/^{144}\text{Nd}$ ratios were normalized to $^{146}\text{Nd}/^{144}\text{Nd} = 0.7219$, and the decay constant used was (σ) 6.54×10^{-12} . The T_{DM} values were calculated using DePaolo (1981) model.

4.3.2 U-Pb isotopes:

Zircon concentrates were extracted from 7 kg rock samples by panning at different sizes (50 - 400 μm) and magnetic separation using a Frantz isodynamic separator. After separation, the grains were placed on epoxy mounts, polished to approximately half thickness, and characterized by back-scattered electron and cathodoluminescence imaging using a JEOL QUANTA 450 scanning electron microscope at the Laboratory of Geochronology of Brasilia University. The images provided the basis for selecting locations for laser ablation analysis. The mounts were cleaned with 3% nitric acid before analysis.

U-Pb isotopic analyses were performed on zircon grains using a Thermo-Fisher Neptune HR-MC-ICP-MS coupled with a Nd:YAG UP213 New Wave laser ablation system, also at the Laboratory of Geochronology of the University of Brasilia. The U-Pb analyses on zircon grains were carried out by the standard-sample bracketing method (Albarède et al., 2004) using the GJ-1 standard zircon (Jackson et al., 2004) in order to quantify the amount of ICP-MS fractionation. The tuned masses were 238, 207, 206, 204 and 202. The integration time was 1 second and the ablation time was 40 second. A 30 μm spot size was used and the laser setting was 10 Hz and 2-3 J/cm². Two to four unknown grains were analyzed between GJ-1 analyses. $^{206}\text{Pb}/^{207}\text{Pb}$ and $^{206}\text{Pb}/^{238}\text{U}$ ratios were time corrected. The raw data were processed off-line and reduced using an Excel worksheet (Bühn et al., 2009). During the analytical sessions the zircon standard 91500 (Jackson et al., 2004) was also analyzed as an external standard.

Common ^{204}Pb was monitored using the ^{202}Hg and ($^{204}\text{Hg} + ^{204}\text{Pb}$) masses. Common Pb corrections were not done due to very low signals for ^{204}Pb (< 30 cps) and high $^{206}\text{Pb}/^{204}\text{Pb}$ ratios. Reported errors are propagated by quadratic addition

$[(2SD_2+2SE_2)/2]$ (SD = standard deviation; SE = standard error) of external reproducibility and within-run precision. External reproducibility is represented by the standard deviation obtained from repeated analyses ($n=20$, ~1.1 % for $^{207}\text{Pb}/^{206}\text{Pb}$ and up to ~2 % for $^{206}\text{Pb}/^{238}\text{U}$) of the GJ-1 zircon standard during the analytical sessions, and the within-run precision is the standard error calculated for each analyses. Concordia diagrams (2σ error ellipses), probability density plots and weighted average ages were calculated using the Isoplot-3/Ex software (Ludwig, 2008). The distribution of ages was using the criteria $6/8 < 1\text{ Ga}$ was used the ratio 6/8 and $6/8 > 1\text{ Ga}$ was used the ratio 7/6 (Nemchin & Cawood, 2005).

4.4 RESULTS

Table 1 and Fig. 4 present the Sr-Nd isotope data for sedimentary rocks sampled from the Jurassic to Upper Cretaceous interval. The data show slight increase in $^{87}\text{Sr}/^{86}\text{Sr}$ ratios in Lower Cretaceous compared to the Middle-Upper Jurassic and Upper Cretaceous intervals. While the Sr isotope ratios for the Middle-Upper Jurassic and early Upper Cretaceous ratios range between 0.70796 to 0.7318 (mean ~0.71675), the late Upper Jurassic ratios range between 0.71337 to 0.72158 (mean ~0.71733). thus, indicating a slightly radiogenic source. The Lower Cretaceous show slightly radiogenic sources. The Upper Cretaceous the Sr isotope ratios decrease in the Sr isotope ratios indicating input of less radiogenic sources.

The Nd data show major isotopic shift around the Upper Jurassic- Lower Cretaceous and the Upper Cretaceous boundary. The Nd data in Jurassic is slightly irregular varying between -12.0 to -7.5. The lower Cretaceous Nd data show old sources $\epsilon_{\text{Nd}(0)} = -11.9$ (Murco Formation), and upper Cretaceous show input from more radiogenic sources $\epsilon_{\text{Nd}(0)} = -5.35$ (Chilcane formation).

Fig. 6 and Table 3 present the U-Pb age spectrum of zircon ages obtained of 10 sandstone samples, from the Middle Jurassic to Upper Cretaceous sedimentary rocks of Arequipa Basin. This data allows us to separate the results into three main groups. The first group present a bimodal age distribution, it is represented by (ARE304, 312, 305, 339). The main populations are Neoproterozoic and Grenville-Sunsas ages. The main population occurs at 0.5 – 0.7 Ga (27.4 – 35.9 %) and 0.9 – 1.3 Ga (23.1% - 38.1%). The second group present unimodal age distribution, it is represented by (ARE 14, 16, 17), mainly population are Neoproterozoic ages 0.5 – 0.7 Ga (34.5 – 37.9 %), and minor

population occurs at 0.9-1.3 (18.4 – 20.8 %), 0.4 – 0.250 Ga (5.7 – 9.5%). The difference with the previous group, is the decrease of sediments of age Grenville - Sunsás. The third group is characterized by a mixed source (ARE332). In this group is characterized by presence of Paleo-Mesoproterozoic, Neoproterozoic and arc ages. The population ages <130 Ma (7.7%), 216 -130 Ma (6.9%), 2.0-1.82 Ga (15.4%), 1.82 – 1.54 Ga (12.3%), 1.3 – 0.9 Ga (22.3%), 0.5 – 0.7 Ga (13.1%). The fourth group is represented by Proterozoic ages (0.5 - 2.0 Ga), it is represented by (ARE 306, 367), where is important the presence of old ages, with peaks of 2.0, 1.6, 1.3, 0.9 Ga

5. DISCUSIONS:

5.1. Interpretation of provenance

The $^{87}\text{Sr}/^{86}\text{Sr}$ vs $\xi\text{Nd}_{(0)}$ isotopes show that the Chilcane Formation have the same isotopic signature that the Chilcane formation, similar to isotopic signature of Central Depression, it is directly influence by volcanic source (Fig. 6). In other hand Middle Jurassic, have similar Sr-Nd isotopic signature of Altiplano sediments (Pinto et al., 2013). It is interpreted as a mixing between the Paleozoic rocks and Permian-Triassic intrusive rocks (Gondwanide magmatism), present in the Eastern cordillera and the erosion Jurassic peralkaline rocks reported by Miscovic et al., 2009, (Fig 5). In the case of Lower cretaceous (Murco formation) the isotopic signature, it is interpreted as old sources mixing with a subordinate volcanic source because show poor Permian-Triassic ages.

The initial ideas about the origin of the sediments of the Middle Jurassic (Puente and Cachios formations), it was interpreted as their sediments came from the Jurassic magmatic arc (to the west of the basin) coeval with the sedimentation of the Arequipa basin (Vicente et al., 1981, Chavez et al., 1981, Leon., et al., 1981; Vicente et al., 2005).

Our analyzes carried out in these units (Puente and Cachios formations), show us the absence of zircons from the coeval Jurassic arc of the time (See Fig 5, Table S1 to S4). This observation is also reported by Wolzlav et al., (2009) in the Jurassic rocks of the Livilcar Formation (Northern Chile), where there are not zircons from the coeval magmatic arc.

Different hypothesis was created about the non-generation of zircons by the Jurassic Magmatic Arc, however, Boekhout et al., (2012) reported zircons coming from the magmatic arc for the lower part of Puente formation around Chala village (near the Costa, to north-west of Arequipa city) on the Coastal Cordillera area.

The most important populations in Middle Jurassic (Puente and Cachios Formation) in Arequipa area have populations between 0.5 – 0.7 Ga and 0.9 – 1.3 Ga and 0.4 – 0.250 Ga, and these ages are characteristic of the Eastern Cordillera (Perez et al., 2014; Reitsman et al., 2010; Miscovic et al., 2009; Chew et al., 2007; 2008). These ages could be associated with the Eastern Cordillera (Perez et al., 2016, Sempere et al., 2002), as a possible like a horts that could have contributed sediment to the Arequipa basin.

The Labra Formation is dominantly formed by Brazilian ages 0.5 – 0.7 Ga, and in minor proportion conformed by Grenville Sunsás ages 0.9 – 1.0 Ga and is the first unit that presents zircons from the magmatic arc ($n = 2$) that is not enough proof to say that they come from the Chocolate arc, this source until is subordinate. The more negative values of $\xi_{\text{Nd}(0)}$ to the top is concordant with the increasing the Brazilian ages. Is important to note the reduction of Permo-Triasic ages, as mentioned above, it is diagnostic of sources of the eastern cordillera (Perez et al., 2014, 2016), is possible to associate this event to onset of the Jurua Orogeny (Upper Jurassic, Caputo et al., 2014), that produce the uplift of basement structures for the eastern sources. It is support because most important peak 0.51 Ga is more linked to the peaks of Sierras Pampeanas basin in northern Argentina (0.56-0.52 Ga; Rapela et al., 1998)

This event (Jurura orogeny) is more clear reflect in the age distribution of the Gramadal Formation (Fig 5), where a strong shift of source occurs with the increasing the of Paleoproterozoic, Mesoproterozoic and Neoproterozoic ages with the peak of ages 0.241, 0.6, 1.6, 2.0 Ga and that only are present in the Brazilian Shield (e.g. Rondonia San Ignacio, Rio Negro Juruena), but the Sr/Sr and $\xi_{\text{Nd}(0)}$ isotopes not reflect the cratonic sources, it is possible because the isotopic signature may be altered by the increasing of Permo-Triassic ages (it is probable another permo-triassic record towards the Brazilian shield?, until unknow) and the transgression processes that was register in this unit of Titonian age (Vicente et al., 1981; Sempere et al., 2002; Alvan et al., 2018), the origin of old sources is supported by Nd crustal ages where T_{DM} varies from 1.24 to 3.26 (average ~2.20), demonstrating this form the older sources. (Fig. 4, Table 3).

In the lower Cretaceous (Hualhuani Formation), a source with Brazilian ages (0.5 – 0.7 Ga) was established again, without Paleoproterozoic ages and a clear decrease of Grenville – Sunsás ages (0.9 – 1.3 Ga). In this unit the presence of detrital zircons from the Jurassic magmatic arc is recorded (peak of 153, 157 Ma in the top and base respectively, Fig 4), as a subordinate population. According the Neoproterozoic peaks (0.6-0.64 Ga) is possible the Araguaia -Paraguaia belt as a potential source, however, the lower Jurassic to Lower cretaceous is not present in Madre de Dios basin (Peru) or Alto Beni Basin (Bolivia) (Baby et al., 2018; Loutherbac et al., 2018. Sempere & Oller., 1995), it may be for erosion or not depositional processes, in this way it is possible that the sediments of this area may be was eroded and deposited in Arequipa Tarapacá Basin, together the uplift of Brazilian shield by the open South Atlantic Ocean. It is possible for these reason that sediments of the Lower cretaceous is very similar to Upper Jurassic but need more studies.

In the Murco Formation the Neoproterozoic and Grenville sources is reactivate again peaks between (0.540-0.620 Ga and 0.9-1.2 Ga), is clear the reduction of Permotriassic population that have directly influence in the $\xi_{Nd(0)}$ (more negative value, -11.94), that which indicates the entry of older sources (Fig 4). This populations are characteristic of Eastern Cordillera, which is linked as potential source.

The Upper cretaceous (Chilcane Formation) is beginning with strong change in provenance sedimentary in this area, because, this unit has important population of the volcanic arc and increasing of Paleoproterozoic (1.8-2.0 Ga), Mesoproterozoic (1.0 – 1.2Ga) and Neoproterozoic (0.55 Ga) and Famatianian ages (0.55Ga) ages (Fig 4). This ages are typical of the Arequipa-Antofalla Basement (Loewy et al., 2004, Casquet et al., 2010, Romero et al., 2013). Along with the Nd-Sr that is made much more positive evidencing an effectively volcanic source, however, the Neoproterozoic source is not reported in the Coastal area, this age is characteristic is of the Brazilian shield (Bahlburg et al., 2006; Perez and Horton, 2014; Ramos, 2010; Reimann et al., 2010). In this sense is possible for this time exist two potential sources, i) the area of the mountain range of the coast which contributes the sediments of ages of the Jurassic magmatic arc and eroding rocks of the Arequipa massif. ii) A source of Neoproterozoic ages of the SW margin of Amazonia (Hurtado et al., 2018; Nie et al., 2010). The exhumation of the coastal area may be associate to compressive Peruvian Phase, where is the change of the

extensive to compressive tectonic setting (Steimann et al., 1929; Jaillard, 1992), establishing in this form the onset of back-arc basin.

5.2. TECTONIC SETTING

The distribution of U-Pb ages in detrital zircons of the formations that conform the Arequipa basin, In the Middle Jurassic to Lower Cretaceous (Puente – Murco Formation), are not compatible with age spectra in typical back-arc basins. The back-arc basins have, as main population, contemporary zircons at the age of development of the concomitant magmatic arc (Cawood et al., 2012, Dickinson & Stern et al., 2016, Boekhout et al., 2017, Martinez et al., 2016). In the case of the units studied, this is not the case, on the contrary, the youngest ages are Permian-Triassic ages (Puente, Cachios and Gramadal Formation, Table 1). For the Upper Jurassic and Lower Cretaceous (Labra – Murco Formation, Table 1), the number of zircons coming possibly from the magmatic arc are very subordinate, showing that the sediments do not come directly from the this area, but from come from older source. In this sense, the tectonic setting were the Arequipa basin in south of Peru need to be re-defined.

The Weighted Average for Puente (ARE 304) is [257.2 ± 3.0 ; MSWD = 0.67; n=3] and Cachios Formation (ARE 305) is [256.1 ± 4.1 Ma; MSWD = 1.08; n=3], these ages are Permian, are not located in the Coastal Cordillera, their localization are only in the eastern Cordillera and are related to Gondwanide orogeny (Perez et al., 2016; Reitsma et al., 2012; Miscovic et al., 2009, Spikings et al., 2016). Then these youngest ages are not associated to jurassic magmatic arc, in the other hand, it is not an important population that allows us to infer the tectonic environment.

The top of Labra Formation (ARE 14), is the first sequence with one sin-sedimentary zircon (159 ± 2 Ma; n=1), this zircon age could be directly related to the concomitant volcanism, however, it shows again that the Jurassic magmatic arc is not a potential source of sediments for the Arequipa basin for this time. However, there is a subordinate contribution of this.

During the Lower Jurassic and Lower Cretaceous subduction in the Central Andes was developed under an extensional regime (Sempere et al., 2002, Pino et al., 2004, Ramos, 2018, references therein). This regime was controlled by the movement of the

continental plate (South America and Africa were still a single continent) to the east, associated with the negative roll-back processes produced a strong extension in the upper plate (Mpodozis & Ramos, 1989; 2009; 2018). The record of the roll-back processes is the migration of the jurassic magmatic arc towards the ocean. It was recorded in the Ilo Batholith (Demouy et al., 2012; Boekhout et al., 2012, 2015), together the heavy Mesozoic oceanic crust (Sdrolias et al., 2005), generated in this way, strong distension in the continental plate, where the accumulation of distensive stress can lead to the generation of a rift (Stern et al., 2002, Ingersoll & Busy, 2012). Under these extensional process during the Late Jurassic and Early Cretaceous was formed in the Salta Rift system, in North of Argentina and Western Bolivia (Ramos et al., 2009, References therein).

The presence of zircons from older sources (Fig. 4), the fluvial sedimentation environment recently proposed by Alvan et al., (2018), and the extended processes (Sempere et al., 2002; Ramos et al., 2018) is a characteristic of continental rift-type environments.

The generation of a passive continental rift is consistent with the age distribution of detrital zircons found in the Jurassic detrital zircons of the Arequipa basin, which are comparable to the established standards for rift type extensional basin established by Cawood et al., (2012) and Cawood and Nemchin, (2000).

6. CONCLUSIONS

-According to our U-Pb results in detrital zircons, we redefined the tectonic environment of the Arequipa basin on its typical-section in southern Peru, as a passive continental rift type basin developed from the Middle Jurassic to the Lower Cretaceous.

-The potential sources of the Middle Jurassic sedimentary rocks of Arequipa Basin are located in the Eastern Cordillera, as possible development horts and graven system where the Eastern Cordillera would be a horts, as an associated process with the extension related to Pangea break-up.

-The Upper Jurassic and the Lower Cretaceous the potential source are in (Brazilian shield) probably in Do Rio Guaporé Arch (Parecis Basin – Brazil), by the response of Sr- Nd isotopic signature and Nd crustal ages, revealing older sources, it that may be

correlative with de Enviar Arc in Amazon basin (Hurtado et al., 2018; Caputo et al., 2016).

The response of mixing of Nd-Sr isotopic signature for Middle Jurassic is possible some interaction with the basalt laves related to the CAMP (Central Atlantic Magmatic Province), or the Jurassic arc in the Easter cordillera reported by Miscovic et al., (2009).

-The upper cretaceous have two possible sources, the first is the Coastal Cordillera, with ages from the coeval arc (~100 Ma), correlative with Toquepala Arc (~91 Ma; Mamani et al., 2010), and peak ages of 1.8, 1.0, 0.4 Ga. In the other hand the second source with Neoproterozoic ages with peak of 0.5 Ga where the typical localization is un South Western of Amazonic Craton.

-The rift-type basin transform to back-arc basin during the beginning of the Cretaceous, where the arc area is associated with the Peruvian compressive phase (~100 Ma; Steimman et al., 1929).

The paleo-drainage for the Middle Jurassic to Early Cretaceous is apparently of the East to West of Gondwana, however, exist subordinate input of the Eastern source onwards.

Capítulo IV: Artigo

Table 1 Sm, Nd, Sr values of sedimentary units, and coordinates of localization.

Nº	Sample	Formation	Lithology	Coordinates		Sm (ppm)	Nd (ppm)	147Sm/144Nd	143Nd/Nd144	$\pm 2\sigma$	eNd	TDM	87Sr/Sr86	$\pm 2\sigma$
				Latitude	Longitude									
1	ARE 304	Puente	Sandstone	- 16.260406°	- 71.722301°	2.219	8.716	0.1539	0.51222	+/-13	-8.15	2.08		
2	ARE 308	Puente	Sandstone	- 16.259460°	- 71.719988°								0.71768	+/-1
3	ARE 309	Puente	Sandstone	- 16.257787°	- 71.719488°	2.979	9.468	0.1902	0.51225	+/-17	-7.57	-	0.71497	+/-2
4	ARE 309-A	Puente	Shale	- 16.257787°	- 71.719488°	3.682	27.271	0.0816	0.512194	+/-14	-8.66	-		
5	ARE 310	Puente	Sandstone	- 16.253852°	- 71.718574°								0.71473	+/-0
6	ARE 310-A	Puente	Shale	- 16.253852°	- 71.718574°	6.221	53.811	0.0699	0.512148	+/-12	-9.56	-		
7	ARE 311-A	Puente	Shale	- 16.249620°	- 71.719684°	5.147	26.606	0.1169	0.512183	+/-12	-8.87	1.34		
8	ARE 311	Puente	Sandstone	- 16.249620°	- 71.719684°	2.604	13.536	0.1163	0.512179	+/-8	-8.95	1.34	0.72157	+/-2
9	ARE 312	Puente	Sandstone	- 16.247378°	- 71.718410°	1.970	8.513	0.1399	0.512252	+/-7	-7.52	1.62	0.71568	+/-2
10	ARE 23	Puente	Sandstone	- 16.249516°	- 71.719356°	2.653	18.011	0.0890	0.51242	+/-10	-4.25	0.77	0.71892	+/-1
11	ARE 305	Cachios	Sandstone	- 16.245150°	- 71.716837°	2.080	8.154	0.1542	0.512239	+/-13	-7.79	2.04	0.71280	+/-1
12	ARE 306	Cachios	Sandstone	- 16.238506°	- 71.710183°	14.643	17.231	0.5137	0.512215	+/-6	-8.24	-	0.71403	+/-1
13	ARE 306-A	Cachios	Shale	- 16.238506°	- 71.710183°	7.263	37.703	0.1165	0.512235	+/-10	-7.87	1.26		
14	CH B	Cachios	Shale	- 16.247552°	- 71.719823°	7.457	43.175	0.1044	0.512217	+/-21	-8.21	1.15	0.72220	+/-3

Capítulo IV: Artigo

15	ARE 343	Cachios	Shale	- 16.243123°	- 71.719960°	7.134	36.160	0.1193	0.512138	+/-15	-9.76	1.45	0.71545	+/-1
16	ARE 342	Cachios	Shale	- 16.244662°	- 71.720383°	14.130	80.705	0.1058	0.512238	+/-2	-7.80	1.13	0.71666	+/-1
17	ARE 361	Cachios	Shale	- 16.247963°	- 71.719278°	7.940	34.016	0.1411	0.511746	+/-21	-17.40	2.73		
18	ARE 341	Cachios	Shale	- 16.245442°	- 71.720122°	7.625	39.136	0.1178	0.512216	+/-15	-8.24	1.30	0.71895	+/-3
19	ARE 307	Cachios	Sandstone	- 16.243875°	- 71.719823°	1.528	6.864	0.1346	0.512021	+/-17	-12.04	1.95	0.71470	+/-1
20	ARE373	Cachios	Shale	- 16.240095°	- 71.718712°	7.475	38.324	0.1179	0.512214	+/-8	-8.27	1.31	0.72165	+/-2
21	ARE 9	Labra	Sandstone	- 16.238376°	- 71.718286°	3.518	17.300	0.1229	0.512202	+/-11	-8.50	1.40	0.71539	+/-1
22	ARE 10	Labra	Sandstone	- 16.237884°	- 71.718429°	6.232	30.078	0.1252	0.512200	+/-2	-8.54	1.44	0.71514	+/-1
23	ARE 10A	Labra	Sandstone	- 16.237931°	- 71.718411°	2.909	13.218	0.1330	0.512181	+/-14	-8.91	1.61	0.71576	+/-3
24	ARE 10B	Labra	Sandstone	- 16.238031°	- 71.718412°	5.001	24.852	0.1216	0.512202	+/-10	-8.51	1.38	0.71657	+/-1
25	ARE 11	Labra	Sandstone	- 16.237832°	- 71.718428°	7.481	40.353	0.1121	0.512213	+/-4	-8.30	1.24	0.71594	+/-1
26	ARE 12	Labra	Sandstone	- 16.237766°	- 71.718643°	2.671	13.014	0.1241	0.512182	+/-8	-8.90	1.45	0.71586	+/-2
27	ARE 13	Labra	Sandstone	- 16.237690°	- 71.718903°	5.460	28.628	0.1153	0.512254	+/-4	-7.49	1.21	0.71458	+/-1
28	ARE 14	Labra	Sandstone	- 16.239065°	- 71.816240°	1.282	6.987	0.1109	0.512147	+/-10	-9.58	1.32	0.71286	+/-1
29	ARE 15	Labra	Sandstone	- 16.236944°	- 71.814125°								0.70796	+/-1
30	ARE 360	Labra	Sandstone	- 16.226974°	- 71.727029°	1.157	7.746	0.0903	0.512124	+/-8	-10.03	1.13	0.73186	+/-1
31	ARE 367	Gramadal	Sandstone	- 16.234595°	- 71.815522°								0.71337	+/-1

Capítulo IV: Artigo

32	ARE 346	Gramadal	Sandstone	- 16.234405°	- 71.815584°	1.446	5.078	0.1721	0.512175	+/-8	-9.03	3.26	0.7145	+/-2
33	ARE 344	Gramadal	Sandstone	- 16.234993°	- 71.815546°	1.410	5.415	0.1574	0.512265	+/-17	-7.28	2.09	0.71987	+/-3
34	ARE 345	Gramadal	Sandstone	- 16.234595°	- 71.815522°	52.637	292.62 7	0.1087	0.512182	+/-6	-8.90	1.24	0.72158	+/-4
35	ARE 16	Hualhuani	Sandstone	- 16.236000°	- 71.812410°	2.132	10.869	0.1186	0.512121	+/-3	-10.08	1.46	0.71079	+/-3
36	ARE 17	Hualhuani	Sandstone	- 16.235477°	- 71.811674°	0.464	1.987	0.1413	0.512167	+/-6	-9.19	1.83		
37	ARE 18	Hualhuani	Sandstone	- 16.234403°	- 71.812350°	0.631	3.364	0.1133	0.512179	+/-1	-8.96	1.30	0.71343	+/-1
38	ARE 340	Murco	Siltstone	- 16.154454°	- 71.835979°								0.70915	+/-2
39	ARE 339	Murco	Sandstone	- 16.148175°	- 71.832086°	1.968	5.116	0.2326	0.512026	+/-13	-11.94		0.70924	+/-1
40	ARE 338	Murco	Sandstone			0.630	5.762	0.0661	0.512279	+/-4	-7.01	0.79	0.70760	+/-1
41	ARE 332	Chilcane	Argilito	- 16.131963°	- 71.822017°	3.009	14.534	0.1251	0.512364	+/-16	-5.35	1.16	0.70786	+/-1

Capítulo IV: Artigo

Table 2: U-Pb percentages ages, by known orogenic event. Based on Reimann et al (2010), Chew et al., (2007), Hurtado et al (2018).

Time interval (Ga)*	Event	Puente Formation				Cachios Formation Paleo Chanel				Labra Formation		Gramadal Formation		Hualhuani Formation		Murco Formation		Chilcane Formation			
		ARE 304		ARE 312		ARE 305		ARE 306		ARE 14		ARE 367		ARE 16		ARE 17		ARE 339		ARE 332	
		n	%	n	%	n	%	n	%	n	%	n	%	n	%	n	%	n	%	n	%
<0.130	Andean arc	0	0.0	0	0.0	0	0.0	0	0.0	0	0.0	0	0.0	0	0.0	0	0.0	0	0.0	10	7.7
0.216- 0.130	Chocolate Arc & Jurassic Extension 216-132 Ma	0	0.0	0	0.0	0	0.0	0	0.0	2	1.9	0	0.0	3	3.4	4	4.8	2	1.5	9	6.9
0.250- 0.216	Triassic rift 250 - 216 Ma	1	0.9	0	0.0	0	0.0	1	1.5	1	0.9	2	2.8	3	3.4	3	3.6	0	0.0	1	0.8
0.4-0.25	Paleozoic Magmatic Arc	7	6.2	8.0	6.3	5.0	6.4	7.0	10.4	7.0	6.6	5.0	7.0	5.0	5.7	8.0	9.5	6.0	4.6	6.0	4.6
0.3-0.25	Permian magmatism 290 - 252 Ma	6	5.3	5	4.0	3	3.8	6	9.0	5	4.7	5	7.0	2	2.3	6	7.1	3	2.3	4	3.1
0.4-0.3	0.4-0.3	1	0.9	3	2.4	2	2.6	1	1.5	2	1.9	0	0.0	3	3.4	2	2.4	3	2.3	2	1.5
0.5-0.4	Famatinian	4	3.5	3	2.4	2	2.6	0	0.0	6	5.7	0	0.0	0	0.0	4	4.8	5	3.8	7	5.4
0.7-0.5	Brazilian/Pampean	31	27.4	44	34.9	28	35.9	20	29.9	38	35.8	8	11.3	33	37.9	29	34.5	40	30.5	17	13.1
0.9-0.7	0.7 - 0.9	7	6.2	7	5.6	7	9.0	5	7.5	10	9.4	6	8.5	8	9.2	5	6.0	7	5.3	6	4.6
1.3-0.9	Grenville - Sunsás	43	38.1	33	26.2	18	23.1	16	23.9	22	20.8	17	23.9	16	18.4	16	19.0	44	33.6	29	22.3
1.54-1.3	Rondonia - San Ignacio mobile belt	4	3.5	10	7.9	6	7.7	4	6.0	5	4.7	9	12.7	4	4.6	1	1.2	7	5.3	5	3.8
1.82- 1.54	Rio Negro - Juruena mobile belt	5	4.4	3	2.4	7	9.0	4	6.0	5	4.7	11	15.5	6	6.9	6	7.1	7	5.3	16	12.3
2.0-1.82	Ventuari-Tapajós (Trans- amazonian) mobile belt	3	2.7	7	5.6	3	3.8	6	9.0	4	3.8	4	5.6	1	1.1	4	4.8	4	3.1	20	15.4
2.2-2.0	Maroni - Itacaiúnas Province	6	5.3	6	4.8	1	1.3	3	4.5	4	3.8	6	8.5	3	3.4	1	1.2	4	3.1	3	2.3
>2.2	Central Amazonian province	2	1.8	5	4.0	1	1.3	1	1.5	2	1.9	3	4.2	5	5.7	3	3.6	5	3.8	1	0.8
		113	100	126	100	78	100	67	100	106	100	71	100	87	100	84	100	131	100	130	100

Table 3: Summary of U-Pb data, localization and major peaks.

Sample	Lithology	Coordinates		Number of concordant/total analyzed zircon	youngest zircon ages \pm 2STD (Ma)	Important age peaks
		Latitude	Longitude			
ARE 304	Sandstone	-16.260406°	-71.722301°	113/142	247 \pm 5	524, 580, 990, 1044
ARE 312	Sandstone	-16.247378°	-71.718410°	126/153	240 \pm 19	557, 603, 980, 1099
ARE 305	Sandstone	-16.245150°	-71.716837°	79/	253 \pm 6	511, 613, 1071
ARE 306	Sandstone	-16.238506°	-71.710183°	67/97	239 \pm 15	260, 547, 627, 1204, 1973
ARE 14	Sandstone	-16.239065°	-71.816240°	106/	159 \pm 2	514, 586, 640, 1057
ARE 367	Sandstone	-16.234595°	-71.815522°	71/135	240 \pm 6	241, 594, 748, 981, 1314, 1615, 2032
ARE 16	Sandstone	-16.236000°	-71.812410°	87/110	157 \pm 6	248, 598, 654, 1022
ARE 17	Sandstone	-16.235477°	-71.811674°	84/110	151 \pm 4	261, 634, 609, 990
ARE 339	Sandstone	-16.148175°	-71.832086°	131/155	137 \pm 7	536, 556, 627, 986, 1204
ARE 332	Siltstone	-16.131963°	-71.822017°	130	100 \pm 6	103, 146, 550, 1001, 1192, 1834

Figure captions:

Figure 1: Localization of the Jurassic basins in west margin of Western Gondwana to the east of Jurassic Magmatic Arc, and the localization and extension of the Arequipa-Tarapaca basin. B) The principal morphological structures in South of Peru and North of Chile. In red-dash is the limit of Arequipa – Tarapacá Basin. 1 is the paleo-high in limit north. In blue-dash and 2 is Mañaza-Lagunillas-Puno high. The abbreviation is CC: Coastal Cordillera, DC: Central Depression, WC: Western Cordillera, AT: Altiplano, EC: Eastern Cordillera, SAZ: Sub-Andean Zone, AZ: Amazon Zone. The maps is based on Jaillard & Santander, 1994; Sempere et al., 2002, 2004, Carlotto et al., 2009, Fernandez Lopez et al., 2014; Naipauer et al., 2015; Oliveros et al., 2012, Alvan et al., 2018.

Figure 2: Geological map, showing the different geological units in Yura area, the map shows the localization of the samples for U-Pb and Sr, Nd isotopes, the coordinates are in table 1. The source of the map is INGEMMET (Geological Survey of Peru) <http://geocatmin.ingemmet.gob.pe/geocatmin/>. The black boxes was the sampled area.

Figure 3: Map of the potential sources, the eastern cordillera represent mainly by the Paleozoic rocks and the intrusive rocks of the Eastern Cordillera, in the other hand the Coastal Cordillera with the rocks of the Arequipa Massif and the Ordovician magmatism. Map based on Ramos et al., 2008; Chew et al., 2007, 2008; Miscovic et al., 2009.

Figure 4: Stratigraphical section, showing the Yura Group (Jurassic Units) and the Cretaceous Units, with the stratigraphic localization of the samples for U-Pb and Sr-Nd isotopes. The columns in ξ Nd (o) and $^{87}\text{Sr}/^{86}\text{Sr}$ in vertical position for comparison with stratigraphic position for the comparison respect the others units.

Figure 5: Detrital zircon U-Pb age spectra: age probability (red-line) and the age histogram (white bars).

Figure 6: The Sr/Sr vs End(t) relation between the poles basaltic and crust sources, where was established Roddaz et al., (2005), based on Pinto et al., (2013), Barragan et al., (1988), Viers et al., (2008), plot our different results, the interpretations in text.

Figure 7: Evolution model of the Arequipa – Tarapacá Basin according the U-Pb ages.

Table list:

Table 1: Percentages of population the zircon detrital age in the different stratigraphic units.

Table 2: Nd-Sr isotopes results and the coordinates of the samples, the results od End(t) was recalculate t=170 Ma.

Table 3: Summary of detrital zircon data.

Table 4: Lu-Hf isotopes results.

Supplementary Data - ANEXO:

Table S1: U-Pb ages ARE304, Base of Puente Formation.

Table S2: U-Pb ages ARE312, Top of Puente Formation.

Table S3: U-Pb ages ARE305, Paleo channel of the base in Cachios Formation.

Table S4: U-Pb ages ARE306, Paleo channel in the top of Cachios Formation

Table S5: U-Pb ages ARE14, Top of the sequence, Labra Formation.

Table S6: U-Pb ages ARE367, Sandstone sequence in Gramadal Formation.

Table S7: U-Pb ages ARE16, Base of the Hualhuani Formation.

Table S8: U-Pb ages ARE17, Top of the Hualhuani Formation.

Table S9: U-Pb ages ARE339, Top of Murco Formation.

Table S10: U-Pb ages ARE332, siltstone of the Chilcane Formation.

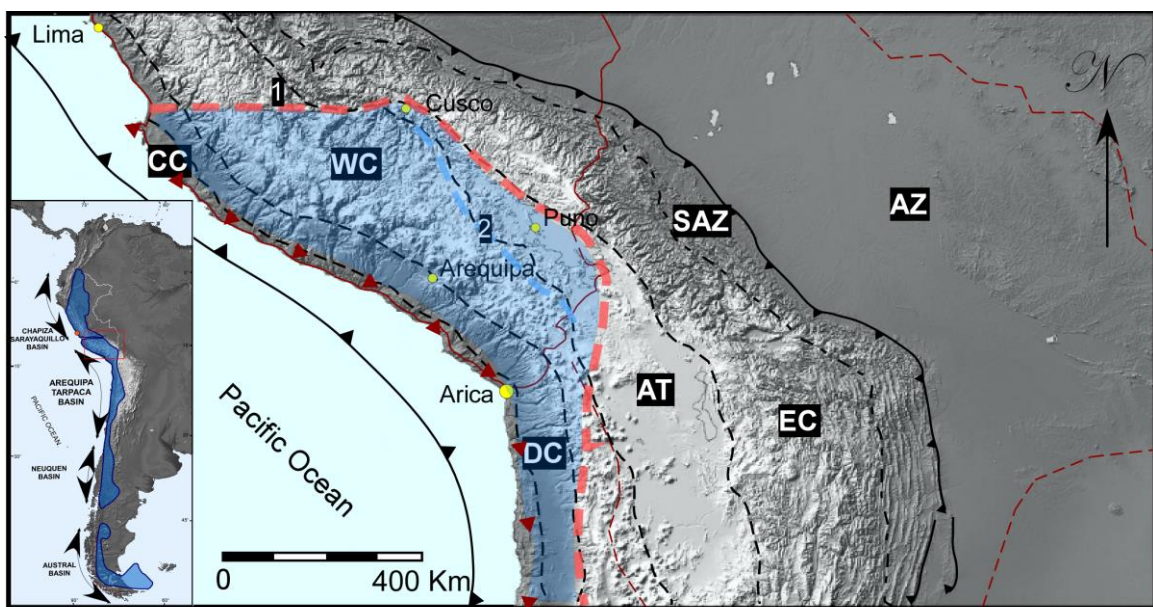


FIGURE 1

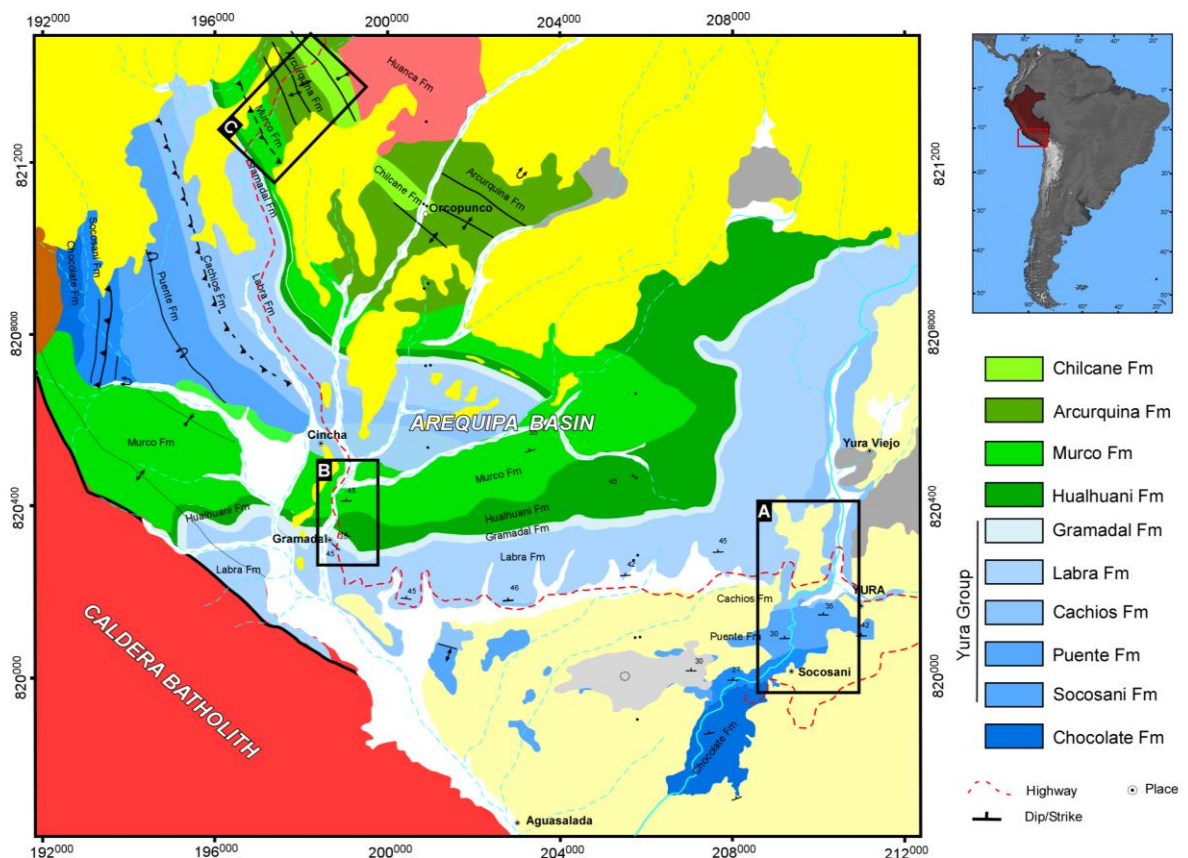


FIGURE 2

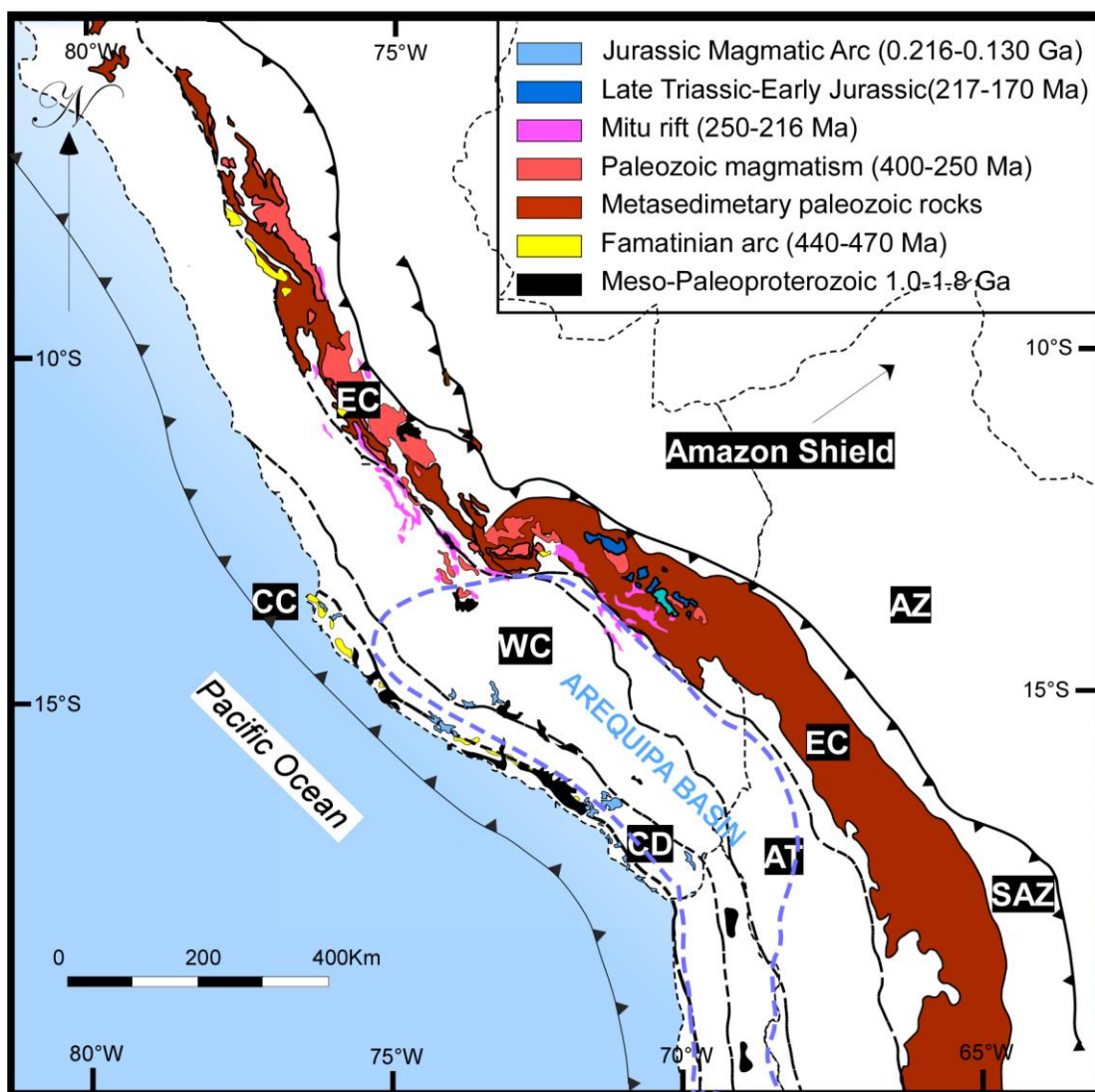


FIGURE 3

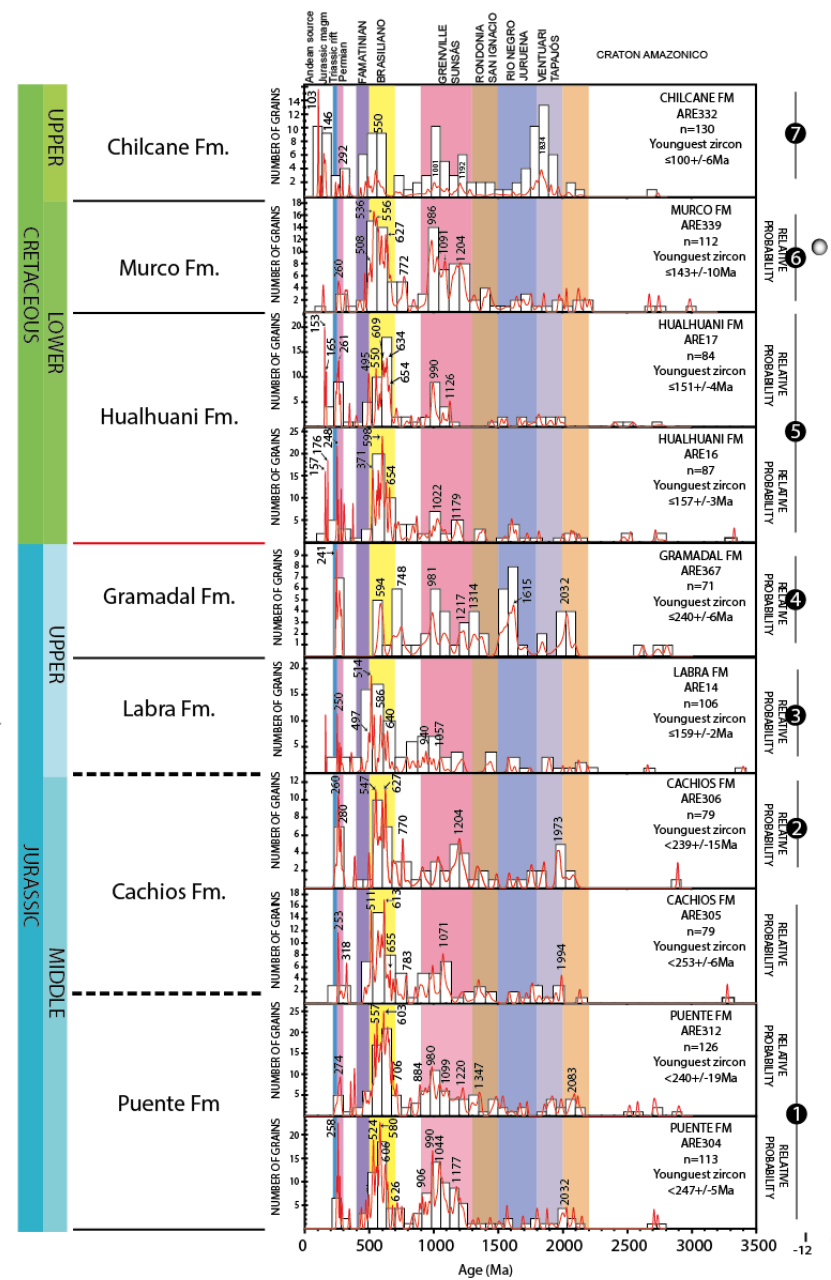


FIGURE 4

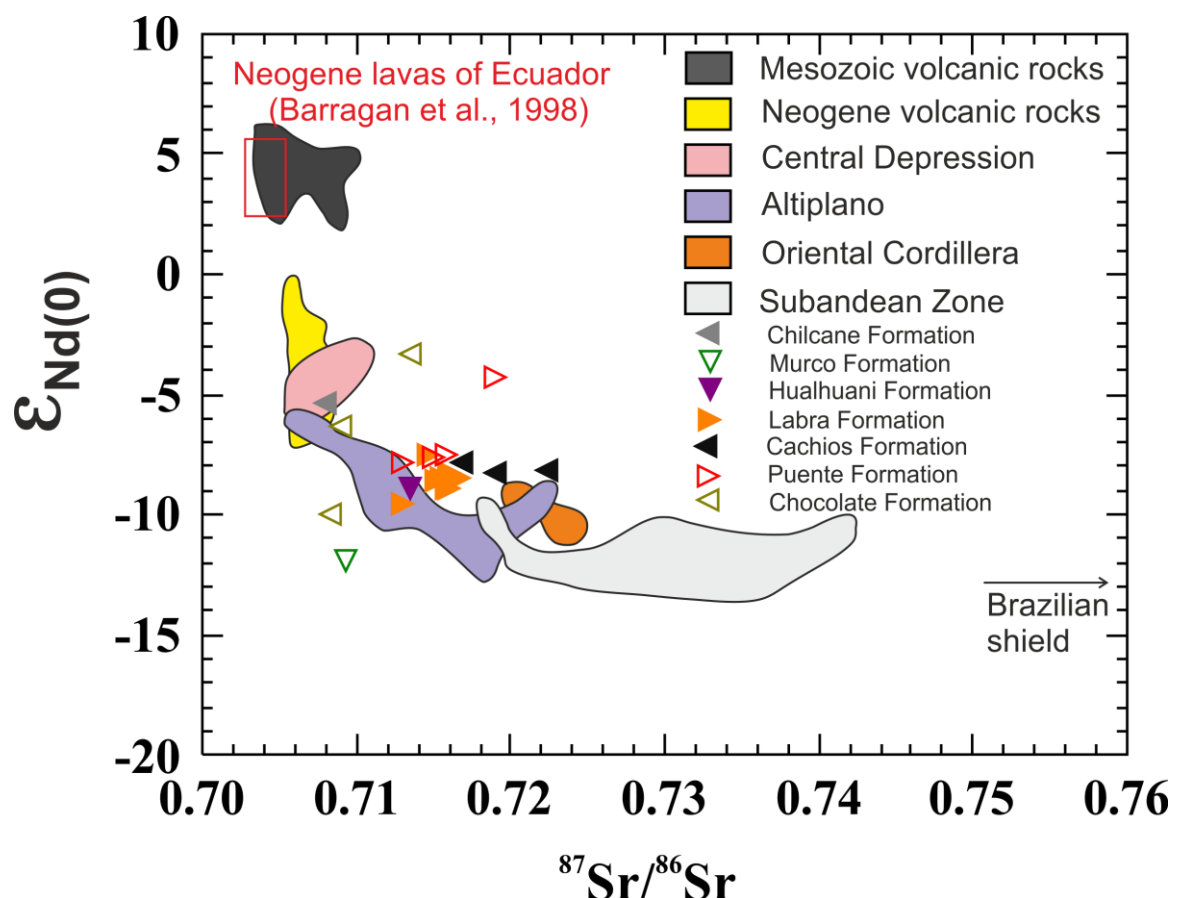


FIGURE 5

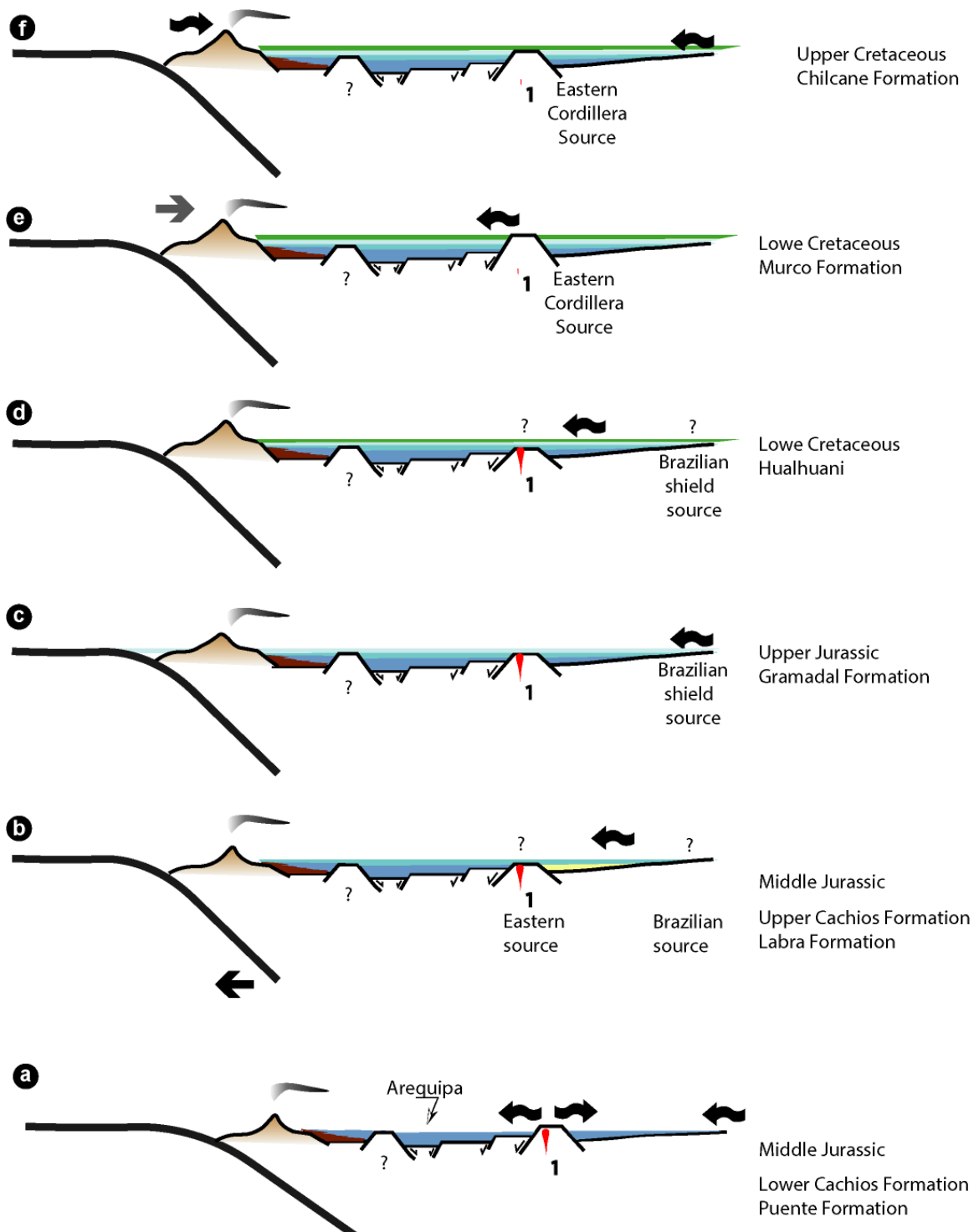


FIGURE 6

4.6 REFERENCES

- Acosta, H., Alvan, A., Hillebrandt, A., Riegraf, W., & Oviedo, M. (2009). nuevos aportes en la sedimentología y paleontología de las formaciones chocolate y socosani (jurásico inferior a medio) en el distrito de yura , arequipa (sur de perú). Sociedad Geológica Del Perú, Volumen Es, 63–77.
- Albarède, F., Telouk, S., Blichert-Toft, J., Boyet, M., Agranier, A., Nelson, B., 2004. Precise and accurate isotopic measurements using multiple-collector ICPMS. *Geochim. Cosmochim. Acta* 68, 2725–2744.
- Aleman, A., & Ramos, V. A. (2000). Northern Andes. Tectonic evolution of South America, 31, 453-480.
- Alván, A., Jacay, J., Caracciolo, L., Sánchez, E., & Trinidad, I. (2018). Sedimentary facies analysis of the Mesozoic clastic rocks in southern Peru (Tacna, 18°S): Towards a paleoenvironmental Re-definition and stratigraphic Re-organization. *Journal of South American Earth Sciences*. <https://doi.org/10.1016/j.jsames.2018.04.014>
- Arcay, D., Lallemand, S., & Doin, M. P. (2008). Back-arc strain in subduction zones: Statistical observations versus numerical modeling. *Geochemistry, Geophysics, Geosystems*, 9(5). <https://doi.org/10.1029/2007GC001875>
- Armijo, R., Lacassin, R., Coudurier-Curveur, A., & Carrizo, D. (2015). Coupled tectonic evolution of Andean orogeny and global climate. *Earth-Science Reviews*, 143, 1–35. <https://doi.org/10.1016/j.earscirev.2015.01.005>
- Aspden, J.A., and McCourt, W.J., 1986, Mesozoic oceanic terrane in the central Andes of Colombia: *Geology*, v. 14, p. 415–418, doi: 10.1130/0091-7613(1986)14<415:MOTITC>2.0.CO;2.
- Baby, P., Calderón, Y., Hurtado, C., Louterbach, M., Espurt, N., Brusset, S., Roddaz, M., Brichau, S., Eude, A., Calvès, G., Quispe, A., Ramirez, L., Bandach, A. and Bolaños, R., The Peruvian subandean foreland basin system: structural overview, geochronologic constraints, and unexplored plays, in *Petroleum Basins and Hydrocarbon Potential of the Andes of Peru and Bolivia*. AAPG Memoir 117, (accepted).
- Bahlburg, H., Carlotto, V., & Cárdenas, J. (2006). Evidence of Early to Middle Ordovician arc volcanism in the Cordillera Oriental and Altiplano of southern Peru, Ollantaytambo Formation and Umachiri beds. *Journal of South American Earth Sciences*, 22(1–2), 52–65. <https://doi.org/10.1016/j.jsames.2006.09.001>
- Bahlburg, H., Vervoort, J. D., Andrew DuFrane, S., Carlotto, V., Reimann, C., & Cárdenas, J. (2011). The U-Pb and Hf isotope evidence of detrital zircons of the Ordovician Ollantaytambo Formation, southern Peru, and the Ordovician provenance

and paleogeography of southern Peru and northern Bolivia. *Journal of South American Earth Sciences*, 32(3), 196–209. <https://doi.org/10.1016/j.jsames.2011.07.002>

Bahlburg, H., Vervoort, J. D., Du Frane, S. A., Bock, B., Augustsson, C., & Reimann, C. (2009). Timing of crust formation and recycling in accretionary orogens: Insights learned from the western margin of South America. *Earth-Science Reviews*, 97(1–4), 215–241. <https://doi.org/10.1016/j.earscirev.2009.10.006>

Batty, E. L. M., & Jaillard, E. (1989). La sedimentación neocomiana (Jurasico terminal-Aptiano) en el sur del Perú, (January), 1–15.

Bellido E. & Guevara C. (1963) Geología del Cuadrángulo de Punta de Bombón y la Clemesí. Comisión Carta Geológica Nacional. Boletín N° 5. p. 10-55

Benavides, V. (1962). Estratigrafía pre-Terciaria de la región de Arequipa. Boletín de la Sociedad geológica del Perú, 38, 5-63.

Boekhout, F., Reitsma, M. J., Spikings, R., Rodriguez, R., Ulianov, A., Gerdes, A., & Schaltegger, U. (2018). New age constraints on the palaeoenvironmental evolution of the late Paleozoic back-arc basin along the western Gondwana margin of southern Peru. *Journal of South American Earth Sciences*, 82, 165–180. <https://doi.org/10.1016/j.jsames.2017.12.016>

Boekhout, F., Sempere, T., Spikings, R., & Schaltegger, U. (2013). Late Paleozoic to Jurassic chronostratigraphy of coastal southern Peru: Temporal evolution of sedimentation along an active margin. *Journal of South American Earth Sciences*, 47, 179–200. <https://doi.org/10.1016/j.jsames.2013.07.003>

Boekhout, F., Spikings, R., Sempere, T., Chiaradia, M., Ulianov, A., & Schaltegger, U. (2012). Mesozoic arc magmatism along the southern Peruvian margin during Gondwana breakup and dispersal. *Lithos*, 146–147, 48–64. <https://doi.org/10.1016/j.lithos.2012.04.015>

Bühn, B., Pimentel, M.M., Matteini, M., Dantas, E.L., 2009. High spatial resolution analysis of Pb and U isotopes for geochronology by laser ablation multicollector inductively coupled plasma mass spectrometry (LA-MC-ICPMS). *Ann. Braz. Acad. Sci.* 81, 99-114.

Caputo, M. V. (2014). Juruá Orogeny: Brazil and Andean Countries. *Brazilian Journal of Geology*, 44(2), 181–190. <https://doi.org/10.5327/Z2317-4889201400020001>

Cardona, A., Cordani, U. G., Ruiz, J., Valencia, V. A., Armstrong, R., Chew, D., Sanchez, A. W. (2009). U-Pb Zircon Geochronology and Nd Isotopic Signatures of the Pre-Mesozoic Metamorphic Basement of the Eastern Peruvian Andes: Growth and Provenance of a Late Neoproterozoic to Carboniferous Accretionary Orogen on the Northwest Margin of Gondwana. *The Journal of Geology*, 117(3), 285–305. <https://doi.org/10.1086/597472>

- Carlotto, V., Cardenas, J. Baez, D., Rodriguez, R. (2008). Alto Estructural Totos-Paras (Ayacucho): Límite Paleogeográfico en la Evolución Mesozoica de las Cuencas de Arequipa y Pucará. XIII Congreso Latinoamericano de Geología, Lima, Perú.
- Casquet, C., Fanning, C. M., Galindo, C., Pankhurst, R. J., Rapela, C. W., & Torres, P. (2010). The Arequipa Massif of Peru: New SHRIMP and isotope constraints on a Paleoproterozoic inlier in the Grenvillian orogen. *Journal of South American Earth Sciences*, 29(1), 128–142. <https://doi.org/10.1016/j.jsames.2009.08.009>
- Cawood, P. A. (2005). Terra Australis Orogen: Rodinia breakup and development of the Pacific and Iapetus margins of Gondwana during the Neoproterozoic and Paleozoic. *Earth-Science Reviews*, 69(3–4), 249–279. <https://doi.org/10.1016/j.earscirev.2004.09.001>
- Cawood, P. A., & Nemchin, A. A. (2000). Provenance record of a rift basin: U/Pb ages of detrital zircons from the Perth Basin, Western Australia. *Sedimentary Geology*, 134(3–4), 209–234. [https://doi.org/10.1016/S0037-0738\(00\)00044-0](https://doi.org/10.1016/S0037-0738(00)00044-0)
- Cawood, P. A., Hawkesworth, C. J., & Dhuime, B. (2012). Detrital zircon record and tectonic setting. *Geology*, 40(10), 875–878. <https://doi.org/10.1130/G32945.1>
- Chen, H., Cooke, D. R., & Baker, M. J. (2013). Mesozoic iron oxide copper-gold mineralization in the Central Andes and the Gondwana supercontinent breakup. *Economic Geology*, 108(1), 37–44. <https://doi.org/10.2113/econgeo.108.1.37>
- Chew, D. M., Cardona, A., & Mišković, A. (2011). Tectonic evolution of western Amazonia from the assembly of Rodinia to its break-up. *International Geology Review*, 53(11–12), 1280–1296. <https://doi.org/10.1080/00206814.2010.527630>
- Chew, D. M., Magna, T., Kirkland, C. L., Miskovic, A., Cardona, A., Spikings, R., & Schaltegger, U. (2008). Detrital zircon fingerprint of the Proto-Andes: Evidence for a Neoproterozoic active margin? *Precambrian Research*, 167(1–2), 186–200. <https://doi.org/10.1016/j.precamres.2008.08.002>
- Chew, D. M., Pedemonte, G., & Corbett, E. (2016). Proto-Andean evolution of the Eastern Cordillera of Peru. *Gondwana Research*, 35(April 2018), 59–78. <https://doi.org/10.1016/j.gr.2016.03.016>
- Chew, D. M., Schaltegger, U., Košler, J., Whitehouse, M. J., Gutjahr, M., Spikings, R. A., & Mišković, A. (2007). U-Pb geochronologic evidence for the evolution of the Gondwanan margin of the north-central Andes. *Bulletin of the Geological Society of America*, 119(5–6), 697–711. <https://doi.org/10.1130/B26080.1>
- Clark, A.H., Farrar, E., Kontak, D.J., Langridge, R.J., Arenas, M.J., France, L.J., McBride, S.L., Woodman, P.L., Wasteneys, H.A., Sandeman, H.A., Douglas, D.A., 1990a. Geologic and geochronologic constraints on the metallogenic evolution of the Andes of southeastern Peru. *Economic Geology* 85, 1520–1583

- Coira, B., Davidson, J., Mpodozis, C., & Ramos, V. (1982). Tectonic and magmatic evolution of the Andes of northern Argentina and Chile. *Earth Science Reviews*, 18(3–4), 303–332. [https://doi.org/10.1016/0012-8252\(82\)90042-3](https://doi.org/10.1016/0012-8252(82)90042-3)
- Dantas, E. L., Alvarenga, C. J. S. de, Santos, R. V., & Pimentel, M. M. (2009). Using Nd isotopes to understand the provenance of sedimentary rocks from a continental margin to a foreland basin in the Neoproterozoic Paraguay Belt, Central Brazil. *Precambrian Research*, 170(1–2), 1–12. <https://doi.org/10.1016/j.precamres.2008.11.005>
- Del Rey, A., Deckart, K., Arriagada, C., & Martínez, F. (2016). Resolving the paradigm of the late Paleozoic–Triassic Chilean magmatism: Isotopic approach. *Gondwana Research*, 37, 172–181. <https://doi.org/10.1016/j.gr.2016.06.008>
- Demouy, S., Paquette, J. L., de Saint Blanquat, M., Benoit, M., Belousova, E. A., O'Reilly, S. Y., ... Sempere, T. (2012). Spatial and temporal evolution of Liassic to Paleocene arc activity in southern Peru unraveled by zircon U-Pb and Hf in-situ data on plutonic rocks. *Lithos*, 155, 183–200. <https://doi.org/10.1016/j.lithos.2012.09.001>
- DePaolo D. J., Linn A. M., Schubert, G. (1991). The Continental Crustal Age Distribution Methods of Determining Mantle Separation Ages From Sm-Nd Isotopic Data and Application to the Southwestern United States. *Journal of Geophysical Research*, 96, 2071–2088. <https://doi.org/http://dx.doi.org/10.1029/90JB02219>
- DePaolo D.J. (1981). Neodymium isotopes in the Colorado Front Range and crust - mantle evolution in the Proterozoic. *Nature*, 291, 193–196.
- Dickinson, W. R., & Gehrels, G. E. (2009). Use of U-Pb ages of detrital zircons to infer maximum depositional ages of strata: A test against a Colorado Plateau Mesozoic database. *Earth and Planetary Science Letters*, 288(1–2), 115–125. <https://doi.org/10.1016/j.epsl.2009.09.013>
- Fernandez-Lopez, S., Carlotto, V., Giraldo, E., & Chacaltana, C. (2014). Bajocian ammonoids from Pumani River area (Ayacucho, Peru): Palaeobiogeographical and palaeoenvironmental implications for the Arequipa Basin. *Journal of South American Earth Sciences*, 49, 51–62. <https://doi.org/10.1016/j.jsames.2013.11.003>
- Folguera, A., Contreras Reyes, E., Heredia, N., Encinas, A., Iannelli, S., Oliveros, V., Dávila, F., Collo, G., Giambiagi, L., Maksymowicz, A., Iglesia Llanos, P., Turienzo, M., Naipauer, M., Orts, D., M., Litvak, V., Alvarez, O., Arriagada, C. (2018). The making of the Chilean- Argentinean Andes, 1–579.
- Gioia, S.M.C.L. and Pimentel, M.M. (2000). The Sm-Nd isotopic method in the geochronology laboratory of the University of Brasília. *Academia Brasileira das Ciências*. vol.72, n.2, pp.219-245. ISSN 0001-3765. <http://dx.doi.org/10.1590/S0001-37652000000200009>.
- Grocott, J., & Taylor, G. K. (2002). Magmatic arc fault systems, deformation partitioning and emplacement of granitic complexes in the Coastal Cordillera, north

Chilean Andes (25° 30'S to 27° 00'S). *Journal of the Geological Society*, 159(4), 425–443. <https://doi.org/10.1144/0016-764901-124>

Hauser, N., Matteini, M., Omarini, R. H., & Pimentel, M. M. (2011). Combined U-Pb and Lu-Hf isotope data on turbidites of the Paleozoic basement of NW Argentina and petrology of associated igneous rocks: Implications for the tectonic evolution of western Gondwana between 560 and 460 Ma. *Gondwana Research*, 19(1), 100–127. <https://doi.org/10.1016/j.gr.2010.04.002>

Hawkesworth, C., Cawood, P., Kemp, T., Storey, C., and Dhuime, B., 2009, A Mater of Preservation: *Science*, v. 323, p. 49–50, doi:10.1126/science.1168549.

Heuret, A., & Lallemand, S. (2005). Plate motions, slab dynamics and back-arc deformation. *Physics of the Earth and Planetary Interiors*, 149(1–2 SPEC. ISS.), 31–51. <https://doi.org/10.1016/j.pepi.2004.08.022>

Horton, B. K., Saylor, J. E., Nie, J., Mora, A., Parra, M., Reyes-Harker, A., & Stockli, D. F. (2010). Linking sedimentation in the northern Andes to basement configuration, Mesozoic extension, and Cenozoic shortening: Evidence from detrital zircon U-Pb ages, Eastern Cordillera, Colombia. *Bulletin of the Geological Society of America*, 122(9–10), 1423–1442. <https://doi.org/10.1130/B30118.1>

Hurtado, C., Roddaz, M., Santos, R. V., Baby, P., Antoine, P., & Dantas, E. L. (2018). Late Cretaceous-early Paleocene drainage shift of Amazonian rivers driven by Equatorial Atlantic Ocean opening and Andean uplift as deduced from the provenance of northern Peruvian sedimentary rocks (Huallaga basin). *Gondwana Research*, <https://doi.org/10.1016/j.gr.2018.05.012>

Jackson, S.E., Pearson, N.J., Griffina, W.L., Belousova, E.A., 2004. The application of laser ablation-inductively coupled plasma-mass spectrometry to in situ U-Pb zircon geochronology. *Chem. Geol.* 211, 47–69.

Jaillard, E. (1995). La sedimentación albiana - tuironiana en el sur del Perú (Arequipa - punq - putina). *Sociedad Geológica Del Perú, Jubilar Al*, 135–157.

Jaillard, E., & Soler, P. (1996). Cretaceous to early Paleogene tectonic evolution of the northern Central Andes (0–18° S) and its relations to geodynamics. *Tectonophysics*, 259(1–3), 41–53.

Jaillard, E., Feist, M., Grambast-Fessard, N., Carlotto, V., 1994. Senonian–Paleocene charophyte succession of the Peruvian Andes. *Cretaceous Research* 15, 445–456.

Jaillard, E., Hérail, G., Monfret, T., Diaz-Martinez, E., Baby, P., Lavenu, A., & Dumont, J. F. (2000). Tectonic evolution of the Andes of Ecuador, Peru, Bolivia and Northernmost Chile. In *Tectonic evolution of South America* (Cordani, U.; Milani, E.; Thomaz Filho, A.; Campos; D.; editors). International Geological Congress : . Río de Janeiro., 31(January), 481–559.

- Jaillard, E., Ordoñez, M., Suárez, Johnny., Toro, J., Iza, D., Lugo, W. (2004). Stratigraphy of the late Cretaceous – Paleogene deposits of the Cordillera Occidental of Central Ecuador: geodynamic implications. *Journal South America Earth Sciences*, 17(1), 49-58.
- Jarrard, R. (1986). Relations among subduction parameters. *Reviews of Geophysics*, 24(2), 217-284. <https://doi.org/10.1029/RG024i002p00217>
- Jenks, W. F. (1948). Geology of the Arequipa quadrangle. *Boletin Instituto Geológico del Perú*, 9, 204.
- Kontak, D.J., Clark, A.H., Farrar, E., Strong, D.F., 1985. The rift associated Permo-Triassic magmatism of the Eastern Cordillera: a precursor to the Andean orogeny. In: Pitcher, W.S., Atherton, M.P., Cobbing, J., and Beckinsale R.D. (Eds.), *Magmatism at a plate edge: The Peruvian Andes*. Blackie, Glasgow, and Halsted Press, New York, pp. 36–44.
- Lamotte, D. F., Fourdan, B., Leleu, S., Lepamentier, F., & de Clarens, P. (2015). Style of rifting and the stages of Pangea breakup. *Tectonics*, 34(5), 1009-1029.
- León, I., 1981. Antecedentes sedimentológicos sobre el Jurásico-Cretácico inferior del sector de Yura (Departamento de Arequipa). Bachelor thesis. Universidad Nacional San Agustín, Perú, pp. 92.
- Litherland, M., Aspen, J.A., and Jemielita, R.A., 1994, The Metamorphic Belts of Ecuador: British Geological Survey Overseas Geology & Mineral Resources Memoir 11, 147 p.
- Loewy, S. L., Connelly, J. N., & Dalziel, I. W. D. (2004). An orphaned basement block: The Arequipa-Antofalla Basement of the central Andean margin of South America. *Bulletin of the Geological Society of America*, 116(1–2), 171–187. <https://doi.org/10.1130/B25226.1>
- López, C., Riquelme, R., Martínez, F., Sanchez, C., & Mestre, A. (2017). Zircon U-Pb geochronology of the mesozoic to lower Cenozoic rocks of the Coastal Cordillera in the Antofagasta region ($22^{\circ}30' - 23^{\circ}00'$ S): Insights to the Andean tectono-magmatic evolution. *Journal of South American Earth Sciences*. <https://doi.org/10.1016/j.jsames.2017.11.005>
- López, C., Riquelme, R., Martínez, F., Sanchez, C., & Mestre, A. (2017). Zircon U-Pb geochronology of the mesozoic to lower Cenozoic rocks of the Coastal Cordillera in the Antofagasta region ($22^{\circ}30' - 23^{\circ}00'$ S): Insights to the Andean tectono-magmatic evolution. *Journal of South American Earth Sciences*, (November). <https://doi.org/10.1016/j.jsames.2017.11.005>.
- Louterbach, M., Roddaz, M., Antoine, P. O., Marivaux, L., Adnet, S., Bailleul, J. Calderon, Y. (2018). Provenance record of late Maastrichtian–late Palaeocene Andean Mountain building in the Amazonian retroarc foreland basin (Madre de Dios basin, Peru). *Terra Nova*, 30(1), 17–23. <https://doi.org/10.1111/ter.12303>

- Ludwig, K. R. 2008. User's Manual for Isoplot 3.0. A geochronological Toolkit for Microsoft Excel. Berkeley Geochronology Center, 4(4), 76.
- Mamani, M., Wörner, G., & Sempere, T. (2010). Geochemical variations in igneous rocks of the Central Andean orocline (13°S to 18°S): Tracing crustal thickening and magma generation through time and space. *Bulletin of the Geological Society of America*, 122(1–2), 162–182. <https://doi.org/10.1130/B26538.1>
- McCourt, W.J., Aspden, J.A., and Brook, M., 1984, New geological and geochronological data from the Colombian Andes: Continental growth by multiple accretion: *Journal of the Geological Society of London*, v. 141, p. 831–845, doi: 10.1144/gsjgs.141.5.0831.
- McGroder, M. F., Lease, R. O., & Pearson, D. M. (2015). Along-strike variation in structural styles and hydrocarbon occurrences, Subandean fold-and-thrust belt and inner foreland, Colombia to Argentina. *Geological Society of America Memoirs*, 212, 79–113. [https://doi.org/10.1130/2015.1212\(05\)](https://doi.org/10.1130/2015.1212(05))
- McLennan, S. M., Hemming, S., McDaniel, D. K., & Hanson, G. N. (1993). Geochemical approaches to sedimentation, provenance, and tectonics.
- Mégard, F. (1979). Estudio geológico de los Andes del Perú Central (Doctoral dissertation, Instituto Geológico Minero y Metalúrgico).
- Mégard, F. (1984). The Andean orogenic period and its major structures in central and northern Peru. *Journal of the Geological Society*, 141(5), 893–900.
- Mišković, A., Spikings, R. A., Chew, D. M., Košler, J., Ulianov, A., & Schaltegger, U. (2009). Tectonomagmatic evolution of Western Amazonia: Geochemical characterization and zircon U-Pb geochronologic constraints from the Peruvian Eastern Cordilleran granitoids. *Bulletin of the Geological Society of America*, 121(9–10), 1298–1324. <https://doi.org/10.1130/B26488.1>
- Mukasa, S.B., 1986. Zircon U–Pb ages of superunits in the Coastal Batholith of Peru: implications for magmatic and tectonic processes. *Geological Society of America Bulletin* 97, 241–254.
- Naipauer, M., Tapia, F., Mescua, J., Farías, M., Pimentel, M. M., & Ramos, V. A. (2015). Detrital and volcanic zircon U-Pb ages from southern Mendoza (Argentina): An insight on the source regions in the northern part of the Neuquén Basin. *Journal of South American Earth Sciences*, 64, 434–451. <https://doi.org/10.1016/j.jsames.2015.09.013>
- Nakakuki, T., & Mura, E. (2013). Dynamics of slab rollback and induced back-arc basin formation. *Earth and Planetary Science Letters*, 361, 287–297. <https://doi.org/10.1016/j.epsl.2012.10.031>
- Nance, R. D., & Murphy, J. B. (2013). Origins of the supercontinent cycle. *Geoscience Frontiers*, 4(4), 439–448.

- Nance, R. D., Murphy, J. B., & Santosh, M. (2014). The supercontinent cycle: a retrospective essay. *Gondwana Research*, 25(1), 4-29.
- Nemchin, A.A., Cawood, P.A., 2005. Discordance of the U–Pb system in detrital zircons: implication for provenance studies of sedimentary rocks. *Sedimentary Geology* 182, 143–162.
- Newell, N.D., 1942. Lower Paleozoic pelecypods: Mytilacea. University of Kansas Publications 10 (2), 1e115.
- Nie, J., Horton, B. K., Saylor, J. E., Mora, A., Mange, M., Garzzone, C. N., ... Parra, M. (2012). Integrated provenance analysis of a convergent retroarc foreland system: U-Pb ages, heavy minerals, Nd isotopes, and sandstone compositions of the Middle Magdalena Valley basin, northern Andes, Colombia. *Earth-Science Reviews*, 110(1–4), 111–126. <https://doi.org/10.1016/j.earscirev.2011.11.002>
- Oliveros, V., Féraud, G., Aguirre, L., Fornari, M., & Morata, D. (2006). The Early Andean Magmatic Province (EAMP): 40 Ar / 39 Ar dating on Mesozoic volcanic and plutonic rocks from the Coastal Cordillera , northern Chile, 157, 311–330. <https://doi.org/10.1016/j.jvolgeores.2006.04.007>
- Oliveros, V., Labbé, M., Rossel, P., Charrier, R., & Encinas, A. (2012). Journal of South American Earth Sciences Late Jurassic paleogeographic evolution of the Andean back-arc basin : New constrains from the Lagunillas Formation , northern Chile (27 30 ' e 28 30 ' S). *Journal of South American Earth Sciences*, 37, 25–40. <https://doi.org/10.1016/j.jsames.2011.12.005>
- Pankhurst, R.J., Rapela, C.W., Fanning, C.M., and Márquez, M., 2006, Gondwanide continental collision and the origin of Patagonia: *Earth-Science Reviews*, v. 76, p. 235–257, doi: 10.1016/j.earscirev.2006.02.001.
- Perelló J.; Carlotto V.; (2003). Porphyry-Style Alteration and Mineralization of the Middle Eocene to Early Oligocene Andahuaylas-Yauri Belt , Cuzco Region , Peru, 98, 1575–1605.
- Perez, N. D., & Horton, B. K. (2014). Oligocene-miocene deformational and depositional history of the andean hinterland basin in the northern altiplano Plateau, Southern Peru. *Tectonics*, 33(9), 1819–1847. <https://doi.org/10.1002/2014TC003647>
- Perez, N. D., & Horton, B. K. (2014). Oligocene-miocene deformational and depositional history of the andean hinterland basin in the northern altiplano Plateau, Southern Peru. *Tectonics*, 33(9), 1819–1847. <https://doi.org/10.1002/2014TC003647>
- Perez, N. D., Horton, B. K., McQuarrie, N., Stübner, K., & Ehlers, T. A. (2016). Andean shortening, inversion and exhumation associated with thin- and thick-skinned deformation in southern Peru. *Geological Magazine*, 153(5–6), 1013–1041. <https://doi.org/10.1017/S0016756816000121>

- Pindell, J. L., & Tabbutt, K. D. (1995). Mesozoic-Cenozoic Andean paleogeography and regional controls on hydrocarbon systems.
- Pamparo, M. B., & Batty, E. L. M. (1994). First palynological data from the Lower Cretaceous of the Arequipa Basin, southern Peru (1, Zbl. Ge ed.). Stuttgart. Deutschland
- Ramos, V. A. (2008). The Basement of the Central Andes: The Arequipa and Related Terranes. Annual Review of Earth and Planetary Sciences, 36(1), 289–324. <https://doi.org/10.1146/annurev.earth.36.031207.124304>
- Ramos, V. A. (2009). Anatomy and global context of the Andes: Main geologic features and the Andean orogenic cycle. Geological Society of America Memoirs, 204(0), 31–65. [https://doi.org/10.1130/2009.1204\(02\)](https://doi.org/10.1130/2009.1204(02))
- Ramos, V. A. (2018). Tectonic Evolution of the Central Andes: From Terrane Accretion to Crustal Delamination, 1–34. <https://doi.org/10.1306/13622115M1172855>
- Ramos, V. A., & Mpodozis, C. (1989). The Andes of Chile and Argentina , in : Geology of the Andes and its Relation to Hydrocarbon and Mineral Resources, 11(December), 33.
- Rapela, C. W., Pankhurst, R. J., Casquet, C., Baldo, E., Saavedra, J., & Galindo, C. (1998). Early evolution of the Proto-Andean margin of South America. Geology, 26(8), 707-710.
- Reimann, C. R., Bahlburg, H., Carlotto, V., Boekhout, F., Berndt, J., & Lopez, S. (2015). Journal of South American Earth Sciences Multi-method provenance model for early Paleozoic sedimentary basins of southern Peru and northern Bolivia (13 e 18 S). Journal of South American Earth Sciences, 64, 94–115. <https://doi.org/10.1016/j.jsames.2015.08.013>
- Reimann, C. R., Bahlburg, H., Kooijman, E., Berndt, J., Gerdes, A., Carlotto, V., & López, S. (2010). Geodynamic evolution of the early Paleozoic Western Gondwana margin 14°S-17°S reflected by the detritus of the Devonian and Ordovician basins of southern Peru and northern Bolivia. Gondwana Research, 18(2–3), 370–384. <https://doi.org/10.1016/j.gr.2010.02.002>
- Reitsma, M. J. (2012). Reconstructing the Late Paleozoic - Early Mesozoic plutonic and sedimentary record of south-east Peru : Orphaned back-arcs along the western margin of Gondwana. <https://doi.org/10.13097/archive-ouverte/unige:23095>
- Roddaz, M., Viers, J., Brusset, S., Baby, P., & Héral, G. (2005). Sediment provenances and drainage evolution of the Neogene Amazonian foreland basin. Earth and Planetary Science Letters, 239(1–2), 57–78. <https://doi.org/10.1016/j.epsl.2005.08.007>
- Romero, D., Valencia, K., Alarcón, P., Peña, D., & Ramos, V. A. (2013). The offshore basement of Perú: Evidence for different igneous and metamorphic domains in the forearc. Journal of South American Earth Sciences, 42, 47–60. <https://doi.org/10.1016/j.jsames.2012.11.003>

- Romeuf, N., Aguirre L., Soler P., Féraud G., Jaillard E., Ruffet G. (1995). Middle Jurassic volcanism in the Northern and Central Andes. *Revista Geológica de Chile*, 22 (2). 245-259.
- Rossel, P., Oliveros, V., Ducea, M. N., Charrier, R., Scaillet, S., Retamal, L., & Figueroa, O. (2013). The Early Andean subduction system as an analog to island arcs: Evidence from across-arc geochemical variations in northern Chile. *Lithos*, 179, 211–230. <https://doi.org/10.1016/j.lithos.2013.08.014>
- Scherrenberg, A. F., Jacay, J., Holcombe, R. J., & Rosenbaum, G. (2012). Stratigraphic variations across the Marañón Fold-Thrust Belt, Peru: Implications for the basin architecture of the West Peruvian Trough. *Journal of South American Earth Sciences*, 38, 147–158. <https://doi.org/10.1016/j.jsames.2012.06.006>
- Scherrenberg, A. F., Kohn, B. P., Holcombe, R. J., & Rosenbaum, G. (2016). Thermotectonic history of the Marañón Fold–Thrust Belt, Peru: Insights into mineralisation in an evolving orogen. *Tectonophysics*, 667, 16–36. <https://doi.org/10.1016/j.tecto.2015.11.007>
- Sdrolias, M., & Müller, R. D. (2006). Controls on back-arc basin formation. *Geochemistry, Geophysics, Geosystems*, 7(4). <https://doi.org/10.1029/2005GC001090>
- Sdrolias, M., & Müller, R. D. (2006). Controls on back-arc basin formation. *Geochemistry, Geophysics, Geosystems*, 7(4). <https://doi.org/10.1029/2005GC001090>
- Sdrolias, M., & Müller, R. D. (2006). Controls on back-arc basin formation. *Geochemistry, Geophysics, Geosystems*, 7(4).
- Sempere, T., Carlier, G., Soler, P., Fornari, M., Carlotto, V., Jacay, J., ... Jiménez, N. (2002). Late Permian-Middle Jurassic lithospheric thinning in Peru and Bolivia, and its bearing on Andean-age tectonics. *Tectonophysics*, 345(1–4), 153–181. [https://doi.org/10.1016/S0040-1951\(01\)00211-6](https://doi.org/10.1016/S0040-1951(01)00211-6)
- Sempere, T., Carlier, G., Soler, P., Fornari, M., Carlotto, V., Jacay, J., Jiménez, N. (2002). Late Permian-Middle Jurassic lithospheric thinning in Peru and Bolivia, and its bearing on Andean-age tectonics. *Tectonophysics*, 345(1–4), 153–181. [https://doi.org/10.1016/S0040-1951\(01\)00211-6](https://doi.org/10.1016/S0040-1951(01)00211-6)
- Sempere, T., Oller, J., & Barrios, L. (1988). Evolución tectosedimentaria de Bolivia durante el Cretácico. In Congreso Geológico Chüeno, 5th, Santiago, Actas (Vol. 3, pp. 37-65).
- Spikings, R., Boekhout, F., & Chiaradia, M. (2016). Characterization of Triassic Rifting in Peru and implications for the early disassembly of western Pangaea, (April). <https://doi.org/10.1016/j.gr.2016.02.008>
- Spikings, R., Cochrane, R., Villagomez, D., Van der Lelij, R., Vallejo, C., Winkler, W., & Beate, B. (2015). The geological history of northwestern South America: From

Pangaea to the early collision of the Caribbean Large Igneous Province (290–75 Ma). *Gondwana Research*, 27(1), 95–139. <https://doi.org/10.1016/j.gr.2014.06.004>

Stern, R. J. (2002). Subduction zones. *Reviews of Geophysics*, 40(4). <https://doi.org/10.1029/2001RG000108>

Stern, R. J., & Dickinson, W. R. (2010). The Gulf of Mexico is a Jurassic backarc basin. *Geosphere*, 6(6), 739–754. <https://doi.org/10.1130/GES00585.1>

Vargas, L. (1970). Geología del cuadrángulo de Arequipa. República del Perú, Ministerio de Energía y Minas, Dirección General de Minería, Servicio de Geología y Minería.

Vicente, J. C. (1981). Elementos de la estratigrafía mesozóica sur-peruana. Cuencas sedimentarias del Jurásico y Cretácico de América del Sur, 1, 319–351.

Vicente, J. C., Beaudoin, B., Chávez, A., & León, I. (1982). La cuenca de Arequipa (Sur Perú) durante el Jurásico-Cretácico inferior. In 5to Congreso Latinoamericano de Geología, Buenos-Aires 1981 (Vol. 1, pp. 121–153).

Vicente, J.C., 2006. Dynamic paleogeography of the Jurassic Andean basin: pattern of regression and general considerations on main features. *Revista Asociación Geológica del Argentina*. 61, 408–437

Wotzlaw, F., Decou, A., Eynatten, H. Von, Wo, G., & Frei, D. (2011). Jurassic to Palaeogene tectono-magmatic evolution of northern Chile and adjacent Bolivia from detrital zircon U-Pb geochronology and heavy mineral provenance. <https://doi.org/10.1111/j.1365-3121.2011.01025.x>

Ziegler, P. A., & Cloetingh, S. (2004). Dynamic processes controlling evolution of rifted basins. *Earth-Science Reviews*, 64(1–2), 1–50. [https://doi.org/10.1016/S0012-8252\(03\)00041-](https://doi.org/10.1016/S0012-8252(03)00041-)

CAPITULO V

5. CONCLUSÃO

De acordo com os resultados obtidos do estudo da proveniência sedimentar das rochas da Bacia Arequipa, podemos concluir o seguinte:

A distribuição das idades dos grãos de zircão detritico do Mesojurássico indica como fontes principais as idades Grenville-Sunsás (1,3 - 0,9Ga), neoproterozoicas (0,7 a 0,5 Ga) e permianas. As potenciais fontes de rochas sedimentares do Arequipa, do Mesojurássico, estão localizadas na Cordilheira Oriental, como possíveis *horts* associados aos eventos de extensão que aconteceram no Jurássico, relacionados à quebra do Gondwana.

A distribuição de idades do Neojurássico e Eocretáceo sugere o arco do Rio Guaporé como a provável fonte relativa ao Escudo Brasileiro.

As assinaturas isotópicas de Nd e Sr e o TDM revelam fontes mais velhas relacionadas ao desenvolvimento do Arco de Envira Melhoria na bacia Amazônica (Hurtado et al, 2018; Caputo et al, 2016).

Duas possíveis fontes são conferidas às unidades do Neocretáceo. A primeira é a Cordilheira Costeira com idades do arco contemporâneo (~100 Ma) correlativo ao desenvolvimento do arco Toquepala (~91 Ma; Mamani et al, 2010); além de picos de 1,8, 1,0 e 0,4 Ga, que são características do Embasamento de Arequipa. Por outro lado, uma segunda fonte foi reconhecida, possui idade neoproterozoica (0,7 - 0,5Ga) e tem como área tipo o sudoeste do Cráton Amazônico e a Cordilheira Oriental.

Admite-se que a paleo-drenagem estabelecida desde o Mesojurássico até o Eocretáceo vai de leste para o oeste do Gondwana; porém, a partir do Neocretáceo a proveniência das fontes muda de oeste para leste, onde começam a aparecer as fontes do arco magmático concomitante (Arco Jurássico).

De acordo com as idades U-Pb em zircões detriticos e as evidências de um grande sistema de extensão, propomos uma redefinição do ambiente tectônico da bacia Arequipa, na seção sul do Peru, como uma bacia de tipo rifte continental passiva que se desenvolveu desde o Mesojurássico até o Eocretáceo.

REFERÊNCIAS BIBLIOGRÁFICAS

- Acosta, H., Alvan, A., Hillebrandt, A., Riegraf, W., & Oviedo, M. (2009). nuevos aportes en la sedimentología y paleontología de las formaciones chocolate y socosani (jurásico inferior a medio) en el distrito de yura , arequipa (sur de perú). Sociedad Geológica Del Perú, Volumen Es, 63–77.
- Albarède, F., Telouk, S., Blichert-Toft, J., Boyet, M., Agranier, A., Nelson, B., 2004. Precise and accurate isotopic measurements using multiple-collector ICPMS. *Geochim. Cosmochim. Acta* 68, 2725-2744.
- Aleman, A., & Ramos, V. A. (2000). Northern Andes. Tectonic evolution of South America, 31, 453-480.
- Alván, A., Jacay, J., Caracciolo, L., Sánchez, E., & Trinidad, I. (2018). Sedimentary facies analysis of the Mesozoic clastic rocks in southern Peru (Tacna, 18°S): Towards a paleoenvironmental Re-definition and stratigraphic Re-organization. *Journal of South American Earth Sciences*. <https://doi.org/10.1016/j.jsames.2018.04.014>
- Alván, A., von Eynatten, H., 2014. Sedimentary facies and stratigraphic architecture in coarse-grained deltas: Anatomy of the Cenozoic Camaná Formation, southern Peru (16°25'S to 17°15'S). *J. South Am. Earth Sci.* 54, 82–108. <https://doi.org/10.1016/j.jsames.2014.04.008>
- Arcay, D., Lallemand, S., & Doin, M. P. (2008). Back-arc strain in subduction zones: Statistical observations versus numerical modeling. *Geochemistry, Geophysics, Geosystems*, 9(5). <https://doi.org/10.1029/2007GC001875>
- Armijo, R., Lacassin, R., Coudurier-Curveur, A., & Carrizo, D. (2015). Coupled tectonic evolution of Andean orogeny and global climate. *Earth-Science Reviews*, 143, 1–35. <https://doi.org/10.1016/j.earscirev.2015.01.005>
- Aspden, J.A., and McCourt, W.J., 1986, Mesozoic oceanic terrane in the central Andes of Colombia: *Geology*, v. 14, p. 415–418, doi: 10.1130/0091-7613(1986)14<415:MOTITC>2.0.CO;2.
- Baby, P., Calderón, Y., Hurtado, C., Loutherbach, M., Espurt, N., Brusset, S., Roddaz, M., Brichau, S., Eude, A., Calvès, G., Quispe, A., Ramirez, L., Bandach, A. and Bolaños, R., The Peruvian subandean foreland basin system: structural overview, geochronologic constraints, and unexplored plays, in Petroleum Basins and Hydrocarbon Potential of the Andes of Peru and Bolivia. AAPG Memoir 117, (accepted).
- Bahlburg, H., Carlotto, V., & Cárdenas, J. (2006). Evidence of Early to Middle Ordovician arc volcanism in the Cordillera Oriental and Altiplano of southern Peru, Ollantaytambo Formation and Umachiri beds. *Journal of South American Earth Sciences*, 22(1–2), 52–65. <https://doi.org/10.1016/j.jsames.2006.09.001>
- Bahlburg, H., Vervoort, J. D., Andrew DuFrane, S., Carlotto, V., Reimann, C., & Cárdenas, J. (2011). The U-Pb and Hf isotope evidence of detrital zircons of the

Ordovician Ollantaytambo Formation, southern Peru, and the Ordovician provenance and paleogeography of southern Peru and northern Bolivia. *Journal of South American Earth Sciences*, 32(3), 196–209. <https://doi.org/10.1016/j.jsames.2011.07.002>

Bahlburg, H., Vervoort, J. D., Du Frane, S. A., Bock, B., Augustsson, C., & Reimann, C. (2009). Timing of crust formation and recycling in accretionary orogens: Insights learned from the western margin of South America. *Earth-Science Reviews*, 97(1–4), 215–241. <https://doi.org/10.1016/j.earscirev.2009.10.006>

Batty, E. L. M., & Jaillard, E. (1989). La sedimentación neocomiana (Jurasico terminalAptiano) en el sur del Peru, (January), 1–15.

Bellido E. & Guevara C. (1963) Geología del Cuadrángulo de Punta de Bombón y la Clemesí. Comisión Carta Geológica Nacional. Boletín N° 5. p. 10-55

Benavides, V. (1962). Estratigrafía pre-Terciaria de la región de Arequipa. Boletín de la Sociedad geológica del Perú, 38, 5-63.

Boekhout, F., Reitsma, M. J., Spikings, R., Rodriguez, R., Ulianov, A., Gerdes, A., & Schaltegger, U. (2018). New age constraints on the palaeoenvironmental evolution of the late Paleozoic back-arc basin along the western Gondwana margin of southern Peru. *Journal of South American Earth Sciences*, 82, 165–180. <https://doi.org/10.1016/j.jsames.2017.12.016>

Boekhout, F., Sempere, T., Spikings, R., & Schaltegger, U. (2013). Late Paleozoic to Jurassic chronostratigraphy of coastal southern Peru: Temporal evolution of sedimentation along an active margin. *Journal of South American Earth Sciences*, 47, 179–200. <https://doi.org/10.1016/j.jsames.2013.07.003>

Boekhout, F., Spikings, R., Sempere, T., Chiaradia, M., Ulianov, A., & Schaltegger, U. (2012). Mesozoic arc magmatism along the southern Peruvian margin during Gondwana breakup and dispersal. *Lithos*, 146–147, 48–64. <https://doi.org/10.1016/j.lithos.2012.04.015>

Bühn, B., Pimentel, M.M., Matteini, M., Dantas, E.L., 2009. High spatial resolution analysis of Pb and U isotopes for geochronology by laser ablation multicollector inductively coupled plasma mass spectrometry (LA-MC-ICPMS). *Ann. Braz. Acad. Sci.* 81, 99-114.

Caputo, M. V. (2014). Juruá Orogeny: Brazil and Andean Countries. *Brazilian Journal of Geology*, 44(2), 181–190. <https://doi.org/10.5327/Z2317-4889201400020001>

Cardona, A., Cordani, U. G., Ruiz, J., Valencia, V. A., Armstrong, R., Chew, D., ... Sanchez, A. W. (2009). U-Pb Zircon Geochronology and Nd Isotopic Signatures of the Pre-Mesozoic Metamorphic Basement of the Eastern Peruvian Andes: Growth and Provenance of a Late Neoproterozoic to Carboniferous Accretionary Orogen on the Northwest Margin of Gondwana. *The Journal of Geology*, 117(3), 285–305. <https://doi.org/10.1086/597472>

- Carlotto, V., Cardenas, J. Baez, D., Rodriguez, R. (2008). Alto Estructural Totos-Paras (Ayacucho): Límite Paleogeográfico en la Evolución Mesozoica de las Cuencas de Arequipa y Pucará. XIII Congreso Latinoamericano de Geología, Lima, Perú.
- Casquet, C., Fanning, C. M., Galindo, C., Pankhurst, R. J., Rapela, C. W., & Torres, P. (2010). The Arequipa Massif of Peru: New SHRIMP and isotope constraints on a Paleoproterozoic inlier in the Grenvillian orogen. *Journal of South American Earth Sciences*, 29(1), 128–142. <https://doi.org/10.1016/j.jsames.2009.08.009>
- Cawood, P. A. (2005). Terra Australis Orogen: Rodinia breakup and development of the Pacific and Iapetus margins of Gondwana during the Neoproterozoic and Paleozoic. *Earth-Science Reviews*, 69(3–4), 249–279. <https://doi.org/10.1016/j.earscirev.2004.09.001>
- Cawood, P. A., & Nemchin, A. A. (2000). Provenance record of a rift basin: U/Pb ages of detrital zircons from the Perth Basin, Western Australia. *Sedimentary Geology*, 134(3–4), 209–234. [https://doi.org/10.1016/S0037-0738\(00\)00044-0](https://doi.org/10.1016/S0037-0738(00)00044-0)
- Cawood, P. A., Hawkesworth, C. J., & Dhuime, B. (2012). Detrital zircon record and tectonic setting. *Geology*, 40(10), 875–878. <https://doi.org/10.1130/G32945.1>
- Chen, H., Cooke, D. R., & Baker, M. J. (2013). Mesozoic iron oxide copper-gold mineralization in the Central Andes and the Gondwana supercontinent breakup. *Economic Geology*, 108(1), 37–44. <https://doi.org/10.2113/econgeo.108.1.37>
- Chew, D. M., Cardona, A., & Mišković, A. (2011). Tectonic evolution of western Amazonia from the assembly of Rodinia to its break-up. *International Geology Review*, 53(11–12), 1280–1296. <https://doi.org/10.1080/00206814.2010.527630>
- Chew, D. M., Magna, T., Kirkland, C. L., Miskovic, A., Cardona, A., Spikings, R., & Schaltegger, U. (2008). Detrital zircon fingerprint of the Proto-Andes: Evidence for a
- Chew, D. M., Pedemonte, G., & Corbett, E. (2016). Proto-Andean evolution of the Eastern Cordillera of Peru. *Gondwana Research*, 35(April 2018), 59–78. <https://doi.org/10.1016/j.gr.2016.03.016>
- Chew, D. M., Schaltegger, U., Košler, J., Whitehouse, M. J., Gutjahr, M., Spikings, R. A., & Mišković, A. (2007). U-Pb geochronologic evidence for the evolution of the Gondwanan margin of the north-central Andes. *Bulletin of the Geological Society of America*, 119(5–6), 697–711. <https://doi.org/10.1130/B26080.1>
- Clark, A.H., Farrar, E., Kontak, D.J., Langridge, R.J., Arenas, M.J., France, L.J., McBride, S.L., Woodman, P.L., Wasteneys, H.A., Sandeman, H.A., Douglas, D.A., 1990a. Geologic and geochronologic constraints on the metallogenic evolution of the Andes of southeastern Peru. *Economic Geology* 85, 1520–1583
- Cobbing, E.J., Ozard, J.M., Snelling, N.J., 1977. Reconnaissance geochronology of the crystalline basement rocks of the Coastal Cordillera of southern Peru. *Bull. Geol. Soc. Am.* 88 (2), 241.

- Coira, B., Davidson, J., Mpodozis, C., & Ramos, V. (1982). Tectonic and magmatic evolution of the Andes of northern Argentina and Chile. *Earth Science Reviews*, 18(3–4), 303–332. [https://doi.org/10.1016/0012-8252\(82\)90042-3](https://doi.org/10.1016/0012-8252(82)90042-3)
- Dantas, E. L., Alvarenga, C. J. S. de, Santos, R. V., & Pimentel, M. M. (2009). Using Nd isotopes to understand the provenance of sedimentary rocks from a continental margin to a foreland basin in the Neoproterozoic Paraguay Belt, Central Brazil. *Precambrian Research*, 170(1–2), 1–12. <https://doi.org/10.1016/j.precamres.2008.11.005>
- Decou, A., von Eynatten, H., Dunkl, I., Frei, D., Wörner, G., 2013. Late Eocene to Early Miocene Andean uplift inferred from detrital zircon fission track and U–Pb dating of Cenozoic forearc sediments (15–18°S). *J. South Am. Earth Sci.* 45, 6–23. <https://doi.org/10.1016/j.jsames.2013.02.003>.
- Del Rey, A., Deckart, K., Arriagada, C., & Martínez, F. (2016). Resolving the paradigm of the late Paleozoic–Triassic Chilean magmatism: Isotopic approach. *Gondwana Research*, 37, 172–181. <https://doi.org/10.1016/j.gr.2016.06.008>
- Demouy, S., Paquette, J. L., de Saint Blanquat, M., Benoit, M., Belousova, E. A., O'Reilly, S. Y., ... Sempere, T. (2012). Spatial and temporal evolution of Liassic to Paleocene arc activity in southern Peru unraveled by zircon U-Pb and Hf in-situ data on plutonic rocks. *Lithos*, 155, 183–200. <https://doi.org/10.1016/j.lithos.2012.09.001>
- DePaolo D. J., Linn A. M., Schubert, G. (1991). The Continental Crustal Age Distribution Methods of Determining Mantle Separation Ages From Sm-Nd Isotopic Data and Application to the Southwestern United States. *Journal of Geophysical Research*, 96, 2071–2088. <https://doi.org/http://dx.doi.org/10.1029/90JB02219>
- DePaolo D.J. (1981). Neodymium isotopes in the Colorado Front Range and crust mantle evolution in the Proterozoic. *Nature*, 291, 193–196.
- Dickinson, W. R., & Gehrels, G. E. (2009). Use of U-Pb ages of detrital zircons to infer maximum depositional ages of strata: A test against a Colorado Plateau Mesozoic database. *Earth and Planetary Science Letters*, 288(1–2), 115–125. <https://doi.org/10.1016/j.epsl.2009.09.013>
- Espinoza, M., Montecino, D., Oliveros, V., Astudillo, N., Vásquez, P., Reyes, R., Celis, C., González, R., Contreras, J., Creixell, C., Martínez, A., 2018. The synrift phase of the early Domeyko Basin (Triassic, northern Chile): Sedimentary, volcanic, and tectonic interplay in the evolution of an ancient subduction-related rift basin. *Basin Res.* <https://doi.org/10.1111/bre.12305>.
- Fernandez-Lopez, S., Carlotto, V., Giraldo, E., & Chacaltana, C. (2014). Bajocian ammonoids from Pumani River area (Ayacucho, Peru): Palaeobiogeographical and palaeoenvironmental implications for the Arequipa Basin. *Journal of South American Earth Sciences*, 49, 51–62. <https://doi.org/10.1016/j.jsames.2013.11.003>

- Folguera, A., Contreras Reyes, E., Heredia, N., Encinas, A., Iannelli, S., Oliveros, V., Dávila, F., Collo, G., Giambiagi, L., Maksymowicz, A., Iglesia Llanos, P., Turienzo, M., Naipauer, M., Orts, D., M., Litvak, V., Alvarez, O., Arriagada, C. (2018). The making of the Chilean- Argentinean Andes, 1–579.
- Garcia, F., 1967. Geología del Norte Grande de Chile. Simp. Geosincl., Andino, 1962. Soc.GeoL Chile Publ., 3:138 pp.
- Gioia, S.M.C. L., Pimentel, M.M., 2000. The Sm-Nd isotopic method in the Geochronology Laboratory of the University of Brasília. Anais Academia Brasileira de Ciências 72, 219-245.
- Grocott, J., & Taylor, G. K. (2002). Magmatic arc fault systems, deformation partitioning and emplacement of granitic complexes in the Coastal Cordillera, north Chilean Andes (25°30'S to 27°00'S). Journal of the Geological Society, 159(4), 425–443. <https://doi.org/10.1144/0016-764901-124>
- Haschke, M., Günther, A., Melnick, D., Echtler, H., Reutter, K. J., Scheuber, E., & Oncken, O. (2006). Central and southern Andean tectonic evolution inferred from arc magmatism. In *The Andes* (pp. 337-353). Springer, Berlin, Heidelberg.
- Hauser, N., Matteini, M., Omarini, R. H., & Pimentel, M. M. (2011). Combined U-Pb and Lu-Hf isotope data on turbidites of the Paleozoic basement of NW Argentina and petrology of associated igneous rocks: Implications for the tectonic evolution of western Gondwana between 560 and 460 Ma. Gondwana Research, 19(1), 100–127. <https://doi.org/10.1016/j.gr.2010.04.002>
- Hawkesworth, C., Cawood, P., Kemp, T., Storey, C., and Dhuime, B., 2009, A Mater of Preservation: Science, v. 323, p. 49–50, doi:10.1126/science.1168549.
- Heuret, A., & Lallemand, S. (2005). Plate motions, slab dynamics and back-arc deformation. Physics of the Earth and Planetary Interiors, 149(1–2 SPEC. ISS.), 31–51. <https://doi.org/10.1016/j.pepi.2004.08.022>
- Horton, B. K., Saylor, J. E., Nie, J., Mora, A., Parra, M., Reyes-Harker, A., & Stockli, D. F. (2010). Linking sedimentation in the northern Andes to basement configuration, Mesozoic extension, and Cenozoic shortening: Evidence from detrital zircon U-Pb ages, Eastern Cordillera, Colombia. Bulletin of the Geological Society of America, 122(9–10), 1423–1442. <https://doi.org/10.1130/B30118.1>
- Hurtado, C., Roddaz, M., Santos, R. V., Baby, P., Antoine, P., & Dantas, E. L. (2018). Late Cretaceous-early Paleocene drainage shift of Amazonian rivers driven by Equatorial Atlantic Ocean opening and Andean uplift as deduced from the provenance of northern Peruvian sedimentary rocks (Huallaga basin). Gondwana Research, <https://doi.org/10.1016/j.gr.2018.05.012>
- Jacay, J. (1992). Estratigrafía y sedimentología del Jurásico curso medio del valle de Chicama y esbozo paleogeográfico del Jurásico Cretáceo del nor Perú (6°300'8° latitud sur). Geológica-Tesis de Ingeniería. Lima–Perú. Sempere, T., Carlier, G., Soler, P.,

- Fornari, M., Carlotto, V., Jacay, J., Arispe, O., Néraudeau, D., Cárdenas, J., Rosas, S., Jiménez, N., 2002. Late Permian-Middle Jurassic lithospheric thinning in Peru and Bolivia, and its bearing on Andean-age tectonics. *Tectonophysics* 345, 153–181. [https://doi.org/10.1016/S0040-1951\(01\)00211-6](https://doi.org/10.1016/S0040-1951(01)00211-6).
- Jackson, S.E., Pearson, N.J., Griffina, W.L., Belousova, E.A., 2004. The application of laser ablation-inductively coupled plasma-mass spectrometry to in situ U-Pb zircon geochronology. *Chem. Geol.* 211, 47-69.
- Jaillard E. and Jacay J. (1989). Les "couches Chicama" du Nord du Pérou: Colmatage d'un bassin né d'une collision oblique au Tithonique. *Comptes Rendus de l'Académie des Sciences, Paris.* 308(II), 1459-1465.
- Jaillard E.(1995). La sedimentación Albiana -Turoniana en el Sur del Perú (Arequipa-Puno-Putina). Sociedad Geológica del Perú, Volumen Jubilar Alberto Benavides. Lima, 135-157.
- Jaillard, E., & Soler, P. (1996). Cretaceous to early Paleogene tectonic evolution of the northern Central Andes (0–18° S) and its relations to geodynamics. *Tectonophysics*, 259(1-3), 41-53.
- Jaillard, E., Feist, M., Grambast-Fessard, N., Carlotto, V., 1994. Senonian–Paleocene charophyte succession of the Peruvian Andes. *Cretaceous Research* 15, 445–456.
- Jaillard, E., Hérail, G., Monfret, T., Diaz-Martinez, E., Baby, P., Laveno, A., & Dumont, J. F. (2000). Tectonic evolution of the Andes of Ecuador, Peru, Bolivia and Northernmost Chile. In *Tectonic evolution of South America* (Cordani, U.; Milani, E.; Thomaz Filho, A.; Campos; D.; editors). International Geological Congress : . Rio de Janeiro., 31(January), 481–559.
- Jaillard, E., Ordoñez, M., Suárez, Johnny., Toro, J., Iza, D., Lugo, W. (2004). Stratigraphy of the late Cretaceous – Paleogene deposits of the Cordillera Occidental of Central Ecuador: geodynamic implications. *Journal South America Earth Sciences*, 17(1), 49-58.
- Jaillard, E., Soler, P., Carlier, G., & Mourier, T. (1990). Geodynamic evolution of the northern and central Andes during early to middle Mesozoic times: a Tethyan model. *Journal of the Geological Society*, 147(6), 1009-1022.
- Jarrard, R. (1986). Relations among subduction parameters. *Reviews of Geophysics*, 24(2), 217-284. <https://doi.org/10.1029/RG024i002p00217>
- Jenks, W. F. (1948). Geology of the Arequipa quadrangle. *Boletín Instituto Geológico del Perú*, 9, 204.
- Kontak, D.J., Clark, A.H., Farrar, E., Strong, D.F., 1985. The rift associated PermoTriassic magmatism of the Eastern Cordillera: a precursor to the Andean orogeny. In: Pitcher, W.S., Atherton, M.P., Cobbing, J., and Beckinsale R.D. (Eds.),

Magmatism at a plate edge: The Peruvian Andes. Blackie, Glasgow, and Halsted Press, New York, pp. 36–44.

Košler, J., Fonneland, H., Sylvester, P., Tubrett, M., Pedersen, R.B. 2002. U–Pb dating of detrital zircons for sediment provenance studies—a comparison of laser ablation ICPMS and SIMS techniques. *Chemical Geology*, 182:605–618.

Lamotte, D. F., Fourdan, B., Leleu, S., Lepamentier, F., & de Clarens, P. (2015). Style of rifting and the stages of Pangea breakup. *Tectonics*, 34(5), 1009-1029.

León, I., 1981. Antecedentes sedimentológicos sobre el Jurásico-Cretácico inferior del sector de Yura (Departamento de Arequipa). Bachelor thesis. Universidad Nacional San Agustín, Perú, pp. 92.

Litherland, M., Aspen, J.A., and Jemielita, R.A., 1994, The Metamorphic Belts of Ecuador: British Geological Survey Overseas Geology & Mineral Resources Memoir 11, 147 p.

Loewy, S. L., Connelly, J. N., & Dalziel, I. W. D. (2004). An orphaned basement block: The Arequipa-Antofalla Basement of the central Andean margin of South America. *Bulletin of the Geological Society of America*, 116(1–2), 171–187. <https://doi.org/10.1130/B25226.1>

López, C., Riquelme, R., Martínez, F., Sanchez, C., & Mestre, A. (2017). Zircon U-Pb geochronology of the mesozoic to lower Cenozoic rocks of the Coastal Cordillera in the Antofagasta region (22°30'–23°00' S): Insights to the Andean tectono-magmatic evolution. *Journal of South American Earth Sciences*, (November). <https://doi.org/10.1016/j.jsames.2017.11.005>.

Louterbach, M., Roddaz, M., Antoine, P. O., Marivaux, L., Adnet, S., Bailleul, J., ... Calderon, Y. (2018). Provenance record of late Maastrichtian–late Palaeocene Andean Mountain building in the Amazonian retroarc foreland basin (Madre de Dios basin, Peru). *Terra Nova*, 30(1), 17–23. <https://doi.org/10.1111/ter.12303>

Ludwig, K. R. 2008. User's Manual for Isoplot 3.0. A geochronological Toolkit for Microsoft Excel. Berkeley Geochronology Center, 4(4), 76.

Mamani, M., Wörner, G., & Sempere, T. (2010). Geochemical variations in igneous rocks of the Central Andean orocline (13°S to 18°S): Tracing crustal thickening and magma generation through time and space. *Bulletin of the Geological Society of America*, 122(1–2), 162–182. <https://doi.org/10.1130/B26538.1>

McCourt, W.J., Aspden, J.A., and Brook, M., 1984, New geological and geochronological data from the Colombian Andes: Continental growth by multiple accretion: *Journal of the Geological Society of London*, v. 141, p. 831–845, doi: 10.1144/gsjgs.141.5.0831.

McGroder, M. F., Lease, R. O., & Pearson, D. M. (2015). Along-strike variation in structural styles and hydrocarbon occurrences, Subandean fold-and-thrust belt and inner

- foreland, Colombia to Argentina. Geological Society of America Memoirs , 212, 79–113. [https://doi.org/10.1130/2015.1212\(05\)](https://doi.org/10.1130/2015.1212(05))
- McLennan, S. M., Hemming, S., McDaniel, D. K., & Hanson, G. N. (1993). Geochemical approaches to sedimentation, provenance, and tectonics.
- Mégard, F. (1979). Estudio geológico de los Andes del Perú Central (Doctoral dissertation, Instituto Geológico Minero y Metalúrgico).
- Mégard, F. (1984). The Andean orogenic period and its major structures in central and northern Peru. Journal of the Geological Society, 141(5), 893-900.
- Mégard, F. (1987). Cordilleran Andes and Marginal Andes: a Review of Andean Geology North of the Arica Elbow (S. Circum-Pacific Orogenic Belts and Evolution of the Pacific Ocean Basin, 18, 71-95.
- Mišković, A., Schaltegger, U., 2009. Crustal growth along a non-collisional cratonic margin: A Lu-Hf isotopic survey of the Eastern Cordilleran granitoids of Peru. Earth Planet. Sci. Lett. 279, 303–315. <https://doi.org/10.1016/j.epsl.2009.01.002>.
- Mišković, A., Spikings, R. A., Chew, D. M., Košler, J., Ulianov, A., & Schaltegger, U. (2009). Tectonomagmatic evolution of Western Amazonia: Geochemical characterization and zircon U-Pb geochronologic constraints from the Peruvian Eastern Cordilleran granitoids. Bulletin of the Geological Society of America, 121(9–10), 1298–1324. <https://doi.org/10.1130/B26488.1>
- Mukasa, S.B., 1986. Zircon U–Pb ages of superunits in the Coastal Batholith of Peru: implications for magmatic and tectonic processes. Geological Society of America Bulletin 97, 241–254.
- Naipauer, M., Tapia, F., Mescua, J., Farías, M., Pimentel, M. M., & Ramos, V. A. (2015). Detrital and volcanic zircon U-Pb ages from southern Mendoza (Argentina): An insight on the source regions in the northern part of the Neuquén Basin. Journal of South American Earth Sciences, 64, 434–451. <https://doi.org/10.1016/j.jsames.2015.09.013>
- Nakakuki, T., & Mura, E. (2013). Dynamics of slab rollback and induced back-arc basin formation. Earth and Planetary Science Letters, 361, 287–297. <https://doi.org/10.1016/j.epsl.2012.10.031>
- Nance, R. D., & Murphy, J. B. (2013). Origins of the supercontinent cycle. Geoscience Frontiers, 4(4), 439-448.
- Nance, R. D., Murphy, J. B., & Santosh, M. (2014). The supercontinent cycle: a retrospective essay. Gondwana Research, 25(1), 4-29.
- Nemchin, A.A., Cawood, P.A., 2005. Discordance of the U–Pb system in detrital zircons: implication for provenance studies of sedimentary rocks. Sedimentary Geology 182, 143–162.

- Neoproterozoic active margin? Precambrian Research, 167(1–2), 186–200. <https://doi.org/10.1016/j.precamres.2008.08.002>
- Newell, N.D., 1942. Lower Paleozoic pelecypods: Mytilacea. University of Kansas Publications 10 (2), 1e115.
- Nie, J., Horton, B. K., Saylor, J. E., Mora, A., Mange, M., Garzzone, C. N., ... Parra, M. (2012). Integrated provenance analysis of a convergent retroarc foreland system: U-Pb ages, heavy minerals, Nd isotopes, and sandstone compositions of the Middle Magdalena Valley basin, northern Andes, Colombia. Earth-Science Reviews, 110(1–4), 111–126. <https://doi.org/10.1016/j.earscirev.2011.11.002>
- Oliveira V, F., 2016. Chronus : Um novo suplemento para a redução de dados U-Pb obtidos por LA-. Diss. Mestr. N°348 91. <https://doi.org/10.13140/RG.2.1.3598.3126>.
- Oliveros, V., Féraud, G., Aguirre, L., Fornari, M., & Morata, D. (2006). The Early Andean Magmatic Province (EAMP): 40 Ar / 39 Ar dating on Mesozoic volcanic and plutonic rocks from the Coastal Cordillera , northern Chile, 157, 311–330. <https://doi.org/10.1016/j.jvolgeores.2006.04.007>
- Oliveros, V., Labbé, M., Rossel, P., Charrier, R., & Encinas, A. (2012). Journal of South American Earth Sciences Late Jurassic paleogeographic evolution of the Andean back-arc basin : New constrains from the Lagunillas Formation , northern Chile (27 30 ' e 28 30 ' S). Journal of South American Earth Sciences, 37, 25–40. <https://doi.org/10.1016/j.jsames.2011.12.005>
- Pamparo, M. B., & Batty, E. L. M. (1994). First palynological data from the Lower Cretaceous of the Arequipa Basin, southern Peru (1, Zbl. Ge ed.). Stuttgart. Deutschland
- Pankhurst, R.J., Rapela, C.W., Fanning, C.M., and Márquez, M., 2006, Gondwanide continental collision and the origin of Patagonia: Earth-Science Reviews, v. 76, p. 235–257, doi: 10.1016/j.earscirev.2006.02.001.
- Perelló J.; Carlotto V.; (2003). Porphyry-Style Alteration and Mineralization of the Middle Eocene to Early Oligocene Andahuaylas-Yauri Belt , Cuzco Region , Peru, 98, 1575–1605.
- Perez, N. D., & Horton, B. K. (2014). Oligocene-miocene deformational and depositional history of the andean hinterland basin in the northern altiplano Plateau, Southern Peru. Tectonics, 33(9), 1819–1847. <https://doi.org/10.1002/2014TC003647>
- Perez, N. D., Horton, B. K., McQuarrie, N., Stübner, K., & Ehlers, T. A. (2016). Andean shortening, inversion and exhumation associated with thin- and thick-skinned deformation in southern Peru. Geological Magazine, 153(5–6), 1013–1041. <https://doi.org/10.1017/S0016756816000121>
- Pindell, J. L., & Tabbutt, K. D. (1995). Mesozoic-Cenozoic Andean paleogeography and regional controls on hydrocarbon systems.

- Pollard, M., Schaltegger, U., Frank, M., Fontboté, L., 2005. Formation of intra-arc volcanosedimentary basins in the western flank of the central Peruvian Andes during Late Cretaceous oblique subduction: Field evidence and constraints from U-Pb ages and Hf isotopes. *Int. J. Earth Sci.* 94, 231–242. <https://doi.org/10.1007/s00531-005-0464-5>.
- Portugal, J. (1974) Mesozoic and Cenozoic Stratigraphy and Tectonic events of Puno-Santa Lucia Area, Department of Puno, Peru. *Am. Ass. Petrol. Geol. Bull.*, 58,982-999.
- Ramos, V. A. (2008). The Basement of the Central Andes: The Arequipa and Related Terranes. *Annual Review of Earth and Planetary Sciences*, 36(1), 289–324. <https://doi.org/10.1146/annurev.earth.36.031207.124304>
- Ramos, V. A. (2009). Anatomy and global context of the Andes: Main geologic features and the Andean orogenic cycle. *Geological Society of America Memoirs*, 204(0), 31–65. [https://doi.org/10.1130/2009.1204\(02\)](https://doi.org/10.1130/2009.1204(02))
- Ramos, V. A. (2018). Tectonic Evolution of the Central Andes: From Terrane Accretion to Crustal Delamination, 1–34. <https://doi.org/10.1306/13622115M1172855>
- Ramos, V. A., & Mpodozis, C. (1989). The Andes of Chile and Argentina , in : *Geology of the Andes and its Relation to Hydrocarbon and Mineral Resources*, 11(December), 33.
- Rapela, C. W., Pankhurst, R. J., Casquet, C., Baldo, E., Saavedra, J., & Galindo, C. (1998). Early evolution of the Proto-Andean margin of South America. *Geology*, 26(8), 707-710.
- Reimann, C. R., Bahlburg, H., Carlotto, V., Boekhout, F., Berndt, J., & Lopez, S. (2015). Journal of South American Earth Sciences Multi-method provenance model for early Paleozoic sedimentary basins of southern Peru and northern Bolivia (13 e 18 S). *Journal of South American Earth Sciences*, 64, 94–115. <https://doi.org/10.1016/j.jsames.2015.08.013>
- Reimann, C. R., Bahlburg, H., Kooijman, E., Berndt, J., Gerdes, A., Carlotto, V., & López, S. (2010). Geodynamic evolution of the early Paleozoic Western Gondwana margin 14°S-17°S reflected by the detritus of the Devonian and Ordovician basins of southern Peru and northern Bolivia. *Gondwana Research*, 18(2–3), 370–384. <https://doi.org/10.1016/j.gr.2010.02.002>
- Reitsma, M. J. (2012). Reconstructing the Late Paleozoic - Early Mesozoic plutonic and sedimentary record of south-east Peru : Orphaned back-arcs along the western margin of Gondwana. <https://doi.org/10.13097/archive-ouverte/unige:23095>
- Resende, Rosana., 2011. Caracterização do mineral zircão através do método de traços de fissão, espectroscopia micro-raman e mev: geocronologia do grupo bauru. Dissertação (Mestrado)—Universidade Estadual Paulista. Faculdade de Ciências e Tecnologia, Presidente Prudente. 113 f.

- Roddaz, M., Viers, J., Brusset, S., Baby, P., & Hérail, G. (2005). Sediment provenances and drainage evolution of the Neogene Amazonian foreland basin. *Earth and Planetary Science Letters*, 239(1–2), 57–78. <https://doi.org/10.1016/j.epsl.2005.08.007>
- Romero, D., Valencia, K., Alarcón, P., Peña, D., & Ramos, V. A. (2013). The offshore basement of Perú: Evidence for different igneous and metamorphic domains in the forearc. *Journal of South American Earth Sciences*, 42, 47–60. <https://doi.org/10.1016/j.jsames.2012.11.003>
- Romeuf, N., Aguirre L., Soler P., Féraud G., Jaillard E., Ruffet G. (1995). Middle Jurassic volcanism in the Northern and Central Andes. *Revista Geológica de Chile*, 22 (2). 245-259.
- Rosas, S., Fontboté, L., Tankard, A., 2007. Tectonic evolution and paleogeography of the Mesozoic Pucará Basin, central Peru. *J. South Am. Earth Sci.* 24, 1–24. <https://doi.org/10.1016/j.jsames.2007.03.002>
- Rossel, P., Oliveros, V., Ducea, M. N., Charrier, R., Scaillet, S., Retamal, L., & Figueroa, O. (2013). The Early Andean subduction system as an analog to island arcs: Evidence from across-arc geochemical variations in northern Chile. *Lithos*, 179, 211–230. <https://doi.org/10.1016/j.lithos.2013.08.014>
- Scherrenberg, A. F., Jacay, J., Holcombe, R. J., & Rosenbaum, G. (2012). Stratigraphic variations across the Marañón Fold-Thrust Belt, Peru: Implications for the basin architecture of the West Peruvian Trough. *Journal of South American Earth Sciences*, 38, 147–158. <https://doi.org/10.1016/j.jsames.2012.06.006>
- Scherrenberg, A. F., Kohn, B. P., Holcombe, R. J., & Rosenbaum, G. (2016). Thermotectonic history of the Marañón Fold–Thrust Belt, Peru: Insights into mineralization in an evolving orogen. *Tectonophysics*, 667, 16–36. <https://doi.org/10.1016/j.tecto.2015.11.007>
- Sdrolias, M., & Müller, R. D. (2006). Controls on back-arc basin formation. *Geochemistry, Geophysics, Geosystems*, 7(4). <https://doi.org/10.1029/2005GC001090>
- Sempere, T., Carlier, G., Soler, P., Fornari, M., Carlotto, V., Jacay, J., Jiménez, N. (2002). Late Permian-Middle Jurassic lithospheric thinning in Peru and Bolivia, and its bearing on Andean-age tectonics. *Tectonophysics*, 345(1–4), 153–181. [https://doi.org/10.1016/S0040-1951\(01\)00211-6](https://doi.org/10.1016/S0040-1951(01)00211-6)
- Sempere, T., Oller, J., & Barrios, L. (1988). Evolución tectosedimentaria de Bolivia durante el Cretácico. In Congreso Geológico Chüeno, 5th, Santiago, Actas (Vol. 3, pp. 37-65).
- Spikings, R., Boekhout, F., & Chiaradia, M. (2016). Characterization of Triassic Rifting in Peru and implications for the early disassembly of western Pangaea, (April). <https://doi.org/10.1016/j.gr.2016.02.008>

- Spikings, R., Cochrane, R., Villagomez, D., Van der Lelij, R., Vallejo, C., Winkler, W., & Beate, B. (2015). The geological history of northwestern South America: From Pangaea to the early collision of the Caribbean Large Igneous Province (290-75 Ma). *Gondwana Research*, 27(1), 95–139. <https://doi.org/10.1016/j.gr.2014.06.004>
- Stern, R. J. (2002). Subduction zones. *Reviews of Geophysics*, 40(4). <https://doi.org/10.1029/2001RG000108>
- Stern, R. J., & Dickinson, W. R. (2010). The Gulf of Mexico is a Jurassic backarc basin. *Geosphere*, 6(6), 739–754. <https://doi.org/10.1130/GES00585.1>
- Stern, R. J., Reagan, M., Ishizuka, O., Ohara, Y., & Whattam, S. (2012). To understand subduction initiation, study forearc crust: To understand forearc crust, study ophiolites. *Lithosphere*, 4(6), 469-483.
- Trinidad, I., 2017. Procedencia sedimentaria de la Cuenca mesooica Arequipa en Tacna (18°S) a traves de los minerales pesados. Universidad Nacional Daniel Alcides Carrión, Perú. Tesis de Ingeniero Geólogo, 120 p.
- Vargas, L. (1970). Geología del cuadrángulo de Arequipa. República del Perú, Ministerio de Energía y Minas, Dirección General de Minería, Servicio de Geología y Minería.
- Vicente, J. C., Beaudoin, B., Chávez, A., & León, I. (1982). La cuenca de Arequipa (Sur Perú) durante el Jurásico-Cretácico inferior. In 5 to Congreso Latinoamericano de Geología, Buenos-Aires 1981 (Vol. 1, pp. 121-153).
- Vicente, J.C., 1981. Elementos de la estratigrafía Mesozoica sur Peruana. Comité Sudamericano del Jurásico y Cretácico. In Volkheimer, I., Musacchio, A., (Eds), Cuencas sedimentarias del jurassico y cretacico de America del sur, v. 1, p. 319-351.
- Vicente, J.C., 2006. Dynamic paleogeography of the Jurassic Andean basin: Pattern of regression and general considerations on main features. *Revista de la Asociación Geológica Argentina*, v. 61, p. 408-437. Vicente, J.C., 2005. Dynamic paleogeography of the Jurassic Andean basin: pattern of transgression and localization of main straits through the magmatic arc. *Revista de la Asociación Geológica Argentina*, v. 60, p. 221-250.
- Wilson, J. J., & García, W. (1962). Geología de los cuadrángulos de Pachía y Palca 36-vy 36-x, Boletín A 4, Instituto Geológico Minero Meturgico – INGEMMET. Lima – Perú, p. 85.
- Wotzlaw, F., Decou, A., Eynatten, H. Von, Wo, G., & Frei, D. (2011). Jurassic to Palaeogene tectono-magmatic evolution of northern Chile and adjacent Bolivia from detrital zircon U-Pb geochronology and heavy mineral provenance. <https://doi.org/10.1111/j.1365-3121.2011.01025.x>

Referências Bibliográficas

- Ziegler, P. A., & Cloetingh, S. (2004). Dynamic processes controlling evolution of rifted basins. *Earth-Science Reviews*, 64(1–2), 1–50.
[https://doi.org/10.1016/S00128252\(03\)00041-2](https://doi.org/10.1016/S00128252(03)00041-2)

Anexo

ANEXOS

Tabela 1. Sumário dos dados de LA-ICPMS da amostra ARE-304.

Spot	^{204}Pb cps	^{206}Pb mV ¹	Th/U	$^{206}\text{Pb}/^{204}\text{Pb}$	1s %	$^{207}\text{Pb}/^{206}\text{Pb}$	1s %	$^{207}\text{Pb}/^{235}\text{U}$	1s %	$^{206}\text{Pb}/^{238}\text{U}$	1s %	Rho	$^{207}\text{Pb}/^{206}\text{Pb}$	2s abs	$^{206}\text{Pb}/^{238}\text{U}$	2s abs	$^{207}\text{Pb}/^{235}\text{U}$	2s abs	% U-Pb disc ⁴	Event
018-ZR13	9	0.0016	0.710	60763	12.75	0.05209	1.05	0.280	1.56	0.0390	1.09	0.70	289	48	247	5	251	7	14.69	Triassic rift 250 - 220 Ma
090-ZR69	7	0.0008	0.527	36161	10.17	0.05029	2.19	0.276	3.00	0.0399	2.01	0.67	208	100	252	10	248	13	-20.93	
050-ZR38	11	0.0027	0.542	92766	13.62	0.05055	1.41	0.284	1.75	0.0407	0.97	0.55	220	64	257	5	254	8	-16.70	
159-ZR125	16	0.0024	0.523	52313	21.38	0.05335	0.76	0.301	1.21	0.0409	0.86	0.71	344	34	258	4	267	6	24.85	Paleozoic Magmatic Arc 0.4-0.25 Ga
106-ZR81	12	0.0005	0.383	17548	13.74	0.05493	2.60	0.313	4.27	0.0413	3.37	0.79	410	114	261	17	276	21	36.27	
097-ZR74	8	0.0034	0.403	377921	66.50	0.05199	0.55	0.309	1.02	0.0431	0.77	0.76	285	25	272	4	273	5	4.45	
067-ZR51	22	0.0045	0.464	132585	18.08	0.05119	0.98	0.321	1.73	0.0455	1.38	0.80	249	45	287	8	283	9	-15.05	
044-ZR32	36	0.0020	0.585	31237	24.46	0.05486	1.43	0.416	2.09	0.0550	1.48	0.71	406	63	345	10	353	12	15	0.4-03 Ga
148-ZR116	14	0.0019	0.927	52369	16.17	0.05645	0.99	0.547	1.53	0.0703	1.11	0.72	470	43	438	9	443	11	6.82	
046-ZR34	13	0.0026	0.655	100466	17.16	0.05635	0.66	0.592	1.18	0.0762	0.90	0.76	466	29	473	8	472	9	-1.50	Famatinian 0.5 - 0.4 Ga
133-ZR104	14	0.0006	0.434	16649	16.58	0.05990	2.69	0.647	4.02	0.0784	2.97	0.74	600	115	486	28	507	32	18.93	
137-ZR106	11	0.0038	0.575	116309	14.95	0.05761	0.63	0.636	1.08	0.0800	0.79	0.73	515	28	496	8	500	8	3.66	
078-ZR60	11	0.0007	0.381	21952	14.38	0.06158	2.06	0.706	3.13	0.0831	2.33	0.74	660	87	515	23	542	26	21.95	
066-ZR50	15	0.0057	0.229	161142	17.98	0.05816	0.53	0.679	1.17	0.0846	0.98	0.83	536	23	524	10	526	10	2.26	
151-ZR119	10	0.0009	0.502	25355	17.02	0.06058	1.84	0.711	2.61	0.0851	1.82	0.69	624	78	527	18	545	22	15.63	
036-ZR27	18	0.0015	0.400	64492	26.96	0.06454	1.67	0.761	2.04	0.0855	1.12	0.55	759	70	529	11	574	18	30.38	
069-ZR53	17	0.0029	0.402	103926	25.68	0.05917	0.69	0.701	1.13	0.0859	0.82	0.72	573	30	531	8	539	9	7.30	
039-ZR29	13	0.0123	0.130	541368	31.66	0.05820	0.41	0.692	0.88	0.0863	0.69	0.78	537	18	533	7	534	7	0.75	
072-ZR56	13	0.0010	2.135	23912	17.65	0.06031	1.51	0.730	2.30	0.0878	1.69	0.74	615	65	542	18	557	20	11.77	Brazilian/Pampean 0.7 - 0.5 Ga
130-ZR101	14	0.0014	0.796	38979	17.31	0.05891	1.21	0.720	1.87	0.0886	1.38	0.74	564	52	547	14	550	16	2.97	
048-ZR36	8	0.0028	0.110	107575	11.94	0.05948	0.71	0.732	1.15	0.0893	0.82	0.71	585	31	551	9	558	10	5.72	
015-ZR10	9	0.0018	0.807	607158	89.32	0.05845	1.00	0.727	1.46	0.0902	1.00	0.68	547	44	557	11	555	12	-1.79	
086-ZR66	8	0.0015	0.435	56213	11.97	0.05976	1.08	0.752	2.20	0.0913	1.89	0.86	595	46	563	20	570	19	5.33	
169-ZR133	8	0.0035	0.095	140256	13.17	0.05940	0.54	0.748	0.92	0.0914	0.65	0.71	582	23	564	7	567	8	3.15	

099-ZR76	14	0.0008	1.344	22659	15.73	0.06165	2.46	0.787	3.43	0.0926	2.37	0.69	662	104	571	26	590	30	13.77		
123-ZR96	47	0.0058	0.022	60363	24.54	0.05903	0.76	0.765	2.48	0.0939	2.34	0.94	568	33	579	26	577	22	-1.86		
016-ZR11	10	0.0013	0.530	61329	20.12	0.05969	1.11	0.773	1.72	0.0940	1.26	0.73	592	48	579	14	582	15	2.24		
107-ZR82	13	0.0035	0.184	119369	13.84	0.06057	0.60	0.787	1.10	0.0943	0.84	0.77	624	26	581	9	590	10	6.97		
056-ZR42	6	0.0051	0.628	292698	33.88	0.06012	0.59	0.783	1.22	0.0945	1.01	0.82	608	25	582	11	587	11	4.27		
030-ZR23	13	0.0031	0.290	221485	57.04	0.05948	0.67	0.778	1.09	0.0948	0.77	0.71	585	29	584	9	584	10	0.08		
119-ZR92	29	0.0015	0.455	21908	24.19	0.05728	2.07	0.751	2.90	0.0950	1.99	0.69	502	90	585	22	569	25	-16.51		
163-ZR129	9	0.0008	0.368	21791	15.75	0.06198	1.70	0.820	2.34	0.0959	1.57	0.67	673	72	590	18	608	21	12.33		
083-ZR65	15	0.0033	0.131	102925	16.14	0.05857	0.86	0.777	1.17	0.0962	0.70	0.60	551	37	592	8	584	10	-7.47		
008-ZR5	11	0.0017	0.404	56118	14.94	0.05827	1.14	0.783	2.66	0.0974	2.37	0.89	540	50	599	27	587	24	-11.05	Brazilian/Pampean 0.7 - 0.5 Ga	
020-ZR15	6	0.0014	0.524	60437	10.47	0.06049	1.33	0.820	1.98	0.0983	1.41	0.72	621	57	605	16	608	18	2.66		
006-ZR3	9	0.0040	0.308	168725	11.08	0.05911	0.77	0.819	1.13	0.1005	0.75	0.66	571	33	617	9	607	10	-8.08		
017-ZR12	9	0.0055	0.287	179733	14.76	0.06089	0.41	0.853	0.88	0.1016	0.69	0.78	635	18	624	8	626	8	1.83		
129-ZR100	13	0.0012	0.356	47219	28.69	0.06130	1.45	0.860	2.26	0.1017	1.69	0.75	650	62	625	20	630	21	3.90		
082-ZR64	14	0.0028	0.343	78052	17.43	0.06241	0.92	0.880	1.50	0.1023	1.12	0.75	688	39	628	13	641	14	8.76		
081-ZR63	14	0.0053	0.252	162035	19.70	0.05979	0.69	0.848	1.42	0.1029	1.19	0.84	596	30	631	14	624	13	-5.96		
062-ZR48	13	0.0038	0.677	143375	17.17	0.06163	0.53	0.891	0.97	0.1048	0.72	0.75	661	23	643	9	647	9	2.81		
122-ZR95	24	0.0019	0.397	32641	23.21	0.06482	1.07	0.938	1.51	0.1050	1.00	0.66	768	45	643	12	672	15	16.28		
150-ZR118	14	0.0093	0.423	215986	19.20	0.06174	0.41	0.945	0.86	0.1111	0.66	0.77	665	18	679	9	676	8	-2.08		
140-ZR109	16	0.0012	0.581	26877	19.47	0.06539	1.30	1.050	1.97	0.1165	1.42	0.72	787	54	710	19	729	20	9.74		
060-ZR46	19	0.0031	0.300	120618	13.65	0.06362	0.70	1.032	1.35	0.1176	1.10	0.81	729	29	717	15	720	14	1.66		
051-ZR39	14	0.0030	0.455	79605	16.14	0.06246	0.85	1.034	2.12	0.1200	1.90	0.90	690	36	731	26	721	22	-5.94		
157-ZR123	11	0.0047	0.339	629212	76.40	0.06380	0.52	1.088	0.94	0.1236	0.69	0.74	735	22	751	10	747	10	-2.21	0.7 - 0.9 Ga	
004-ZR2	14	0.0080	0.270	203892	16.75	0.07077	0.56	1.352	1.85	0.1385	1.72	0.93	951	23	836	27	868	21	12.04		
091-ZR70	12	0.0016	0.309	50080	14.03	0.07255	1.18	1.398	2.06	0.1398	1.65	0.80	1001	47	843	26	888	24	15.79		
108-ZR83	9	0.0080	0.338	283072	12.53	0.07058	0.49	1.441	0.93	0.1481	0.69	0.75	945	20	890	12	906	11	5.81		
111-ZR86	11	0.0041	0.430	147975	13.07	0.07176	1.15	1.487	1.73	0.1503	1.24	0.71	979	47	903	21	925	21	7.82		

117-ZR90	13	0.0018	0.168	63373	32.31	0.07446	1.63	1.557	2.61	0.1517	2.01	0.77	1054	65	910	34	953	32	13.63	
025-ZR18	15	0.0060	0.759	175700	16.08	0.07051	0.36	1.480	0.78	0.1522	0.59	0.75	943	15	913	10	922	9	3.18	Grenville - Sunsás 1.3 - 0.9 Ga
098-ZR75	20	0.0169	0.201	15311966	97.26	0.07348	0.38	1.581	0.86	0.1560	0.67	0.78	1027	15	935	12	963	11	8.99	
144-ZR113	10	0.0010	0.294	29033	15.04	0.07388	1.30	1.603	2.10	0.1574	1.61	0.76	1038	52	942	28	971	26	9.26	
021-ZR16	10	0.0029	0.525	98761	16.47	0.07226	0.61	1.605	1.08	0.1611	0.81	0.75	993	25	963	15	972	13	3.07	
005-ZR2N	8	0.0059	0.262	260319	10.41	0.07050	0.53	1.573	2.00	0.1618	1.89	0.95	943	22	967	34	960	25	-2.53	
110-ZR85	29	0.0020	0.371	25920	32.02	0.07385	1.37	1.667	1.88	0.1637	1.24	0.66	1037	55	978	22	996	24	5.76	
131-ZR102	15	0.0062	0.209	159413	20.58	0.07337	0.52	1.667	0.90	0.1647	0.63	0.70	1024	21	983	12	996	11	4.02	
101-ZR78	10	0.0111	0.104	381418	13.80	0.07255	0.36	1.662	0.74	0.1661	0.52	0.71	1001	15	991	10	994	9	1.08	
029-ZR22	7	0.0054	0.194	294676	28.52	0.07349	0.42	1.684	0.78	0.1661	0.54	0.69	1028	17	991	10	1002	10	3.57	
164-ZR130	11	0.0115	0.219	314559	15.44	0.07307	0.90	1.680	1.17	0.1667	0.65	0.55	1016	36	994	12	1001	15	2.18	
092-ZR71	10	0.0077	0.232	274019	13.31	0.07312	0.51	1.721	1.24	0.1707	1.07	0.86	1017	20	1016	20	1016	16	0.13	
038-ZR28N	12	0.0071	0.282	201863	18.37	0.07314	0.51	1.710	2.21	0.1696	2.12	0.96	1018	20	1010	40	1012	28	0.80	
079-ZR61	21	0.0029	0.350	65516	19.20	0.07348	2.46	1.754	4.24	0.1732	3.43	0.81	1027	98	1029	65	1029	54	-0.22	
087-ZR67	7	0.0023	0.514	141898	33.58	0.07380	0.68	1.768	1.25	0.1737	0.99	0.79	1036	27	1033	19	1034	16	0.31	
141-ZR110	12	0.0049	0.229	268664	36.24	0.07392	0.50	1.762	0.99	0.1729	0.78	0.78	1039	20	1028	15	1032	13	1.10	
007-ZR4	10	0.0069	0.244	259879	13.12	0.07402	0.38	1.778	0.77	0.1742	0.56	0.72	1042	15	1035	11	1037	10	0.67	
088-ZR68N	8	0.0063	0.504	253417	13.47	0.07406	0.45	1.816	0.83	0.1778	0.59	0.71	1043	18	1055	12	1051	11	-1.14	
089-ZR68B	10	0.0059	0.491	208165	14.11	0.07416	0.44	1.739	0.88	0.1701	0.67	0.76	1046	18	1012	12	1023	11	3.19	
034-ZR25	11	0.0013	0.428	42657	13.52	0.07446	1.18	1.787	1.81	0.1740	1.32	0.73	1054	47	1034	25	1041	23	1.88	
175-ZR139	19	0.0121	0.467	437567	38.05	0.07462	0.54	1.720	1.68	0.1671	1.54	0.92	1058	22	996	28	1016	21	5.86	Grenville - Sunsás 1.3 - 0.9 Ga
041-ZR31	16	0.0079	0.501	194204	18.18	0.07465	0.55	1.866	1.37	0.1813	1.20	0.88	1059	22	1074	24	1069	18	-1.40	
171-ZR135	9	0.0013	1.230	183121	73.74	0.07482	1.13	1.734	2.15	0.1680	1.79	0.83	1064	45	1001	33	1021	28	5.86	
127-ZR98	21	0.0134	0.323	445134	45.62	0.07491	0.38	1.786	0.79	0.1729	0.59	0.74	1066	15	1028	11	1040	10	3.57	
152-ZR120	15	0.0024	0.240	69887	22.25	0.07505	0.84	1.766	1.53	0.1706	1.22	0.80	1070	34	1016	23	1033	20	5.08	
096-ZR73	26	0.0035	0.936	118678	18.92	0.07511	1.21	1.980	1.53	0.1912	0.86	0.56	1072	48	1128	18	1109	20	-5.25	
138-ZR107	12	0.0032	0.405	94922	19.15	0.07518	0.65	1.805	1.21	0.1741	0.95	0.79	1073	26	1035	18	1047	16	3.61	

160-ZR126	10	0.0029	0.527	114640	12.70	0.07596	0.70	1.911	1.16	0.1824	0.84	0.73	1094	28	1080	17	1085	15	1.25		
132-ZR103	13	0.0042	0.376	117563	15.63	0.07611	0.51	1.842	0.89	0.1755	0.63	0.71	1098	20	1042	12	1061	12	5.06		
102-ZR79	13	0.0027	0.660	69167	18.66	0.07702	0.69	1.875	1.22	0.1766	0.94	0.77	1122	27	1048	18	1072	16	6.57		
103-ZR80	6	0.0095	0.300	390676	10.66	0.07743	0.43	1.960	0.83	0.1836	0.61	0.73	1132	17	1087	12	1102	11	4.02		
116-ZR89	12	0.0047	0.309	149273	14.83	0.07846	1.40	1.983	2.08	0.1833	1.49	0.72	1159	55	1085	30	1110	28	6.36		
161-ZR127	8	0.0042	0.212	143290	16.51	0.07848	0.77	2.085	1.35	0.1927	1.05	0.77	1159	30	1136	22	1144	18	1.99		
126-ZR97	13	0.0046	0.292	133932	15.43	0.07874	0.49	2.125	0.90	0.1957	0.66	0.73	1166	19	1152	14	1157	12	1.13		
052-ZR40	13	0.0053	0.286	203220	21.90	0.07891	0.56	2.079	0.96	0.1910	0.68	0.71	1170	22	1127	14	1142	13	3.66		
073-ZR57	11	0.0129	0.183	462896	13.05	0.07923	0.33	2.126	0.76	0.1946	0.57	0.75	1178	13	1146	12	1157	10	2.68		
109-ZR84	12	0.0045	0.309	145153	14.50	0.07970	0.72	2.032	1.37	0.1849	1.11	0.81	1190	28	1094	22	1126	19	8.06	Grenville - Sunsás 1.3 - 0.9 Ga	
168-ZR132	9	0.0076	0.312	385091	22.39	0.08013	0.41	2.305	0.99	0.2086	0.82	0.83	1200	16	1221	18	1214	14	-1.76		
013-ZR8	6	0.0047	0.209	185645	18.67	0.08026	0.94	2.317	1.56	0.2093	1.19	0.76	1203	37	1225	27	1217	22	-1.81		
143-ZR112	11	0.0040	0.275	246786	43.27	0.08078	0.67	2.373	1.17	0.2130	0.88	0.76	1216	26	1245	20	1235	17	-2.38		
173-ZR137	7	0.0012	0.194	51631	11.54	0.08095	1.59	2.260	2.40	0.2025	1.76	0.73	1220	62	1189	38	1200	34	2.57		
076-ZR58	12	0.0030	0.244	78153	16.89	0.08136	0.54	2.348	1.63	0.2093	1.49	0.92	1230	21	1225	33	1227	23	0.42		
059-ZR45	13	0.0062	0.234	221678	15.97	0.08446	0.60	2.502	1.42	0.2149	1.23	0.87	1303	23	1255	28	1273	20	3.73	Rondonia - San Ignacio mobile belt 1.54-1.3 Ga	
093-ZR72	24	0.0174	0.441	591126	14.24	0.08625	0.48	2.635	1.10	0.2216	0.92	0.84	1344	18	1290	22	1311	16	3.99		
009-ZR6	11	0.0041	0.421	151052	16.21	0.09052	0.47	3.075	0.96	0.2464	0.75	0.78	1437	18	1420	19	1427	15	1.17		
028-ZR21	9	0.0023	0.371	73703	14.03	0.09397	0.70	3.371	1.37	0.2602	1.12	0.82	1508	26	1491	30	1498	21	1.12		
026-ZR19	9	0.0096	0.334	358231	12.68	0.09695	0.31	3.604	0.72	0.2696	0.53	0.74	1566	12	1539	15	1550	11	1.76	Rio Negro - Juruena mobile belt 1.82 - 1.54 Ga	
142-ZR111	9	0.0209	0.267	665043	14.41	0.09735	0.75	3.710	1.03	0.2764	0.60	0.58	1574	28	1573	17	1573	16	0.06		
049-ZR37	13	0.0064	0.450	213153	22.47	0.10367	0.42	4.412	1.84	0.3086	1.75	0.95	1691	16	1734	53	1715	30	-2.55		
014-ZR9	10	0.0052	0.525	195960	13.28	0.10998	0.39	4.977	1.01	0.3282	0.85	0.85	1799	14	1830	27	1815	17	-1.71		
055-ZR41	14	0.0030	0.502	98384	17.37	0.11054	0.68	4.970	1.23	0.3261	0.96	0.78	1808	25	1819	30	1814	21	-0.61	Ventuari-Tapajós (Trans-amazonian) mobile belt 2.0 - 1.82 Ga	
027-ZR20	14	0.0105	1.162	305035	19.34	0.11489	0.28	5.298	0.70	0.3344	0.53	0.75	1878	10	1860	17	1869	12	0.98		
118-ZR91	10	0.0083	1.275	266444	14.60	0.11718	1.09	5.270	1.65	0.3261	1.19	0.72	1914	39	1820	38	1864	28	4.92		
120-ZR93	11	0.0051	0.591	162230	14.32	0.12269	0.84	5.743	1.34	0.3395	0.97	0.73	1996	30	1884	32	1938	23	5.60		

047-ZR35	20	0.0051	0.497	227440	22.39	0.12322	0.95	6.043	1.28	0.3557	0.77	0.60	2003	34	1962	26	1982	22	2.09	
077-ZR59	17	0.0072	0.522	184201	18.34	0.12337	1.55	6.311	2.36	0.3710	1.74	0.74	2005	55	2034	61	2020	41	-1.43	
010-ZR7	15	0.0152	0.228	1478248	67.35	0.12504	0.34	6.443	0.79	0.3737	0.61	0.77	2029	12	2047	21	2038	14	-0.86	Maroni - Itacaiúnas Province 2.2 -2.0 Ga
058-ZR44	14	0.0090	0.288	262911	15.87	0.12888	0.37	6.359	1.14	0.3579	1.01	0.89	2083	13	1972	34	2027	20	5.31	
057-ZR43	10	0.0013	1.510	40961	13.77	0.12891	1.02	6.839	1.97	0.3848	1.64	0.83	2083	36	2098	59	2091	35	-0.73	
045-ZR33	20	0.0111	0.324	408052	12.98	0.13375	0.46	7.133	0.88	0.3868	0.65	0.74	2148	16	2108	23	2128	16	1.86	
146-ZR114	33	0.0106	0.313	194830	24.88	0.18604	0.31	12.778	0.97	0.4981	0.84	0.87	2707	10	2606	36	2663	18	3.76	Central Amazonian province >2.2Ga
031-ZR23	21	0.0074	0.297	209801	19.69	0.18916	0.44	12.582	2.72	0.4823	2.66	0.98	2735	14	2537	111	2649	51	7.22	

Tabela 2. Sumário dos dados de LA-ICPMS da amostra ARE-312.

Spot	^{204}Pb cps	^{206}Pb mV ¹	Th/U	$^{206}\text{Pb}/^{204}\text{Pb}$	1s%	$^{207}\text{Pb}/^{206}\text{Pb}$	1s %	$^{207}\text{Pb}/^{235}\text{U}$	1s %	$^{206}\text{Pb}/^{238}\text{U}$	1s %	Rho	$^{207}\text{Pb}/^{206}\text{Pb}$	2s abs	$^{206}\text{Pb}/^{238}\text{U}$	2s abs	$^{207}\text{Pb}/^{235}\text{U}$	2s abs	% U-Pb disc ⁴	Events
013-ZR9	67	0.0029	0.357	16307	33.04	0.05380	1.87	0.282	4.39	0.0380	3.95	0.90	363	83	240	19	252	20	33.70	Paleozoic Magmatic Arc 0.4-0.25 Ga
170-ZR131	8	0.0007	0.662	26645	12.46	0.05097	3.55	0.289	4.65	0.0411	2.97	0.64	240	160	260	15	258	21	-8.46	
014-ZR9N	9	0.0006	0.367	19666	14.68	0.05278	2.15	0.300	3.27	0.0412	2.44	0.75	319	96	260	12	266	15	18.46	
128-ZR97	20	0.0031	0.360	98770	16.18	0.04997	0.94	0.297	2.04	0.0431	1.77	0.87	194	43	272	9	264	9	-40.20	
150-ZR115	12	0.0008	0.473	27506	15.39	0.05348	2.13	0.325	3.17	0.0440	2.31	0.73	349	95	278	13	286	16	20.40	
057-ZR42	12	0.0026	0.291	84736	14.67	0.05332	0.69	0.414	1.15	0.0563	0.84	0.73	342	31	353	6	352	7	-3.24	
086-ZR65	11	0.0020	0.099	78040	11.47	0.05405	0.92	0.454	1.36	0.0609	0.93	0.68	373	41	381	7	380	9	-2.08	
079-ZR60	9	0.0015	0.985	73969	29.59	0.05468	1.13	0.463	1.72	0.0614	1.25	0.72	399	50	384	9	386	11	3.78	
017-ZR11N	14	0.0009	0.509	22124	18.30	0.05738	1.63	0.579	2.39	0.0732	1.72	0.72	506	71	455	15	464	18	10.05	Famatinian 0.5 - 0.4 Ga
016-ZR11	9	0.0015	0.458	54585	12.34	0.05705	1.09	0.589	1.71	0.0749	1.27	0.74	494	48	465	11	470	13	5.71	
095-ZR72	7	0.0014	0.371	56215	10.80	0.05757	1.47	0.618	2.20	0.0778	1.60	0.73	513	64	483	15	488	17	5.92	
160-ZR123	7	0.0005	0.559	19626	12.42	0.05533	2.63	0.622	3.65	0.0815	2.50	0.69	426	115	505	24	491	28	-18.72	
049-ZR36	7	0.0015	0.507	115048	48.95	0.05944	1.43	0.671	1.97	0.0818	1.29	0.66	583	62	507	13	521	16	13.04	
038-ZR27N	12	0.0024	0.417	72065	15.15	0.05745	0.67	0.669	1.19	0.0844	0.91	0.76	509	29	523	9	520	10	-2.66	
173-ZR134	10	0.0028	0.692	98759	12.60	0.05881	0.72	0.697	1.36	0.0860	1.09	0.80	560	31	532	11	537	11	5.08	
037-ZR27	10	0.0048	0.356	169544	15.51	0.05762	0.49	0.691	0.90	0.0870	0.65	0.73	515	21	538	7	534	7	-4.41	
106-ZR81	9	0.0038	0.218	119671	14.07	0.05870	0.88	0.705	1.22	0.0870	0.75	0.62	556	38	538	8	542	10	3.25	
144-ZR111	8	0.0015	0.359	55934	13.05	0.05794	1.21	0.702	1.90	0.0878	1.41	0.74	528	53	543	15	540	16	-2.89	
044-ZR31	9	0.0013	0.499	47883	12.94	0.06010	1.09	0.741	1.73	0.0894	1.30	0.75	607	47	552	14	563	15	9.06	

053-ZR38	10	0.0081	0.070	244822	15.67	0.05782	0.35	0.718	0.98	0.0901	0.83	0.85	523	15	556	9	550	8	-6.35	
023-ZR15	9	0.0071	0.349	399031	26.63	0.05879	0.44	0.732	0.81	0.0903	0.57	0.70	559	19	557	6	557	7	0.40	Brazilian/Pampean 0.7 - 0.5 Ga
030-ZR22	15	0.0031	0.922	72073	20.77	0.05857	1.76	0.732	2.55	0.0907	1.81	0.71	551	76	559	19	558	22	-1.53	
182-ZR141	18	0.0042	0.501	67171	21.15	0.05979	0.56	0.756	1.03	0.0917	0.78	0.76	596	24	565	8	572	9	5.16	
067-ZR50	9	0.0006	0.813	26739	11.42	0.06036	2.58	0.767	3.92	0.0921	2.93	0.75	617	109	568	32	578	34	7.87	
120-ZR93	16	0.0028	0.695	55469	21.56	0.05970	1.20	0.765	3.28	0.0930	3.03	0.92	593	52	573	33	577	29	3.30	
131-ZR100	13	0.0046	0.637	151864	16.92	0.05872	0.66	0.757	1.21	0.0934	0.94	0.78	557	29	576	10	572	11	-3.42	
036-ZR26	13	0.0007	1.090	32703	38.44	0.05883	2.54	0.763	3.72	0.0940	2.69	0.72	561	109	579	30	576	32	-3.29	
145-ZR112	12	0.0016	0.924	52682	15.70	0.06116	1.58	0.795	2.35	0.0943	1.70	0.72	645	67	581	19	594	21	9.96	
039-ZR28	8	0.0023	0.490	81991	13.57	0.05895	0.72	0.772	1.13	0.0949	0.79	0.70	565	31	585	9	581	10	-3.44	
112-ZR87	11	0.0019	0.420	68246	12.71	0.05915	1.08	0.781	1.66	0.0957	1.21	0.73	573	47	589	14	586	15	-2.94	
175-ZR136	9	0.0017	0.458	64603	11.66	0.05979	1.25	0.799	1.84	0.0969	1.30	0.71	596	54	596	15	596	17	-0.02	
163-ZR126	8	0.0034	0.636	120202	13.00	0.05922	0.68	0.798	1.18	0.0977	0.89	0.76	575	29	601	10	596	11	-4.50	
138-ZR105	14	0.0013	0.232	44449	14.39	0.06072	1.15	0.823	1.76	0.0983	1.29	0.73	629	49	604	15	610	16	3.98	
003-ZR1	19	0.0035	1.291	76692	21.22	0.06198	0.73	0.841	2.36	0.0984	2.21	0.94	674	31	605	26	620	22	10.20	
192-ZR149	17	0.0019	0.508	69369	15.79	0.05968	1.32	0.812	2.38	0.0987	1.94	0.82	592	57	607	22	604	22	-2.50	
007-ZR5	10	0.0101	0.307	328379	15.43	0.05941	0.31	0.812	0.70	0.0991	0.50	0.72	582	14	609	6	604	6	-4.69	
055-ZR40	11	0.0014	0.772	38645	16.69	0.05977	1.24	0.818	1.89	0.0992	1.37	0.73	595	53	610	16	607	17	-2.44	
186-ZR145	8	0.0014	0.298	56881	11.14	0.06221	1.04	0.859	1.71	0.1001	1.30	0.76	681	44	615	15	629	16	9.78	
180-ZR139	10	0.0007	0.345	23502	13.84	0.06093	2.45	0.850	3.19	0.1012	2.01	0.63	637	104	621	24	625	30	2.43	
162-ZR125	7	0.0017	0.939	80286	10.82	0.06101	0.97	0.859	1.60	0.1021	1.21	0.76	639	42	627	14	629	15	1.99	
185-ZR144	7	0.0019	1.144	72210	12.14	0.06056	1.04	0.854	1.74	0.1022	1.34	0.77	624	45	628	16	627	16	-0.62	
045-ZR32	12	0.0017	0.207	46974	17.92	0.06043	1.06	0.855	1.99	0.1026	1.65	0.83	619	45	630	20	627	19	-1.76	
159-ZR122	8	0.0058	0.308	216316	12.70	0.06129	0.40	0.867	0.96	0.1026	0.79	0.82	649	17	630	9	634	9	3.01	Brazilian/Pampean 0.7 - 0.5 Ga
089-ZR68	7	0.0076	0.023	352377	12.05	0.06142	0.51	0.882	0.92	0.1042	0.66	0.72	654	22	639	8	642	9	2.32	
174-ZR135	8	0.0019	0.407	75887	11.67	0.06094	0.95	0.879	1.44	0.1046	1.01	0.70	637	41	641	12	640	14	-0.70	
059-ZR44	10	0.0012	0.452	31690	16.25	0.06085	1.49	0.881	2.13	0.1050	1.48	0.69	634	64	644	18	642	20	-1.56	
071-ZR54	8	0.0014	1.683	53500	13.11	0.06091	1.26	0.884	1.88	0.1053	1.34	0.71	636	54	645	16	643	18	-1.41	
109-ZR84	9	0.0063	0.311	285491	15.38	0.06151	0.70	0.902	1.01	0.1064	0.63	0.62	657	30	652	8	653	10	0.84	
006-ZR4	75	0.0073	0.343	75298	27.95	0.06322	1.35	0.929	2.04	0.1065	1.48	0.73	716	57	653	18	667	20	8.82	
122-ZR95	28	0.0009	0.277	17036	22.90	0.06723	1.70	0.996	2.58	0.1075	1.91	0.74	845	70	658	24	702	26	22.13	
152-ZR117	10	0.0010	0.669	38183	15.73	0.06139	1.51	0.921	2.31	0.1088	1.71	0.74	653	64	666	22	663	22	-1.96	

056-ZR41	23	0.0023	0.501	93573	26.30	0.06069	1.04	0.912	2.70	0.1090	2.46	0.91	628	45	667	31	658	26	-6.21	
015-ZR10	13	0.0064	0.239	198459	23.85	0.06190	0.38	0.944	0.74	0.1106	0.51	0.70	671	16	676	7	675	7	-0.80	
165-ZR128	7	0.0013	0.516	118010	61.30	0.06113	2.13	0.940	2.96	0.1116	2.02	0.68	644	90	682	26	673	29	-5.94	
074-ZR55	21	0.0038	0.268	136735	13.64	0.06171	1.42	0.961	1.81	0.1129	1.05	0.58	664	60	690	14	684	18	-3.86	
035-ZR25	7	0.0041	0.093	161445	12.42	0.06438	0.68	1.030	1.63	0.1160	1.44	0.88	754	28	708	19	719	17	6.17	
061-ZR46	6	0.0079	0.226	351458	9.73	0.06286	0.60	1.009	1.03	0.1164	0.75	0.73	703	25	710	10	708	10	-0.90	
153-ZR118	8	0.0021	0.264	69436	15.03	0.06526	1.06	1.208	1.98	0.1342	1.64	0.83	783	44	812	25	804	22	-3.74	
097-ZR74	7	0.0054	0.263	227978	11.22	0.06922	0.96	1.291	1.66	0.1352	1.30	0.78	905	39	818	20	842	19	9.69	0.7 - 0.9 Ga
133-ZR102	9	0.0059	0.367	246546	11.13	0.07266	0.51	1.480	0.97	0.1477	0.73	0.76	1005	21	888	12	922	12	11.61	
115-ZR88	19	0.0059	0.292	168111	18.81	0.06520	0.89	1.331	1.97	0.1481	1.72	0.87	781	37	890	29	859	23	-14.03	
191-ZR148	7	0.0023	0.244	130222	20.25	0.07047	0.97	1.454	1.78	0.1496	1.45	0.81	942	40	899	24	911	21	4.60	
019-ZR13	16	0.0030	0.217	66936	19.26	0.07212	0.75	1.539	1.93	0.1548	1.74	0.90	989	31	928	30	946	24	6.20	
070-ZR53	8	0.0038	0.165	120565	13.87	0.07003	0.56	1.503	1.19	0.1557	0.98	0.83	929	23	933	17	932	14	-0.38	
104-ZR79	10	0.0019	0.210	65088	14.62	0.06938	1.35	1.513	2.78	0.1582	2.40	0.86	910	55	947	42	936	34	-4.01	Grenville - Sunsás 1.3 - 0.9 Ga
008-ZR6	12	0.0029	0.253	94533	14.63	0.07113	0.81	1.643	1.22	0.1675	0.83	0.68	961	33	999	15	987	15	-3.90	
168-ZR129	6	0.0010	0.321	41577	10.92	0.07233	2.02	1.706	3.37	0.1710	2.67	0.79	995	81	1018	50	1011	43	-2.27	
004-ZR2	9	0.0035	0.201	134796	12.86	0.07264	0.51	1.644	0.93	0.1642	0.68	0.73	1004	21	980	12	987	12	2.40	
026-ZR18	12	0.0020	3.425	62686	19.45	0.07274	1.13	1.768	3.62	0.1763	3.42	0.94	1007	45	1047	66	1034	46	-3.96	
068-ZR51	12	0.0070	0.675	238776	14.93	0.07277	0.54	1.528	1.57	0.1523	1.42	0.91	1008	22	914	24	942	19	9.32	
069-ZR52	10	0.0060	0.187	216052	15.40	0.07339	0.78	1.615	1.56	0.1596	1.30	0.83	1025	31	954	23	976	19	6.85	
054-ZR39	9	0.0028	0.419	315495	67.03	0.07367	0.58	1.679	0.98	0.1653	0.70	0.71	1032	23	986	13	1001	12	4.47	
010-ZR8	12	0.0040	0.610	120920	16.22	0.07388	0.58	1.801	1.06	0.1768	0.80	0.76	1038	23	1049	16	1046	14	-1.07	
111-ZR86	11	0.0031	0.387	110613	12.59	0.07406	0.85	1.769	1.44	0.1732	1.10	0.76	1043	34	1030	21	1034	19	1.28	
058-ZR43	9	0.0017	0.224	68111	18.41	0.07426	0.99	1.780	1.60	0.1738	1.19	0.75	1048	40	1033	23	1038	21	1.46	
085-ZR64	20	0.0028	0.642	85415	18.39	0.07430	1.25	1.797	1.58	0.1753	0.89	0.56	1050	50	1041	17	1044	21	0.78	
096-ZR73	19	0.0028	0.256	61716	23.13	0.07442	0.91	1.893	2.98	0.1844	2.82	0.94	1053	36	1091	56	1078	39	-3.63	
033-ZR23	13	0.0087	0.180	664728	69.92	0.07457	0.41	1.663	1.25	0.1617	1.12	0.90	1057	17	966	20	994	16	8.57	
077-ZR58	38	0.0030	0.299	42674	24.77	0.07503	1.00	1.690	2.04	0.1633	1.75	0.85	1069	40	975	32	1005	26	8.79	
060-ZR45	15	0.0017	0.730	47628	16.88	0.07558	1.16	1.827	1.55	0.1753	0.96	0.62	1084	46	1041	18	1055	20	3.96	
155-ZR120	16	0.0027	0.298	55734	21.10	0.07570	0.68	1.870	1.21	0.1791	0.93	0.77	1087	27	1062	18	1070	16	2.29	
047-ZR34	35	0.0040	0.520	57188	25.66	0.07608	0.50	1.848	1.07	0.1762	0.87	0.81	1097	20	1046	17	1063	14	4.67	
193-ZR150	9	0.0023	0.397	82856	21.55	0.07642	1.63	1.754	3.10	0.1665	2.61	0.84	1106	64	993	48	1029	40	10.25	

189-ZR146	4	0.0017	0.648	312450	67.94	0.07679	1.07	1.935	1.75	0.1827	1.34	0.76	1116	42	1082	27	1093	23	3.02	
181-ZR140	12	0.0020	0.286	78812	15.73	0.07701	0.85	1.938	1.27	0.1825	0.86	0.68	1121	34	1081	17	1094	17	3.61	
028-ZR20	8	0.0010	0.724	39523	10.90	0.07780	1.44	2.049	2.37	0.1910	1.85	0.78	1142	57	1127	38	1132	32	1.30	
139-ZR106	9	0.0022	0.419	101527	11.73	0.07815	0.76	2.041	1.28	0.1894	0.96	0.75	1151	30	1118	20	1129	17	2.83	
050-ZR37	12	0.0045	0.279	115538	18.79	0.07891	0.63	2.196	1.18	0.2018	0.93	0.78	1170	25	1185	20	1180	16	-1.28	
134-ZR103	5	0.0033	0.344	147762	10.10	0.07956	0.56	2.126	1.13	0.1938	0.91	0.80	1186	22	1142	19	1157	16	3.74	
179-ZR138	6	0.0033	0.710	134907	10.83	0.08027	0.61	2.217	1.08	0.2003	0.81	0.75	1204	24	1177	17	1186	15	2.20	
176-ZR137	6	0.0027	0.353	118753	10.27	0.08092	1.15	2.312	1.43	0.2072	0.76	0.53	1220	45	1214	17	1216	20	0.47	
190-ZR147	6	0.0060	0.222	237137	11.41	0.08105	0.52	2.331	1.07	0.2085	0.86	0.80	1223	20	1221	19	1222	15	0.13	
184-ZR143	9	0.0044	0.332	132836	14.89	0.08114	0.49	2.343	1.14	0.2094	0.96	0.84	1225	19	1226	22	1225	16	-0.06	
140-ZR107	10	0.0010	0.317	37669	13.75	0.08374	2.02	2.524	2.83	0.2186	1.95	0.69	1286	78	1274	45	1279	41	0.93	
117-ZR90	39	0.0080	0.424	145615	25.39	0.08405	0.64	2.515	1.41	0.2170	1.20	0.85	1294	25	1266	28	1276	20	2.12	
161-ZR124	7	0.0021	0.625	84475	10.90	0.08514	0.86	2.597	1.44	0.2212	1.09	0.76	1319	33	1288	25	1300	21	2.30	
034-ZR24	11	0.0018	0.620	63513	13.58	0.08632	0.80	2.726	1.54	0.2290	1.26	0.82	1345	31	1329	30	1335	23	1.21	
130-ZR99	9	0.0103	0.359	334822	14.38	0.08642	0.42	2.666	1.34	0.2237	1.22	0.91	1348	16	1302	29	1319	20	3.41	
088-ZR67	11	0.0106	0.264	389172	16.06	0.08711	0.42	2.688	1.89	0.2238	1.80	0.96	1363	16	1302	42	1325	28	4.49	
108-ZR83	11	0.0028	0.617	93842	13.76	0.09126	0.85	3.108	1.29	0.2469	0.90	0.70	1452	32	1423	23	1435	20	2.02	Rondonia - San Ignacio mobile belt 1.54-1.3 Ga
132-ZR101	12	0.0101	0.660	391373	14.23	0.09243	0.74	3.042	1.18	0.2387	0.83	0.71	1476	28	1380	21	1418	18	6.53	
137-ZR104	7	0.0034	0.192	130577	11.20	0.09282	0.67	2.978	1.12	0.2327	0.83	0.73	1484	25	1348	20	1402	17	9.14	
107-ZR82	21	0.0028	0.689	93580	16.99	0.09355	1.10	3.344	1.59	0.2592	1.09	0.68	1499	41	1486	29	1491	25	0.89	
142-ZR109	9	0.0045	0.452	172686	19.49	0.09509	0.49	3.501	1.00	0.2670	0.78	0.79	1530	19	1526	21	1527	16	0.26	
090-ZR69	115	0.0122	0.386	95612	39.40	0.09550	0.60	3.623	1.53	0.2751	1.36	0.89	1538	23	1567	38	1555	24	-1.87	
098-ZR75	13	0.0043	0.484	135056	16.05	0.09868	1.11	3.828	1.41	0.2813	0.78	0.56	1599	41	1598	22	1599	23	0.08	
048-ZR35	9	0.0072	0.331	302006	14.01	0.10228	0.43	4.211	0.86	0.2986	0.65	0.75	1666	16	1684	19	1676	14	-1.09	
172-ZR133	7	0.0066	0.430	301456	11.45	0.10532	0.38	4.371	0.86	0.3010	0.67	0.78	1720	14	1696	20	1707	14	1.38	Rio Negro - Juruena mobile belt 1.82 - 1.54 Ga
009-ZR7	8	0.0048	0.534	155172	13.90	0.11341	0.50	5.650	1.07	0.3613	0.87	0.81	1855	18	1988	30	1924	18	-7.19	
149-ZR114	10	0.0036	1.356	191522	33.31	0.11545	0.65	5.058	1.34	0.3177	1.12	0.83	1887	23	1779	35	1829	23	5.74	Ventuari-Tapajós (Trans-amazonian) mobile belt 2.0 - 1.82 Ga
164-ZR127	7	0.0097	0.185	356054	12.10	0.11661	1.26	4.993	2.64	0.3105	2.29	0.87	1905	45	1743	70	1818	44	8.49	
005-ZR3	13	0.0025	0.532	75032	15.52	0.11727	0.55	5.523	0.99	0.3416	0.74	0.74	1915	20	1894	24	1904	17	1.09	
100-ZR77	15	0.0112	0.329	357239	17.07	0.11794	0.99	5.575	1.54	0.3428	1.12	0.73	1925	35	1900	37	1912	26	1.30	
119-ZR92	11	0.0044	0.911	152961	12.93	0.12169	0.62	5.807	1.11	0.3460	0.84	0.76	1981	22	1916	28	1947	19	3.30	

116-ZR89	23	0.0038	0.500	72158	21.82	0.12223	0.67	6.182	1.44	0.3668	1.22	0.85	1989	24	2014	42	2002	25	-1.26	
118-ZR91	16	0.0042	0.554	138541	17.51	0.12688	0.97	6.762	1.51	0.3865	1.09	0.72	2055	34	2106	39	2081	26	-2.49	
099-ZR76	6	0.0035	0.573	143674	15.20	0.12761	0.90	6.683	1.57	0.3798	1.23	0.78	2065	32	2075	44	2070	28	-0.49	Maroni - Itacaiúnas Province 2.2 -2.0 Ga
091-ZR70	9	0.0032	1.398	119131	13.17	0.12868	0.70	6.537	1.19	0.3684	0.89	0.75	2080	24	2022	31	2051	21	2.79	
151-ZR116	12	0.0048	0.702	145846	14.79	0.12946	0.46	6.106	1.22	0.3421	1.07	0.88	2091	16	1897	35	1991	21	9.29	
018-ZR12	8	0.0053	0.571	184115	14.07	0.13107	0.37	7.291	0.84	0.4034	0.65	0.78	2112	13	2185	24	2148	15	-3.42	
110-ZR85	9	0.0039	0.322	179510	26.45	0.13227	0.66	7.073	1.35	0.3878	1.12	0.83	2128	23	2113	40	2121	24	0.74	
062-ZR47	12	0.0086	0.625	281309	16.93	0.16566	0.58	10.085	0.99	0.4415	0.71	0.72	2514	20	2357	28	2443	18	6.24	
148-ZR113	11	0.0129	0.455	565737	40.99	0.17205	0.43	11.123	0.87	0.4688	0.66	0.76	2578	14	2478	27	2533	16	3.85	
158-ZR121	64	0.0110	0.330	390719	12.23	0.18555	0.47	14.388	3.31	0.5623	3.25	0.98	2703	16	2876	150	2776	62	-6.40	Central Amazonian province >2.2Ga
025-ZR17	10	0.0038	0.406	151070	12.09	0.18714	0.55	13.930	0.97	0.5398	0.71	0.73	2717	18	2783	32	2745	18	-2.41	
029-ZR21	35	0.0156	0.376	213559	26.68	0.20891	0.64	15.353	2.02	0.5330	1.88	0.93	2897	21	2754	84	2837	38	4.94	

Tabela 3. Sumário dos dados de LA-ICPMS da amostra ARE-305.

Spot	^{204}Pb cps	^{206}Pb mV ¹	Th/U	$^{206}\text{Pb}/^{204}\text{Pb}$	1s %	$^{207}\text{Pb}/^{206}\text{Pb}$	1s %	$^{207}\text{Pb}/^{235}\text{U}$	1s %	$^{206}\text{Pb}/^{238}\text{U}$	1s %	Rho	$^{207}\text{Pb}/^{206}\text{Pb}$	2s abs	$^{206}\text{Pb}/^{238}\text{U}$	2s abs	$^{207}\text{Pb}/^{235}\text{U}$	2s abs	% U-Pb disc ^d	Events
090-ZR69	8	0.0019	0.684	83310	25.38	0.05092	1.08	0.282	1.69	0.0401	1.24	0.74	237	49	253	6	252	8	-6.94	Permian magmatism 0.3 - 0.25 Ma
070-ZR53	12	0.0012	0.888	36835	15.45	0.05235	1.38	0.292	2.22	0.0404	1.69	0.76	301	63	255	8	260	10	15.15	
101-ZR78	6	0.0014	0.585	65163	13.03	0.05126	1.39	0.292	2.06	0.0412	1.47	0.72	252	63	261	8	260	9	-3.24	
053-ZR40	9	0.0010	0.485	30189	14.47	0.05396	1.94	0.370	3.54	0.0497	2.94	0.83	370	86	313	18	320	19	15.36	
003-ZR1	7	0.0015	0.335	58307	11.81	0.05291	0.99	0.373	1.57	0.0511	1.16	0.74	325	45	321	7	322	9	1.14	
052-ZR39	12	0.0017	0.535	64127	24.35	0.05876	1.29	0.604	2.10	0.0745	1.61	0.77	558	56	463	14	479	16	17.06	
143-ZR112	35	0.0015	0.628	46092	48.99	0.06385	2.30	0.689	2.77	0.0782	1.51	0.54	737	96	486	14	532	23	34.09	Famatinian 0.5 - 0.4 Ga
131-ZR102	6	0.0018	0.402	66535	12.68	0.05597	0.88	0.625	1.74	0.0810	1.45	0.84	451	39	502	14	493	14	-11.26	Brazilian/Pampean 0.7 - 0.5 Ga
062-ZR47	14	0.0053	0.466	119192	19.36	0.05785	0.48	0.657	1.01	0.0824	0.80	0.80	524	21	510	8	513	8	2.67	
014-ZR10	13	0.0025	0.267	90427	13.21	0.05828	0.88	0.664	1.26	0.0826	0.83	0.65	540	38	512	8	517	10	5.29	
094-ZR73	12	0.0020	0.390	79853	22.94	0.05756	0.83	0.659	1.35	0.0830	0.99	0.74	513	36	514	10	514	11	-0.22	
065-ZR50	12	0.0012	0.422	36293	17.78	0.05693	1.21	0.665	2.12	0.0848	1.70	0.80	489	53	524	17	518	17	-7.28	

114-ZR89	11	0.0023	0.775	75318	23.27	0.05927	2.39	0.698	3.76	0.0855	2.88	0.77	577	102	529	29	538	31	8.41	
035-ZR26	10	0.0013	1.052	46572	13.52	0.05939	1.54	0.700	2.15	0.0855	1.46	0.68	581	66	529	15	539	18	9.04	
104-ZR81	10	0.0015	0.309	46859	13.88	0.05878	1.14	0.720	1.73	0.0889	1.25	0.72	559	49	549	13	551	15	1.83	
020-ZR16	10	0.0030	0.255	110663	12.87	0.05887	0.66	0.732	1.20	0.0902	0.93	0.77	562	29	556	10	558	10	1.02	
045-ZR34	11	0.0074	0.074	312545	17.07	0.05976	0.47	0.753	1.04	0.0914	0.85	0.82	595	20	564	9	570	9	5.23	
081-ZR62	8	0.0013	0.484	46874	12.39	0.05995	1.19	0.759	1.75	0.0918	1.24	0.71	602	51	566	13	573	15	5.90	
102-ZR79	14	0.0024	0.212	60627	25.54	0.05943	0.75	0.762	1.77	0.0931	1.56	0.88	583	32	574	17	575	15	1.58	
095-ZR74	6	0.0014	1.939	63700	15.76	0.05846	1.45	0.751	2.19	0.0932	1.60	0.73	547	63	574	18	569	19	-4.97	
073-ZR56	23	0.0016	0.495	22635	27.03	0.05519	3.32	0.712	4.26	0.0936	2.64	0.62	420	145	577	29	546	36	-37.36	
124-ZR97	13	0.0029	0.199	85599	16.11	0.05959	0.91	0.788	1.24	0.0959	0.76	0.61	589	39	591	9	590	11	-0.30	
140-ZR109	25	0.0031	0.094	56950	34.12	0.06229	3.24	0.825	4.71	0.0961	3.40	0.72	684	135	591	38	611	43	13.57	
043-ZR32	11	0.0014	0.372	160065	71.96	0.05645	1.50	0.757	2.94	0.0973	2.50	0.85	470	66	598	28	572	26	-27.30	
006-ZR4	7	0.0009	0.277	37208	12.08	0.05970	1.71	0.803	2.71	0.0975	2.07	0.76	593	73	600	24	598	24	-1.15	
106-ZR83	7	0.0010	0.342	30757	14.92	0.05894	1.80	0.793	2.53	0.0975	1.74	0.69	565	77	600	20	593	23	-6.22	
005-ZR3	8	0.0015	0.277	69249	14.28	0.06047	1.41	0.827	2.32	0.0992	1.80	0.78	620	60	610	21	612	21	1.66	
018-ZR14	11	0.0059	0.110	1048038	73.69	0.06050	0.49	0.832	0.93	0.0998	0.70	0.75	621	21	613	8	615	9	1.31	
119-ZR92	6	0.0041	0.267	161449	11.69	0.06034	0.70	0.830	1.13	0.0998	0.81	0.72	616	30	613	9	614	10	0.40	
017-ZR13	9	0.0017	0.297	62662	13.30	0.06039	0.97	0.831	1.76	0.0998	1.42	0.81	618	42	613	17	614	16	0.71	
141-ZR110	45	0.0017	0.536	12880	47.96	0.06399	2.93	0.888	4.34	0.1007	3.19	0.73	741	121	618	38	645	41	16.57	
039-ZR28	12	0.0012	0.309	27688	14.95	0.05741	1.52	0.819	2.33	0.1034	1.73	0.74	507	66	634	21	607	21	-25.01	
040-ZR29	8	0.0019	0.732	71203	12.63	0.05999	0.88	0.866	1.52	0.1047	1.19	0.78	603	38	642	14	634	14	-6.40	
123-ZR96	17	0.0108	0.332	296833	28.13	0.06080	0.43	0.902	0.83	0.1076	0.60	0.72	632	19	659	7	653	8	-4.24	
019-ZR15	11	0.0070	0.376	203217	16.58	0.06573	1.04	1.010	1.35	0.1115	0.78	0.58	798	43	681	10	709	14	14.61	
054-ZR41	7	0.0029	0.063	115884	11.01	0.06402	0.77	1.019	1.39	0.1154	1.09	0.79	742	33	704	15	713	14	5.13	
060-ZR45	11	0.0046	0.431	136201	16.43	0.06597	0.90	1.054	2.21	0.1159	1.98	0.90	805	37	707	26	731	23	12.25	
068-ZR51	24	0.0040	0.502	87166	22.08	0.06019	0.87	1.010	2.18	0.1216	1.96	0.90	610	37	740	27	709	22	-21.22	
115-ZR90	14	0.0036	0.100	97603	17.26	0.06884	0.77	1.217	1.34	0.1282	1.03	0.77	894	32	778	15	808	15	13.03	0.7 - 0.9 Ga
038-ZR27	21	0.0047	0.112	88114	24.69	0.06553	0.54	1.171	1.11	0.1296	0.89	0.80	791	23	786	13	787	12	0.72	
011-ZR9	12	0.0063	0.423	198924	20.00	0.06765	0.76	1.322	1.25	0.1418	0.92	0.74	858	31	855	15	856	14	0.40	
111-ZR86	9	0.0018	0.476	58884	15.26	0.07165	0.97	1.460	1.60	0.1478	1.21	0.76	976	39	889	20	914	19	8.96	
135-ZR106	8	0.0008	0.327	32939	15.69	0.06886	2.56	1.429	4.02	0.1505	3.08	0.77	895	104	904	52	901	47	-1.04	Grenville - Sunsás
109-ZR84	9	0.0014	0.898	47319	16.29	0.07042	1.21	1.473	1.85	0.1517	1.34	0.73	941	49	910	23	919	22	3.22	1.3 - 0.9 Ga

015-ZR11	117	0.0130	0.094	60667	53.76	0.07380	0.41	1.621	4.37	0.1593	4.33	0.99	1036	17	953	77	979	54	8.02	
063-ZR48	11	0.0017	1.075	63868	22.68	0.07139	0.87	1.585	1.43	0.1610	1.07	0.75	968	35	962	19	964	18	0.63	
133-ZR104	7	0.0018	0.673	73929	15.79	0.07212	1.10	1.642	1.81	0.1651	1.38	0.77	989	45	985	25	986	23	0.44	
116-ZR91	8	0.0062	0.311	229873	13.19	0.07191	0.66	1.644	1.02	0.1658	0.69	0.67	983	27	989	13	987	13	-0.58	
120-ZR93	8	0.0034	0.668	129185	12.19	0.07160	0.74	1.666	1.29	0.1688	1.00	0.77	975	30	1005	19	996	16	-3.15	
009-ZR7	9	0.0018	0.532	77537	12.35	0.07285	0.98	1.710	1.97	0.1702	1.66	0.85	1010	40	1013	31	1012	25	-0.35	
105-ZR82	7	0.0023	0.461	88218	11.82	0.07400	0.93	1.808	1.40	0.1772	0.98	0.70	1041	37	1052	19	1048	18	-0.99	
044-ZR33	7	0.0062	0.365	301776	24.00	0.07467	0.45	1.773	1.01	0.1722	0.82	0.81	1060	18	1024	16	1035	13	3.36	
042-ZR31	9	0.0093	0.105	380509	12.34	0.07499	0.32	1.783	0.84	0.1725	0.68	0.81	1068	13	1026	13	1039	11	3.98	
122-ZR95	16	0.0037	0.538	67796	18.74	0.07518	0.72	1.862	1.27	0.1796	0.99	0.77	1073	29	1065	19	1068	17	0.78	
051-ZR38	11	0.0033	0.240	115860	13.72	0.07530	0.55	1.745	1.02	0.1681	0.78	0.76	1077	22	1002	14	1025	13	6.96	
100-ZR77	11	0.0014	0.409	55673	24.45	0.07574	1.71	2.123	3.22	0.2033	2.70	0.84	1088	68	1193	59	1156	44	-9.63	
079-ZR60	15	0.0080	0.285	274371	22.82	0.07591	0.90	2.065	3.31	0.1972	3.16	0.96	1093	36	1161	67	1137	45	-6.19	
125-ZR98	9	0.0017	0.704	62292	12.11	0.07681	0.87	1.900	1.50	0.1794	1.17	0.78	1116	34	1064	23	1081	20	4.71	
007-ZR5	10	0.0022	0.278	81578	12.56	0.08017	0.85	2.260	1.50	0.2044	1.18	0.79	1201	33	1199	26	1200	21	0.16	
059-ZR44	14	0.0080	0.422	223064	20.21	0.08119	0.71	2.362	1.29	0.2110	1.01	0.79	1226	28	1234	23	1231	18	-0.65	
010-ZR8	73	0.0014	0.366	3392	49.04	0.08439	1.85	2.642	2.92	0.2271	2.24	0.76	1302	71	1319	53	1312	43	-1.34	
041-ZR30	8	0.0020	0.217	77368	12.46	0.08594	0.80	2.626	1.41	0.2216	1.11	0.78	1337	31	1290	26	1308	21	3.49	
072-ZR55	10	0.0045	0.534	140266	14.86	0.08627	0.44	2.741	0.97	0.2304	0.78	0.80	1344	17	1337	19	1340	14	0.56	Rondonia - San Ignacio mobile belt 1.54-1.3 Ga
034-ZR25	20	0.0025	0.535	74685	31.07	0.08746	0.75	2.799	1.12	0.2321	0.75	0.67	1371	29	1345	18	1355	17	1.84	
084-ZR65	6	0.0032	0.269	135544	10.78	0.08964	0.78	2.994	2.09	0.2423	1.90	0.91	1418	30	1398	48	1406	32	1.36	
126-ZR99	41	0.0011	0.722	7062	37.03	0.09065	1.84	2.871	2.58	0.2297	1.77	0.69	1439	69	1333	43	1374	39	7.40	
110-ZR85	12	0.0084	0.503	199322	19.95	0.09766	0.54	3.926	2.85	0.2916	2.77	0.97	1580	20	1649	81	1619	46	-4.39	
103-ZR80	9	0.0065	0.302	220214	15.14	0.10171	0.58	4.350	1.84	0.3102	1.71	0.93	1656	21	1741	52	1703	30	-5.18	
074-ZR57	14	0.0090	0.358	376943	35.96	0.10502	0.60	4.812	1.76	0.3323	1.61	0.92	1715	22	1850	52	1787	29	-7.88	Rio Negro - Juruena mobile belt 1.82 - 1.54 Ga
061-ZR46	23	0.0054	0.674	128353	21.03	0.10715	0.58	4.100	1.33	0.2775	1.14	0.85	1751	21	1579	32	1654	22	9.86	
058-ZR43	9	0.0071	0.368	246137	12.88	0.10786	0.46	4.528	1.07	0.3044	0.89	0.83	1763	17	1713	27	1736	18	2.85	
136-ZR107	14	0.0132	0.375	350317	17.83	0.11088	0.85	5.341	2.99	0.3494	2.85	0.95	1814	31	1932	95	1876	51	-6.49	
091-ZR70	23	0.0061	0.558	162757	24.76	0.11459	0.92	5.836	1.73	0.3694	1.42	0.82	1873	33	2026	49	1952	30	-8.16	
033-ZR24	12	0.0027	1.464	85794	14.69	0.11909	0.62	5.759	1.06	0.3507	0.78	0.73	1943	22	1938	26	1940	18	0.24	Ventuari-Tapajós (Trans-amazonian) mobile belt 2.0 - 1.82 Ga
016-ZR12	8	0.0054	0.717	187476	13.69	0.12201	0.50	5.960	1.20	0.3542	1.03	0.85	1986	18	1955	35	1970	21	1.56	
048-ZR35	9	0.0055	0.635	177252	15.08	0.12214	0.43	6.042	0.86	0.3588	0.65	0.76	1988	15	1976	22	1982	15	0.57	

055-ZR42	15	0.0084	0.269	225196	16.99	0.13226	0.48	6.614	0.98	0.3626	0.77	0.78	2128	17	1995	26	2061	17	6.27	Maroni - Itacaiúnas Province 2.2 -2.0 Ga
050-ZR37	9	0.0090	0.571	266698	15.66	0.26422	0.38	23.621	0.84	0.6483	0.64	0.77	3272	12	3222	33	3253	16	1.54	Central Amazonian province >2.2Ga

Tabela 4. Sumário dos dados de LA-ICPMS da amostra ARE-306.

Spot	^{204}Pb cps	^{206}Pb mV ¹	Th/U	$^{206}\text{Pb}/^{204}\text{Pb}$	1s%	$^{207}\text{Pb}/^{206}\text{Pb}$	1s %	$^{207}\text{Pb}/^{235}\text{U}$	1s %	$^{206}\text{Pb}/^{238}\text{U}$	1s %	Rho	$^{207}\text{Pb}/^{206}\text{Pb}$	2s abs	$^{206}\text{Pb}/^{238}\text{U}$	2s abs	$^{207}\text{Pb}/^{235}\text{U}$	2s abs	% U-Pb disc ⁴	Events
103-ZR81	8	0.0007	0.837	25966	11.32	0.05219	2.97	0.272	4.44	0.0378	3.27	0.74	294	133	239	15	244	19	18.50	Triassic rift 250 - 216 Ma
030-ZR24	12	0.0006	0.706	19993	15.23	0.05074	2.83	0.285	3.99	0.0407	2.79	0.70	229	128	257	14	254	18	-12.20	Permian magmatism 0.3 - 0.25 Ga
078-ZR62	13	0.0012	0.375	33451	16.67	0.05241	1.33	0.296	2.07	0.0410	1.55	0.75	303	60	259	8	263	10	14.65	
023-ZR17	13	0.0014	0.425	50898	13.43	0.04947	1.92	0.286	2.49	0.0419	1.54	0.62	170	88	265	8	255	11	-55.61	
096-ZR76	8	0.0005	0.366	21402	15.59	0.05455	2.96	0.325	3.92	0.0432	2.55	0.65	394	130	273	14	286	19	30.81	
110-ZR88	9	0.0014	0.635	50571	14.80	0.05354	1.54	0.330	2.12	0.0446	1.41	0.66	352	69	282	8	289	11	19.97	
025-ZR19	40	0.0010	0.407	4195	49.74	0.05453	3.29	0.354	4.60	0.0471	3.19	0.69	393	144	296	18	308	24	24.56	
017-ZR13	18	0.0024	0.531	58039	19.31	0.05326	0.82	0.458	1.68	0.0623	1.42	0.84	340	37	390	11	383	11	-14.62	0.4 - 0.3 Ga
098-ZR78	11	0.0030	0.401	69338	17.54	0.06008	0.83	0.669	1.35	0.0807	1.00	0.74	607	36	500	10	520	11	17.49	Brazilian/ Pampean 0.7 - 0.5 Ga
074-ZR58	7	0.0023	0.274	99738	18.22	0.05871	0.84	0.700	1.31	0.0865	0.93	0.71	556	36	535	10	539	11	3.85	
007-ZR5	22	0.0021	0.205	38307	25.58	0.06167	1.21	0.759	1.86	0.0892	1.37	0.73	663	52	551	14	573	16	16.85	
066-ZR52	14	0.0011	0.372	28453	18.22	0.05838	1.72	0.720	2.55	0.0894	1.84	0.72	544	75	552	19	550	22	-1.44	
006-ZR4	11	0.0018	0.787	64633	16.03	0.05873	0.80	0.725	1.90	0.0895	1.69	0.89	557	35	552	18	553	16	0.87	
079-ZR63	9	0.0016	0.880	107836	42.36	0.05817	1.32	0.719	1.82	0.0896	1.20	0.66	536	57	553	13	550	15	-3.19	
047-ZR37	13	0.0014	0.482	34414	22.57	0.05844	2.34	0.731	3.55	0.0908	2.65	0.75	546	100	560	28	557	30	-2.52	
045-ZR35	8	0.0007	0.664	28016	11.35	0.06066	1.66	0.784	2.64	0.0937	2.01	0.76	627	71	578	22	588	23	7.92	
024-ZR18	38	0.0037	0.318	20894	39.24	0.06241	0.74	0.809	1.79	0.0940	1.59	0.89	688	31	579	18	602	16	15.87	
118-ZR94	15	0.0020	0.201	60372	17.64	0.05804	1.55	0.765	2.33	0.0956	1.70	0.73	531	67	589	19	577	20	-10.87	
105-ZR83	12	0.0033	0.274	97357	16.52	0.05902	0.76	0.794	1.48	0.0975	1.21	0.82	568	33	600	14	593	13	-5.68	
005-ZR3	26	0.0027	0.375	47881	23.04	0.05854	0.90	0.793	1.39	0.0982	0.99	0.71	550	39	604	11	593	12	-9.74	
026-ZR20	13	0.0023	0.330	66281	16.55	0.05914	0.91	0.805	1.42	0.0987	1.03	0.73	572	39	607	12	600	13	-6.10	
076-ZR60	12	0.0028	0.246	86862	15.30	0.06010	0.72	0.846	1.16	0.1020	0.83	0.72	607	31	626	10	622	11	-3.12	
028-ZR22	30	0.0025	0.271	24105	38.36	0.06098	1.82	0.859	2.63	0.1022	1.87	0.71	639	77	627	22	630	25	1.78	
057-ZR45	10	0.0026	0.089	162229	53.79	0.06127	0.65	0.865	1.23	0.1024	0.98	0.80	649	28	628	12	633	12	3.17	
034-ZR26	12	0.0006	0.598	20439	15.85	0.05401	3.09	0.768	4.37	0.1031	3.07	0.70	372	136	632	37	578	38	-70.23	
093-ZR73	7	0.0011	0.588	49507	21.99	0.06017	1.38	0.860	2.19	0.1036	1.65	0.76	610	59	636	20	630	20	-4.26	

018-ZR14	11	0.0020	0.510	63118	14.84	0.06160	0.84	0.955	1.63	0.1125	1.35	0.82	660	36	687	18	681	16	-4.10	
108-ZR86	7	0.0006	0.610	24613	12.76	0.06255	3.14	0.989	4.60	0.1146	3.34	0.73	693	131	700	44	698	46	-0.98	
086-ZR68	13	0.0039	0.065	121340	16.28	0.06821	0.92	1.095	1.78	0.1165	1.48	0.83	875	38	710	20	751	19	18.83	
088-ZR70	9	0.0045	0.364	135561	16.91	0.06610	0.63	1.143	1.20	0.1255	0.95	0.79	809	26	762	14	774	13	5.87	
106-ZR84	9	0.0030	0.169	109796	13.19	0.06454	0.72	1.117	1.34	0.1255	1.07	0.80	759	30	762	15	761	14	-0.36	0.7 - 0.9 Ga
065-ZR51	11	0.0010	0.465	34300	15.07	0.06216	1.62	1.130	3.40	0.1318	2.96	0.87	680	68	798	44	768	36	-17.42	
113-ZR89	15	0.0022	0.431	76686	18.67	0.06345	1.86	1.293	3.85	0.1478	3.35	0.87	724	78	889	55	843	44	-22.81	
050-ZR40	9	0.0040	0.310	165920	24.72	0.07101	0.89	1.493	1.76	0.1525	1.48	0.84	958	36	915	25	928	21	4.47	
010-ZR8	79	0.0049	0.292	9325	24.29	0.07208	2.26	1.565	3.57	0.1574	2.74	0.77	988	91	942	48	956	44	4.64	
060-ZR48	15	0.0016	0.414	49518	16.87	0.07368	1.31	1.931	2.57	0.1900	2.18	0.85	1033	52	1122	45	1092	34	-8.61	
048-ZR38	10	0.0016	0.394	63339	14.03	0.07374	1.03	1.722	1.65	0.1694	1.23	0.74	1034	42	1009	23	1017	21	2.48	
094-ZR74	6	0.0050	0.439	360546	32.85	0.07376	0.55	1.783	0.91	0.1753	0.61	0.68	1035	22	1041	12	1039	12	-0.60	
077-ZR61	22	0.0033	0.143	102236	14.91	0.07488	0.65	1.842	1.13	0.1784	0.84	0.75	1065	26	1058	16	1060	15	0.69	
020-ZR16	18	0.0146	0.215	340655	20.67	0.07640	1.61	1.881	2.11	0.1786	1.32	0.62	1106	64	1059	26	1074	28	4.20	
055-ZR43	19	0.0029	0.437	88686	15.28	0.07774	0.79	2.260	2.20	0.2108	2.02	0.92	1140	31	1233	45	1200	31	-8.13	Grenville - Sunsás
080-ZR64	9	0.0034	0.192	119887	15.44	0.07908	0.96	2.252	1.88	0.2065	1.57	0.84	1174	38	1210	35	1197	26	-3.08	1.3 - 0.9 Ga
039-ZR31	10	0.0035	0.255	112109	15.01	0.07908	0.97	2.332	2.00	0.2138	1.70	0.85	1174	38	1249	39	1222	28	-6.40	
095-ZR75	3	0.0040	0.221	198752	7.96	0.07984	0.59	2.117	2.50	0.1923	2.40	0.96	1193	23	1134	50	1154	34	4.98	
084-ZR66	8	0.0007	0.709	28301	11.99	0.08007	2.21	2.104	3.27	0.1906	2.38	0.73	1199	86	1125	49	1150	44	6.19	
054-ZR42	16	0.0073	0.581	242221	18.79	0.08021	0.49	2.466	1.52	0.2230	1.39	0.91	1202	19	1298	33	1262	22	-7.96	
070-ZR56	9	0.0073	0.240	278456	13.49	0.08072	0.56	2.318	1.05	0.2082	0.81	0.77	1215	22	1219	18	1218	15	-0.39	
107-ZR85	7	0.0018	0.386	63363	13.08	0.08149	0.83	2.405	1.44	0.2140	1.11	0.77	1233	32	1250	25	1244	21	-1.38	
099-ZR79	4	0.0015	0.220	62264	10.48	0.08195	1.09	2.296	1.69	0.2031	1.24	0.74	1244	42	1192	27	1211	24	4.19	
104-ZR82	110	0.0090	0.277	285538	79.49	0.08586	0.69	2.932	4.81	0.2476	4.75	0.99	1335	26	1426	121	1390	72	-6.83	
008-ZR6	19	0.0068	0.118	140365	19.02	0.08700	1.21	2.946	3.04	0.2456	2.76	0.91	1361	46	1416	70	1394	46	-4.05	Rondonia - San Ignacio mobile belt 1.54-1.3 Ga
063-ZR49	16	0.0040	0.626	112534	23.43	0.08700	1.12	3.100	2.21	0.2584	1.87	0.85	1361	43	1482	49	1433	34	-8.91	
019ZR15	33	0.0052	0.354	138270	21.01	0.09314	0.63	3.559	2.41	0.2771	2.29	0.95	1491	24	1577	64	1540	38	-5.75	
119-ZR95	11	0.0055	0.343	187363	17.67	0.09808	0.61	3.691	1.00	0.2729	0.70	0.70	1588	23	1555	19	1569	16	2.05	
003-ZR1	47	0.0094	0.679	111143	45.03	0.10161	0.83	4.457	2.88	0.3181	2.73	0.95	1654	30	1781	85	1723	47	-7.68	Juruena mobile belt 1.82 - 1.54 Ga
044-ZR34	10	0.0026	0.404	87794	13.67	0.10743	0.88	4.800	2.34	0.3241	2.14	0.91	1756	32	1810	67	1785	39	-3.04	
117-ZR93	13	0.0047	0.392	148500	15.31	0.10785	0.69	4.711	1.18	0.3168	0.88	0.74	1763	25	1774	27	1769	20	-0.59	
109-ZR87	68	0.0095	0.507	9961	7.98	0.11274	0.71	5.523	2.53	0.3553	2.40	0.95	1844	26	1960	81	1904	43	-6.27	Ventuari-Tapajós (Trans-amazonian)
015-ZR11	19	0.0044	0.705	128433	21.80	0.11382	0.47	5.290	0.89	0.3370	0.66	0.74	1861	17	1872	21	1867	15	-0.60	

073-ZR57	9	0.0090	0.664	347909	20.40	0.12015	0.50	6.160	1.21	0.3718	1.04	0.86	1958	18	2038	36	1999	21	-4.05	mobile belt 2.0 - 1.82 Ga
097-ZR77	6	0.0020	1.532	92952	12.77	0.12083	1.11	5.715	1.96	0.3430	1.57	0.80	1969	39	1901	51	1934	34	3.43	
046-ZR36	13	0.0035	0.671	158284	10.78	0.12103	1.03	6.089	2.11	0.3648	1.81	0.85	1971	37	2005	62	1989	37	-1.71	
069-ZR55	11	0.0058	0.796	162937	15.75	0.12159	0.52	5.694	0.95	0.3396	0.69	0.73	1980	19	1885	23	1930	16	4.80	
040-ZR32	7	0.0067	0.176	257356	14.60	0.12464	1.12	6.390	1.43	0.3718	0.81	0.57	2024	39	2038	28	2031	25	-0.70	Maroni - Itacaiúnas Province 2.2 - 2.0 Ga
116-ZR92	17	0.0020	0.405	45282	26.60	0.12793	2.10	6.878	3.26	0.3899	2.46	0.76	2070	73	2122	89	2096	57	-2.54	
075-ZR59	9	0.0023	0.653	69975	14.90	0.12929	1.09	6.680	1.60	0.3747	1.11	0.70	2088	38	2052	39	2070	28	1.76	
027-ZR21	6	0.0068	0.320	339256	22.37	0.20886	0.41	16.066	0.86	0.5578	0.65	0.76	2897	13	2858	30	2881	16	1.35	Central Amazonian province >2.2Ga

Tabela 5. Sumário dos dados de LA-ICPMS da amostra ARE-14.

Spot	^{204}Pb cps	^{206}Pb mV ¹	Th/U	$^{206}\text{Pb}/^{204}\text{Pb}$	1s%	$^{207}\text{Pb}/^{206}\text{Pb}$	1s %	$^{207}\text{Pb}/^{235}\text{U}$	1s %	$^{206}\text{Pb}/^{238}\text{U}$	1s %	Rho	$^{207}\text{Pb}/^{206}\text{Pb}$	2s abs	$^{206}\text{Pb}/^{238}\text{U}$	2s abs	$^{207}\text{Pb}/^{235}\text{U}$	2s abs	% U-Pb disc ⁴	Events
036-ZR22B	4	0.0006	0.272	29108	8.06	0.04977	0.85	0.172	1.16	0.0250	0.69	0.59	184	39	159	2	161	3	13.45	Jurassic Arc 216-132 Ma
049-ZR33	5	0.0006	0.174	32766	9.80	0.05087	0.86	0.178	1.25	0.0254	0.83	0.66	235	39	162	3	167	4	31.20	Triassic rift 250 - 216 Ma
066-ZR44B	1	0.0009	0.591	56267	5.62	0.05045	1.27	0.275	1.52	0.0396	0.76	0.50	216	58	250	4	247	7	-15.98	250 - 216 Ma
060-ZR42	1	0.0004	0.920	27895	4.26	0.05216	1.15	0.285	1.41	0.0397	0.73	0.52	293	52	251	4	255	6	14.31	
048-ZR35-COMP	2	0.0003	0.298	20646	4.95	0.05361	1.26	0.300	1.60	0.0406	0.91	0.57	354	56	256	5	266	7	27.68	Permian magmatism 0.3 - 0.25 Ga
077-ZR53	4	0.0007	0.489	39503	8.08	0.05166	0.94	0.302	1.22	0.0424	0.69	0.56	270	43	268	4	268	6	0.94	
070-ZR48	1	0.0005	0.356	30970	8.88	0.05246	1.27	0.321	1.58	0.0444	0.85	0.54	305	58	280	5	283	8	8.36	
028-ZR20-COMP	1	0.0012	0.252	73958	4.16	0.05282	0.68	0.335	2.23	0.0460	2.10	0.94	321	31	290	12	293	11	9.68	
079-ZR59-COMP	1	0.0006	0.462	37585	6.14	0.05645	1.15	0.446	2.29	0.0573	1.94	0.85	470	51	359	14	375	14	23.51	0.4 - 0.3 Ga
053-ZR38-COMP	2	0.0012	0.354	66401	4.94	0.05558	0.69	0.441	1.46	0.0576	1.23	0.84	436	31	361	9	371	9	17.19	
014-ZR9-COMP	2	0.0012	0.525	71415	7.43	0.05745	1.26	0.555	4.42	0.0701	4.22	0.96	509	55	437	36	448	32	14.21	
031-ZR21	5	0.0002	0.486	10795	13.01	0.05729	1.64	0.557	1.95	0.0705	0.98	0.50	503	71	439	8	450	14	12.66	
065-ZR47-COMP	2	0.0005	1.604	32535	6.79	0.05958	1.00	0.633	1.62	0.0770	1.21	0.75	588	43	478	11	498	13	18.69	Famatinian 0.5 - 0.4 Ga
011-ZR7	7	0.0010	0.293	39107	13.74	0.05695	0.78	0.626	1.25	0.0797	0.91	0.73	490	34	495	9	494	10	-1.00	
039-ZR29-COMP	2	0.0010	0.497	57061	7.79	0.05817	0.78	0.640	1.40	0.0798	1.10	0.78	536	34	495	10	503	11	7.70	
005-ZR2-COMP	1	0.0016	0.430	89445	6.53	0.05752	0.52	0.635	1.43	0.0800	1.28	0.89	512	23	496	12	499	11	3.02	
009-ZR6-COMP	1	0.0017	0.618	98237	4.55	0.05715	1.06	0.640	3.66	0.0812	3.48	0.95	497	46	503	34	502	29	-1.20	
058-ZR43-COMP	1	0.0024	0.156	148807	6.20	0.05716	0.56	0.642	1.54	0.0815	1.38	0.90	498	25	505	13	504	12	-1.45	
057-ZR42-COMP	1	0.0012	0.334	73051	6.27	0.05853	0.85	0.663	2.58	0.0821	2.41	0.93	550	37	509	24	516	21	7.45	

028-ZR18	3	0.0005	0.179	25360	9.04	0.06312	0.97	0.920	1.27	0.1057	0.73	0.58	712	41	648	9	662	12	9.10	Brazilian/Pampean
074-ZR54-COMP	2	0.0014	0.922	77394	9.36	0.06212	0.67	0.944	1.37	0.1102	1.13	0.83	678	29	674	14	675	13	0.59	0.7 - 0.5 Ga
019-ZR14-COMP	1	0.0011	0.434	67457	11.37	0.06275	1.02	0.955	2.57	0.1103	2.33	0.91	700	43	675	30	681	25	3.59	
075-ZR55-COMP	1	0.0009	0.457	50146	6.90	0.06516	1.13	1.044	1.81	0.1162	1.36	0.75	779	47	709	18	726	19	9.04	
006-ZR3-COMP	1	0.0008	0.703	46270	8.59	0.06703	1.00	1.180	2.08	0.1277	1.78	0.86	839	41	775	26	791	23	7.64	
048-ZR32	3	0.0007	0.395	41892	8.27	0.06521	0.65	1.165	1.23	0.1295	0.98	0.80	781	27	785	14	784	13	-0.52	
030-ZR22-COMP	2	0.0006	0.561	34812	6.53	0.06759	0.86	1.214	2.36	0.1303	2.16	0.92	856	36	789	32	807	26	7.80	
045-ZR29	8	0.0020	0.288	96117	13.07	0.06423	1.14	1.166	1.50	0.1317	0.90	0.60	749	48	797	13	785	16	-6.43	0.7 - 0.9 Ga
008-ZR4	4	0.0003	0.271	18329	8.51	0.06878	1.14	1.297	1.75	0.1368	1.27	0.73	892	47	826	20	844	20	7.36	
009-ZR5	3	0.0031	0.233	159577	10.95	0.06878	0.53	1.317	1.52	0.1389	1.38	0.90	892	22	838	22	853	17	6.04	
041-ZR27	4	0.0027	0.109	129695	10.24	0.07081	0.77	1.369	1.77	0.1402	1.55	0.88	952	31	846	25	876	21	11.15	
017-ZR10	5	0.0017	0.414	104148	25.97	0.07022	0.56	1.406	1.00	0.1452	0.74	0.74	935	23	874	12	891	12	6.52	
059-ZR41	1	0.0001	0.546	7121	4.08	0.07021	1.39	1.411	2.65	0.1458	2.23	0.84	934	56	877	36	894	31	6.13	
025-ZR17-COMP	2	0.0003	0.607	18133	6.21	0.07267	1.99	1.515	2.84	0.1511	1.99	0.70	1005	80	907	34	936	34	9.70	
030-ZR20	2	0.0006	0.397	34150	6.14	0.07016	0.83	1.473	1.16	0.1523	0.72	0.62	933	34	914	12	919	14	2.09	
034-ZR24-COMP	1	0.0003	0.595	19086	5.78	0.07387	1.32	1.566	2.75	0.1537	2.39	0.87	1038	53	922	41	957	34	11.19	
021-ZR13	5	0.0014	0.279	56165	13.13	0.07190	0.85	1.550	1.17	0.1563	0.72	0.61	983	34	936	12	950	14	4.78	
027-ZR17	5	0.0018	0.189	72643	15.61	0.07158	0.65	1.549	1.02	0.1570	0.70	0.68	974	26	940	12	950	13	3.51	
015-ZR10-COMP	1	0.0011	0.220	63126	7.03	0.07096	0.67	1.539	3.01	0.1573	2.91	0.97	956	27	942	51	946	37	1.53	
004-ZR1	7	0.0012	0.511	46565	14.00	0.07123	0.90	1.582	1.25	0.1611	0.80	0.64	964	36	963	14	963	16	0.12	
067-ZR49-COMP	2	0.0022	0.285	134103	8.74	0.07366	0.55	1.648	1.18	0.1622	0.97	0.82	1032	22	969	17	989	15	6.11	
061-ZR43	1	0.0004	0.260	28102	3.18	0.07535	1.00	1.729	1.59	0.1664	1.18	0.74	1078	40	992	22	1019	20	7.92	Grenville - Sunsás 1.3 - 0.9 Ga
075-ZR51	7	0.0013	0.800	53924	12.00	0.07230	0.57	1.668	1.03	0.1673	0.78	0.75	994	23	997	14	997	13	-0.31	
027-ZR19-COMP	1	0.0015	0.115	88471	8.11	0.07242	1.61	1.752	2.58	0.1754	1.98	0.77	998	65	1042	38	1028	33	-4.43	
044-ZR31-COMP	1	0.0026	0.296	243344	35.47	0.07399	0.48	1.759	1.32	0.1724	1.17	0.89	1041	19	1025	22	1031	17	1.51	
057-ZR39	1	0.0010	0.313	64031	5.73	0.07411	0.64	1.744	1.08	0.1707	0.79	0.73	1044	26	1016	15	1025	14	2.75	
047-ZR31	4	0.0016	0.408	66614	10.37	0.07457	0.55	1.731	0.99	0.1683	0.74	0.74	1057	22	1003	14	1020	13	5.11	
044-ZR28	7	0.0043	0.098	162173	12.88	0.07469	0.55	1.852	1.15	0.1798	0.94	0.82	1060	22	1066	19	1064	15	-0.52	
050-ZR34	3	0.0005	0.939	28195	9.06	0.07638	0.79	1.973	1.41	0.1873	1.11	0.78	1105	31	1107	22	1106	19	-0.16	
013-ZR8-COMP	16	0.0007	0.301	40587	5.27	0.07947	1.22	2.109	3.55	0.1924	3.31	0.93	1184	48	1135	69	1152	48	4.17	
056-ZR38	1	0.0012	0.355	74355	3.18	0.07959	0.55	2.211	1.09	0.2014	0.87	0.80	1187	22	1183	19	1184	15	0.32	
054-ZR36	2	0.0016	0.256	95520	8.20	0.08044	0.66	2.222	1.29	0.2003	1.05	0.81	1208	26	1177	22	1188	18	2.55	

080-ZR56	6	0.0008	0.380	32176	11.81	0.08070	0.61	2.230	1.11	0.2004	0.86	0.77	1214	24	1178	18	1191	16	2.99	
029-ZR19	5	0.0025	0.418	115352	12.76	0.08122	0.68	2.349	0.97	0.2097	0.59	0.60	1227	26	1227	13	1227	14	-0.05	
054-ZR39-COMP	1	0.0008	0.199	46857	5.07	0.08146	0.72	2.117	1.36	0.1885	1.09	0.80	1232	28	1113	22	1154	19	9.68	
035-ZR25-COMP	68	0.0034	0.353	81395	24.78	0.08875	2.23	2.695	3.01	0.2202	1.99	0.66	1399	84	1283	46	1327	44	8.27	
049-ZR36-COMP	13	0.0068	0.063	177986	17.34	0.08897	0.56	2.688	1.86	0.2191	1.74	0.93	1403	21	1277	40	1325	27	8.99	Rondonia - San Ignacio mobile belt 1.54-1.3 Ga
069-ZR51-COMP	1	0.0042	0.279	264471	5.74	0.09014	0.59	3.088	1.09	0.2484	0.84	0.77	1429	23	1430	21	1430	17	-0.12	
084-ZR60	4	0.0004	0.522	19374	10.30	0.09028	1.25	3.022	1.71	0.2427	1.12	0.65	1431	47	1401	28	1413	26	2.13	
083-ZR59	5	0.0054	0.334	227575	13.62	0.09080	0.55	3.125	1.29	0.2496	1.11	0.86	1442	21	1436	28	1439	20	0.41	
026-ZR18-COMP	2	0.0042	0.037	258939	6.95	0.09739	0.37	3.793	1.49	0.2825	1.40	0.94	1575	14	1604	40	1591	24	-1.86	
020-ZR12	4	0.0002	1.232	10475	14.37	0.09752	1.25	3.496	2.79	0.2600	2.47	0.88	1577	47	1490	66	1526	44	5.54	Rio Negro - Juruena mobile belt 1.82 - 1.54 Ga
068-ZR50-COMP	5	0.0057	0.331	273206	10.18	0.09757	0.50	3.423	2.46	0.2545	2.38	0.97	1578	19	1461	62	1510	38	7.40	
010-ZR6	4	0.0048	0.170	249755	9.56	0.09998	0.48	3.678	1.14	0.2668	0.96	0.84	1624	18	1524	26	1567	18	6.12	
040-ZR26	5	0.0025	0.515	107123	11.17	0.10678	0.58	4.423	1.09	0.3004	0.85	0.78	1745	21	1693	25	1717	18	2.96	
077-ZR57-COMP	3	0.0022	0.678	124331	9.24	0.11536	0.46	5.344	1.75	0.3359	1.64	0.94	1886	17	1867	53	1876	30	0.99	
069-ZR47	1	0.0028	0.453	171062	5.92	0.11580	0.48	5.400	0.92	0.3382	0.69	0.75	1892	17	1878	22	1885	16	0.76	Ventuari-Tapajós (Trans-amazonian) mobile belt 2.0 - 1.82 Ga
039-ZR25	6	0.0038	0.557	169126	11.31	0.11626	0.48	5.151	1.05	0.3213	0.86	0.82	1900	17	1796	27	1845	18	5.44	
016-ZR11-COMP	3	0.0073	0.664	1043300	66.17	0.12275	0.43	5.884	3.87	0.3476	3.83	0.99	1997	15	1923	127	1959	66	3.67	
029-ZR21-COMP	17	0.0061	0.364	451631	47.28	0.12657	0.54	5.845	2.60	0.3349	2.52	0.97	2051	19	1862	81	1953	45	9.21	Marconi - Icataiúmas Province 2.2 - 2.0 Ga
024-ZR16-COMP	30	0.0026	0.293	27047	22.86	0.13136	0.39	6.801	2.35	0.3755	2.29	0.97	2116	14	2055	80	2086	41	2.89	
018-ZR13-COMP	2	0.0023	0.701	135869	7.91	0.13188	0.51	7.370	2.23	0.4053	2.14	0.96	2123	18	2193	79	2157	40	-3.32	
033-ZR23-COMP	2	0.0047	0.346	312182	15.13	0.13693	0.42	7.656	2.55	0.4055	2.49	0.98	2189	15	2194	92	2191	45	-0.25	
067-ZR45	5	0.0046	0.267	216814	12.23	0.18002	0.40	12.740	0.90	0.5132	0.71	0.79	2653	13	2670	31	2661	17	-0.65	Central Amazonian province >2.2Ga
025-ZR15	6	0.0082	0.604	345831	10.63	0.28572	0.54	23.991	1.01	0.6089	0.76	0.76	3394	17	3066	37	3268	20	9.69	

Tabela 6. Sumário dos dados de LA-ICPMS da amostra ARE-367.

Spot	204Pb cps	206Pb mV ¹	Th/U	206Pb/204Pb	1s %	207Pb/206Pb	1s %	207Pb/235U	1s %	206Pb/238U	1s %	Rho	207Pb/206Pb	2s abs	206Pb/238U	2s abs	207Pb/235U	2s abs	% U-Pb disc ⁴	Events
020-ZR15	11	0.0014	0.471	39029	16.78	0.05195	1.15	0.272	1.73	0.0379	1.25	0.72	283	52	240	6	244	8	15.27	Triassic rift 250 - 216 Ma
024-ZR17	12	0.0017	0.640	43736	19.30	0.05189	0.97	0.274	1.60	0.0383	1.22	0.76	281	44	242	6	246	7	13.58	
046-ZR35	26	0.0024	0.262	38512	24.11	0.05442	1.26	0.302	2.61	0.0402	2.26	0.86	389	56	254	11	268	12	34.63	Permian magmatism 0.3 - 0.25 Ma
013-ZR8	8	0.0005	0.769	21978	13.21	0.05184	3.06	0.289	4.91	0.0404	3.82	0.78	279	137	255	19	258	22	8.31	
040-ZR31	12	0.0011	0.634	44446	14.25	0.05166	1.51	0.299	2.47	0.0420	1.92	0.78	271	68	265	10	266	12	2.06	

033-ZR24	10	0.0011	0.435	36979	15.83	0.05271	3.17	0.310	3.82	0.0427	2.10	0.55	316	141	270	11	275	18	14.80	
014-ZR9	11	0.0022	0.486	83125	19.41	0.05116	1.22	0.313	1.90	0.0444	1.41	0.74	248	55	280	8	277	9	-12.98	
140-ZR109	10	0.0012	0.285	45973	16.48	0.05718	3.69	0.732	4.89	0.0928	3.19	0.65	498	159	572	35	557	42	-14.80	
137-ZR106	7	0.0018	0.223	79754	9.95	0.05879	1.15	0.765	2.02	0.0943	1.62	0.80	559	50	581	18	577	18	-3.89	
145-ZR112	14	0.0006	1.298	16045	17.97	0.05986	3.16	0.780	4.47	0.0944	3.14	0.70	598	134	582	35	585	39	2.79	Brazilian/Pampean
029-ZR22	14	0.0010	0.531	47457	40.85	0.05515	2.23	0.719	3.81	0.0945	3.07	0.80	418	98	582	34	550	32	-39.23	
053-ZR40	7	0.0006	0.384	23260	12.15	0.06034	3.00	0.798	4.44	0.0959	3.25	0.73	616	127	590	37	595	40	4.19	Brazilian/Pampean
165-ZR128	9	0.0014	0.394	80836	34.42	0.06113	1.33	0.822	1.96	0.0976	1.39	0.71	644	57	600	16	609	18	6.78	0.7 - 0.5 Ga
146-ZR113	14	0.0023	0.530	53874	20.89	0.05850	3.45	0.891	4.36	0.1104	2.63	0.60	548	147	675	34	647	41	-23.14	
118-ZR92	8	0.0022	0.418	91824	13.67	0.06133	1.43	0.943	3.16	0.1115	2.80	0.88	651	61	682	36	675	31	-4.75	
127-ZR99	79	0.0023	0.357	2598	14.60	0.06782	2.82	1.089	3.96	0.1164	2.75	0.69	863	115	710	37	748	41	17.73	
134-ZR104	10	0.0023	0.051	82662	34.47	0.06239	3.54	1.030	4.39	0.1197	2.57	0.59	688	147	729	35	719	45	-5.97	
155-ZR120	23	0.0059	0.375	164073	22.53	0.06031	0.58	1.019	3.39	0.1225	3.32	0.98	615	25	745	47	713	34	-21.25	0.9 - 0.7 Ga
153-ZR118	13	0.0014	0.329	39285	16.10	0.06504	1.47	1.103	2.26	0.1230	1.68	0.74	776	61	748	24	755	24	3.64	
025-ZR18	12	0.0015	0.368	41863	18.06	0.06944	1.48	1.233	4.07	0.1288	3.78	0.93	912	60	781	55	816	45	14.36	
043-ZR32	13	0.0029	0.122	76243	23.83	0.06779	2.82	1.396	4.69	0.1494	3.73	0.79	862	115	897	62	887	55	-4.09	
148-ZR115	8	0.0011	0.149	51868	16.78	0.07259	2.32	1.531	4.42	0.1530	3.74	0.85	1002	93	918	64	943	54	8.46	
063-ZR48	14	0.0023	0.334	84821	14.07	0.06702	1.52	1.485	2.90	0.1607	2.45	0.84	838	63	961	44	924	35	-14.60	
123-ZR95	4	0.0042	0.271	210815	8.93	0.07402	0.72	1.683	1.46	0.1649	1.21	0.83	1042	29	984	22	1002	18	5.57	
003-ZR1B	16	0.0042	0.183	100899	30.02	0.06987	2.14	1.592	3.36	0.1652	2.56	0.76	925	87	986	47	967	41	-6.59	
128-ZR100	9	0.0023	0.102	115837	27.01	0.07282	0.94	1.675	1.99	0.1668	1.71	0.86	1009	38	995	31	999	25	1.40	
130-ZR102	10	0.0020	0.207	84632	15.46	0.07216	1.67	1.788	3.05	0.1797	2.53	0.83	991	67	1065	50	1041	39	-7.55	
004-ZR1N	12	0.0011	0.338	37673	26.31	0.07233	3.15	1.769	4.47	0.1774	3.15	0.70	995	125	1053	61	1034	57	-5.77	
158-ZR123	19	0.0008	1.567	25650	15.48	0.07234	2.74	1.839	3.84	0.1844	2.67	0.69	995	109	1091	53	1060	50	-9.58	Grenville - Sunsás
007-ZR4	14	0.0027	0.264	91879	17.86	0.07490	1.04	1.920	3.02	0.1859	2.81	0.93	1066	42	1099	57	1088	40	-3.09	1.3 - 0.9 Ga
054-ZR41	11	0.0036	0.204	147898	18.34	0.07537	1.34	2.052	3.04	0.1975	2.70	0.89	1078	53	1162	57	1133	41	-7.75	
160-ZR125	14	0.0019	0.671	52271	19.94	0.07556	1.05	2.055	3.22	0.1972	3.03	0.94	1083	42	1160	64	1134	44	-7.10	
119-ZR93	10	0.0032	0.074	180675	33.76	0.07680	1.04	2.014	2.15	0.1902	1.85	0.86	1116	41	1122	38	1120	29	-0.56	
138-ZR107	4	0.0032	0.226	154542	9.56	0.07986	0.81	2.136	2.61	0.1940	2.46	0.94	1194	32	1143	51	1161	36	4.25	
059-ZR46	14	0.0019	0.151	61278	15.96	0.08018	1.04	2.233	1.72	0.2020	1.32	0.77	1201	41	1186	29	1192	24	1.27	
076-ZR59	11	0.0024	0.197	81882	15.46	0.08074	1.04	2.385	1.88	0.2142	1.52	0.81	1215	41	1251	35	1238	27	-2.98	
113-ZR87	10	0.0047	0.234	183103	13.11	0.08140	0.60	2.514	3.22	0.2240	3.14	0.98	1231	23	1303	74	1276	46	-5.83	

068-ZR53	17	0.0018	0.197	44956	24.82	0.08383	2.51	2.659	4.55	0.2301	3.77	0.83	1289	96	1335	91	1317	66	-3.59	
115-ZR89	11	0.0023	0.297	110982	36.33	0.08431	1.50	2.885	2.69	0.2481	2.21	0.82	1300	58	1429	56	1378	40	-9.92	Rondonia - San Ignacio mobile belt 1.54-1.3 Ga
034-ZR25	12	0.0077	0.238	255739	15.35	0.08468	0.86	2.772	1.85	0.2374	1.59	0.86	1308	33	1373	39	1348	27	-4.95	
057-ZR44	16	0.0041	0.215	131014	34.82	0.08573	1.64	2.766	2.15	0.2340	1.33	0.62	1332	63	1355	33	1346	32	-1.74	
027-ZR20	36	0.0032	0.212	59272	22.86	0.08698	1.19	3.101	3.58	0.2586	3.36	0.94	1360	45	1482	89	1433	54	-8.99	
154-ZR119	13	0.0025	0.318	72723	16.42	0.08754	0.87	2.678	1.98	0.2219	1.74	0.88	1372	33	1292	41	1322	29	5.87	
147-ZR114	10	0.0032	0.543	130134	13.89	0.09400	0.84	3.278	2.26	0.2529	2.07	0.91	1508	31	1453	54	1476	35	3.63	
104-ZR80	3	0.0020	0.423	106894	8.36	0.09410	1.28	3.456	3.69	0.2664	3.45	0.93	1510	48	1522	93	1517	57	-0.81	
107-ZR83	9	0.0045	0.214	236167	16.64	0.09556	1.73	3.670	4.27	0.2785	3.88	0.91	1539	65	1584	109	1565	67	-2.90	
143-ZR110	14	0.0028	0.772	71250	18.30	0.09593	0.79	3.400	1.33	0.2571	1.00	0.75	1546	29	1475	26	1505	21	4.63	
045-ZR34	12	0.0011	0.158	31391	16.00	0.09719	2.16	3.846	4.63	0.2869	4.08	0.88	1571	80	1626	117	1602	73	-3.52	Rio Negro - Juruena mobile belt 1.82 - 1.54 Ga
144-ZR111	12	0.0022	0.530	66082	15.81	0.09733	1.35	3.736	3.05	0.2784	2.70	0.89	1574	50	1583	76	1579	48	-0.61	
114-ZR88	11	0.0041	0.471	118271	24.01	0.09744	2.38	3.708	3.53	0.2760	2.58	0.73	1576	88	1571	72	1573	56	0.29	
125-ZR97	12	0.0037	0.608	139295	16.45	0.09784	0.63	3.496	1.72	0.2591	1.55	0.90	1583	24	1485	41	1526	27	6.19	
129-ZR101	12	0.0051	0.178	175499	18.70	0.09802	0.88	4.081	2.06	0.3020	1.82	0.89	1587	33	1701	54	1651	33	-7.20	
056-ZR43	86	0.0145	0.113	54187	46.66	0.09936	0.64	3.832	2.14	0.2797	2.01	0.94	1612	24	1590	56	1600	34	1.38	
124-ZR96	8	0.0048	0.277	190143	11.20	0.09976	0.64	3.755	1.09	0.2730	0.81	0.74	1620	24	1556	22	1583	17	3.92	
028-ZR21	12	0.0211	0.245	531298	17.53	0.09986	0.86	4.136	3.15	0.3003	3.01	0.95	1621	32	1693	89	1661	51	-4.41	
035-ZR26	11	0.0062	0.088	429857	63.69	0.09988	1.57	4.063	2.54	0.2950	1.96	0.77	1622	58	1666	57	1647	41	-2.75	
080-ZR63	11	0.0044	0.395	168409	20.52	0.10093	2.82	4.077	4.87	0.2929	3.95	0.81	1641	103	1656	115	1650	78	-0.91	
009-ZR6	19	0.0058	0.289	174582	38.01	0.10451	1.17	4.415	2.21	0.3063	1.84	0.83	1706	43	1723	55	1715	36	-0.99	
105-ZR81	3	0.0030	0.024	156118	17.30	0.11180	3.01	5.645	4.37	0.3661	3.14	0.72	1829	107	2011	108	1923	74	-9.97	Ventuari-Tapajós (Trans-amazonian) mobile belt 2.0 - 1.82 Ga
086-ZR67	21	0.0160	0.426	391725	19.94	0.11231	0.77	4.762	3.05	0.3075	2.93	0.96	1837	28	1728	89	1778	51	5.93	
108-ZR84	5	0.0029	0.108	111431	25.42	0.11976	1.73	5.845	3.10	0.3539	2.54	0.82	1953	61	1953	85	1953	53	-0.04	
066-ZR51	11	0.0046	0.082	227562	37.43	0.12164	2.08	5.897	3.05	0.3515	2.20	0.72	1980	73	1942	74	1961	52	1.95	
026-ZR19	17	0.0032	0.607	75962	23.38	0.12365	1.24	6.730	2.57	0.3947	2.21	0.86	2010	44	2145	81	2077	45	-6.72	Maroni - Itacaiúnas Province 2.2 - 2.0 Ga
030-ZR23	9	0.0036	0.733	152712	15.52	0.12384	1.28	6.577	2.45	0.3852	2.06	0.84	2012	45	2100	73	2056	43	-4.38	
157-ZR122	11	0.0116	0.416	338508	16.61	0.12478	0.65	6.534	3.01	0.3798	2.92	0.97	2026	23	2075	103	2051	52	-2.44	
050-ZR39	9	0.0066	0.591	660959	55.77	0.12524	0.73	6.552	1.32	0.3794	1.04	0.79	2032	26	2074	37	2053	23	-2.04	
008-ZR5	23	0.0037	0.491	72330	28.75	0.12627	1.31	6.510	4.58	0.3739	4.37	0.95	2047	46	2048	152	2047	79	-0.06	
039-ZR30	15	0.0039	0.477	94496	19.15	0.12955	0.81	6.728	1.37	0.3767	1.03	0.76	2092	28	2061	36	2076	24	1.49	
149-ZR116	16	0.0138	0.539	403040	20.47	0.17612	0.91	11.364	1.59	0.4680	1.25	0.79	2617	30	2475	51	2554	30	5.43	

060-ZR47	18	0.0017	0.394	44190	19.46	0.18884	1.36	15.195	4.61	0.5835	4.39	0.95	2732	44	2963	207	2828	86	-8.46	Central Amazonian province >2.2Ga
169-ZR132	15	0.0165	0.493	453648	24.55	0.19722	0.88	14.977	2.61	0.5507	2.42	0.93	2803	29	2828	111	2814	49	-0.89	

Tabela 7. Sumário dos dados de LA-ICPMS da amostra ARE-16.

Spot		^{204}Pb cps	^{206}Pb mV ¹	Th/U	$^{206}\text{Pb}/^{204}\text{Pb}$	1s %	$^{207}\text{Pb}/^{206}\text{Pb}$	1s %	$^{207}\text{Pb}/^{235}\text{U}$	1s %	$^{206}\text{Pb}/^{238}\text{U}$	1s %	Rho	$^{207}\text{Pb}/^{206}\text{Pb}$	2s abs	$^{206}\text{Pb}/^{238}\text{U}$	2s abs	$^{207}\text{Pb}/^{235}\text{U}$	2s abs	% U-Pb disc ⁴	Events
045-ZR32-COMP	4	0.0006	0.259	37074	8.65	0.05050	1.63	0.171	1.95	0.0246	1.01	0.52	218	75	157	3	161	6	28.18	Jurassic Arc 216-130 Ma	
036-ZR26-COMP	2	0.0003	0.250	16151	6.68	0.05284	1.53	0.183	2.21	0.0251	1.55	0.70	322	69	160	5	171	7	50.33		
018-ZR13	3	0.0007	0.623	36394	10.21	0.04971	0.96	0.190	1.19	0.0277	0.59	0.50	181	44	176	2	177	4	2.69		
058-ZR43-COMP	1	0.0005	0.625	26665	7.45	0.05471	1.63	0.295	2.04	0.0391	1.16	0.57	400	72	248	6	263	9	38.16		
052-ZR37-COMP	1	0.0025	0.273	156987	5.78	0.05163	0.70	0.280	2.89	0.0393	2.78	0.96	269	32	248	14	250	13	7.67		
057-ZR42	3	0.0008	0.769	43161	7.37	0.05181	0.80	0.282	1.06	0.0394	0.60	0.56	277	36	249	3	252	5	9.96		
045-ZR32	3	0.0007	0.614	40204	10.83	0.05201	1.16	0.293	1.49	0.0409	0.85	0.57	286	53	258	4	261	7	9.63		
059-ZR44	3	0.0008	0.326	46958	8.88	0.05310	0.99	0.325	1.22	0.0444	0.61	0.50	333	44	280	3	286	6	15.94		
046-ZR33-COMP	2	0.0012	0.165	65957	7.97	0.05292	0.79	0.350	1.51	0.0480	1.23	0.82	325	35	302	7	305	8	7.08		
059-ZR44-COMP	1	0.0010	0.244	250094	75.21	0.05432	1.09	0.361	2.33	0.0482	2.03	0.87	384	49	303	12	313	13	21.03	0.4 - 0.3 Ga	
024-ZR16	6	0.0014	0.591	63061	12.24	0.05416	0.76	0.443	1.05	0.0593	0.62	0.59	378	34	371	4	372	7	1.63		
009-ZR6-COMP	1	0.0004	0.270	21715	6.96	0.05908	1.07	0.678	1.89	0.0833	1.51	0.80	570	46	516	15	526	15	9.54		
020-ZR15-COMP	3	0.0010	0.392	62779	8.50	0.05835	0.78	0.679	1.32	0.0844	1.00	0.76	543	34	522	10	526	11	3.86		
034-ZR24	5	0.0005	0.907	28080	11.52	0.05850	0.87	0.684	1.28	0.0848	0.86	0.67	548	38	525	9	529	10	4.35		
008-ZR5-COMP	1	0.0005	0.257	31382	7.36	0.05994	0.97	0.702	1.41	0.0849	0.96	0.68	602	42	525	10	540	12	12.70		
068-ZR50-COMP	2	0.0002	0.199	11264	7.07	0.06433	2.00	0.759	2.52	0.0855	1.48	0.59	753	83	529	15	573	22	29.70		
007-ZR4-COMP	2	0.0005	1.062	35021	11.72	0.05928	0.85	0.708	1.40	0.0867	1.04	0.75	577	37	536	11	544	12	7.18		
008-ZR05	2	0.0037	0.029	203777	7.79	0.05841	0.77	0.712	2.61	0.0884	2.47	0.94	545	34	546	26	546	22	-0.12		
010-ZR07	4	0.0030	0.027	141938	9.44	0.05837	0.53	0.724	0.93	0.0900	0.66	0.72	544	23	556	7	553	8	-2.21		
065-ZR47-COMP	3	0.0010	0.726	62118	9.79	0.05917	0.79	0.735	1.87	0.0900	1.65	0.89	573	34	556	18	559	16	3.07		
036-ZR26	5	0.0006	0.046	32830	22.65	0.05931	0.82	0.743	1.21	0.0909	0.81	0.67	578	35	561	9	564	10	3.07	Brazilian/Pampean 0.7 - 0.5 Ga	
016-ZR11	5	0.0024	0.649	122533	12.34	0.05901	0.67	0.750	0.93	0.0921	0.53	0.57	567	29	568	6	568	8	-0.12		

005-ZR02	4	0.0014	0.554	103111	32.12	0.05896	0.69	0.749	0.94	0.0921	0.53	0.56	565	30	568	6	568	8	-0.47	
077-ZR57	3	0.0010	0.633	43729	11.04	0.06064	0.86	0.786	1.41	0.0940	1.06	0.75	627	37	579	12	589	13	7.54	
007-ZR04	6	0.0022	0.135	91247	15.63	0.05940	0.67	0.772	0.91	0.0943	0.49	0.54	582	29	581	5	581	8	0.16	
019-ZR14	6	0.0002	0.925	6914	9.73	0.06163	1.90	0.816	2.30	0.0960	1.25	0.54	661	80	591	14	606	21	10.66	
064-ZR46	7	0.0002	0.483	9698	13.76	0.05900	1.47	0.783	1.83	0.0962	1.03	0.56	567	63	592	12	587	16	-4.45	
029-ZR21-COMP	1	0.0010	0.517	56412	9.11	0.05928	0.91	0.788	1.86	0.0964	1.58	0.85	577	39	593	18	590	17	-2.73	
035-ZR25	4	0.0033	0.115	166637	9.91	0.05840	0.60	0.782	0.96	0.0971	0.65	0.67	545	26	597	7	586	9	-9.63	
078-ZR58	3	0.0012	0.001	67536	10.20	0.06023	0.75	0.810	1.16	0.0975	0.80	0.69	612	32	600	9	603	11	1.97	
069-ZR51-COMP	1	0.0005	0.187	28645	7.05	0.06291	1.23	0.849	1.95	0.0979	1.46	0.75	705	52	602	17	624	18	14.59	
039-ZR29-COMP	2	0.0014	0.242	84095	9.24	0.05943	1.10	0.803	1.69	0.0980	1.23	0.73	583	47	603	14	599	15	-3.40	
015-ZR10-COMP	1	0.0031	1.011	183838	6.82	0.05917	0.65	0.800	1.13	0.0981	0.85	0.75	573	28	603	10	597	10	-5.16	
028-ZR20-COMP	2	0.0024	0.448	141383	9.99	0.06217	0.65	0.843	1.73	0.0984	1.56	0.90	680	28	605	18	621	16	11.03	
049-ZR36	3	0.0008	0.209	50979	14.30	0.06091	0.85	0.846	1.21	0.1007	0.78	0.65	636	36	618	9	622	11	2.77	
025-ZR17-COMP	1	0.0018	0.355	111155	6.83	0.06066	0.68	0.844	2.75	0.1009	2.64	0.96	627	29	620	31	621	25	1.22	
005-ZR2-COMP	2	0.0009	0.245	51374	8.13	0.06200	0.70	0.870	1.11	0.1017	0.77	0.70	674	30	625	9	635	10	7.34	Brazilian/Pampean 0.7 - 0.5 Ga
006-ZR03	4	0.0013	0.449	57419	11.89	0.06050	0.63	0.856	0.89	0.1027	0.51	0.57	621	27	630	6	628	8	-1.39	
069-ZR51	4	0.0015	0.268	69101	12.58	0.06174	0.67	0.876	1.18	0.1030	0.89	0.76	665	29	632	11	639	11	5.01	
037-ZR27	3	0.0008	0.230	37108	10.04	0.06181	0.80	0.904	1.12	0.1061	0.68	0.61	668	34	650	8	654	11	2.62	
014-ZR09	7	0.0018	0.440	78636	15.45	0.06074	0.50	0.897	0.84	0.1070	0.56	0.67	630	22	656	7	650	8	-4.06	
040-ZR30	4	0.0002	0.072	11961	10.56	0.06273	1.83	0.932	2.24	0.1077	1.24	0.55	699	77	659	16	668	22	5.70	
030-ZR22	4	0.0008	0.336	41884	9.75	0.06511	1.84	0.967	2.33	0.1078	1.38	0.59	778	77	660	17	687	23	15.18	
068-ZR50	4	0.0016	0.455	86485	8.60	0.06242	0.59	0.980	1.11	0.1138	0.86	0.78	689	25	695	11	693	11	-0.90	
010-ZR7-COMP	2	0.0031	0.132	183322	11.23	0.06225	0.69	0.999	1.65	0.1164	1.46	0.88	683	29	710	20	703	17	-3.94	
064-ZR46-COMP	2	0.0004	0.231	22467	7.16	0.06790	1.11	1.114	1.90	0.1189	1.51	0.79	865	46	724	21	760	20	16.28	
037-ZR27-COMP	1	0.0004	0.369	22162	5.03	0.07134	0.96	1.175	1.74	0.1194	1.40	0.81	967	39	727	19	789	19	24.81	
067-ZR49-COMP	1	0.0015	0.199	91734	9.61	0.06624	0.94	1.175	2.86	0.1286	2.68	0.94	814	39	780	39	789	31	4.17	0.7 - 0.9 Ga
004-ZR1-COMP	7	0.0044	0.206	180853	10.15	0.06840	0.42	1.304	1.40	0.1383	1.28	0.92	881	18	835	20	847	16	5.22	
014-ZR9-COMP	1	0.0003	0.270	20431	5.69	0.07334	0.96	1.402	1.77	0.1387	1.44	0.81	1023	39	837	23	890	21	18.21	
033-ZR23	4	0.0011	0.338	46963	12.84	0.06968	0.73	1.378	1.11	0.1435	0.76	0.68	919	30	864	12	880	13	5.96	
047-ZR34	5	0.0004	0.623	78977	56.65	0.07037	1.11	1.395	1.52	0.1438	0.98	0.64	939	45	866	16	887	18	7.78	
049-ZR36-COMP	1	0.0013	0.233	82166	8.53	0.06938	0.90	1.449	2.32	0.1515	2.11	0.91	910	37	909	36	910	28	0.11	Grenville - Sunsás 1.3 - 0.9 Ga
048-ZR35-COMP	1	0.0013	0.196	78900	10.88	0.07205	0.82	1.543	2.50	0.1553	2.33	0.93	987	33	931	40	948	31	5.71	

066-ZR48-COMP	1	0.0020	0.039	123537	6.86	0.07163	0.82	1.599	1.29	0.1619	0.93	0.72	976	33	967	17	970	16	0.87	
044-ZR31	10	0.0023	0.117	113058	11.78	0.07293	0.91	1.675	1.20	0.1666	0.69	0.57	1012	37	993	13	999	15	1.87	
075-ZR55	4	0.0011	0.398	57942	13.11	0.07318	0.54	1.750	1.01	0.1734	0.77	0.76	1019	22	1031	15	1027	13	-1.16	
055-ZR40-COMP	3	0.0013	0.172	76011	9.52	0.07331	0.99	1.700	2.33	0.1681	2.07	0.89	1023	40	1002	38	1008	30	2.03	
038-ZR28	3	0.0027	0.246	136721	10.60	0.07338	0.58	1.809	0.94	0.1787	0.65	0.69	1025	23	1060	13	1049	12	-3.46	
060-ZR45	4	0.0023	0.327	109769	10.26	0.07416	0.86	1.779	1.25	0.1740	0.82	0.65	1046	35	1034	16	1038	16	1.13	
025-ZR17	5	0.0008	0.985	37242	10.55	0.07417	0.65	1.791	1.02	0.1751	0.70	0.69	1046	26	1040	13	1042	13	0.56	
035-ZR25-COMP	2	0.0006	0.300	33368	5.50	0.07525	1.08	1.777	2.11	0.1713	1.78	0.84	1075	43	1019	34	1037	27	5.21	
027-ZR19	4	0.0023	0.149	371795	69.18	0.07559	0.55	1.948	1.01	0.1869	0.77	0.76	1084	22	1105	16	1098	14	-1.89	
073-ZR53	6	0.0004	0.615	20360	17.28	0.07833	0.97	2.030	1.67	0.1879	1.31	0.78	1155	38	1110	27	1125	23	3.93	
006-ZR3-COMP	2	0.0017	0.211	102372	7.01	0.07911	0.41	2.125	0.90	0.1948	0.70	0.79	1175	16	1147	15	1157	12	2.34	
020-ZR15	4	0.0027	0.236	134510	9.66	0.07914	0.73	2.230	1.07	0.2044	0.68	0.64	1176	29	1199	15	1191	15	-1.98	
004-ZR01	6	0.0028	0.357	118293	13.19	0.07989	0.47	2.336	0.80	0.2121	0.53	0.66	1194	18	1240	12	1223	11	-3.81	
029-ZR21	5	0.0017	0.405	83000	8.70	0.08046	0.70	2.271	1.07	0.2047	0.73	0.68	1208	27	1200	16	1203	15	0.65	
024-ZR16-COMP	1	0.0031	0.205	193643	7.71	0.08662	0.57	2.715	2.02	0.2273	1.90	0.94	1352	22	1320	45	1332	30	2.35	
074-ZR54	4	0.0018	0.278	83895	11.55	0.08785	0.58	2.693	1.02	0.2223	0.75	0.74	1379	22	1294	18	1326	15	6.18	Rondonia - San Ignacio mobile belt
050-ZR37	5	0.0007	0.325	34961	10.82	0.08821	0.82	2.857	1.31	0.2348	0.95	0.72	1387	32	1360	23	1371	20	1.97	1.54-1.3 Ga
080-ZR60	2	0.0045	0.229	251926	8.32	0.09608	0.80	3.632	1.22	0.2741	0.84	0.69	1549	30	1562	23	1557	19	-0.80	
017-ZR12-COMP	1	0.0035	0.456	205149	7.15	0.09865	0.43	3.801	1.81	0.2795	1.72	0.95	1599	16	1589	48	1593	29	0.63	
039-ZR29	12	0.0013	0.633	66685	11.82	0.09876	0.80	3.910	1.18	0.2871	0.78	0.66	1601	30	1627	22	1616	19	-1.63	Rio Negro - Juruena mobile belt
013-ZR8-COMP	1	0.0013	0.304	77643	7.09	0.09904	0.62	3.683	2.15	0.2697	2.03	0.94	1606	23	1539	55	1568	34	4.17	1.82 - 1.54 Ga
044-ZR31-COMP	2	0.0048	0.262	293541	8.63	0.10052	0.43	4.078	1.19	0.2942	1.05	0.88	1634	16	1662	31	1650	19	-1.76	
038-ZR28-COMP	2	0.0044	0.481	256097	9.60	0.10535	0.53	4.558	1.61	0.3138	1.47	0.92	1720	19	1759	45	1742	27	-2.26	
055-ZR40	3	0.0024	0.580	122083	10.37	0.11070	0.43	4.696	0.80	0.3076	0.57	0.70	1811	16	1729	17	1766	13	4.53	
058-ZR43	5	0.0018	0.699	85743	12.92	0.12288	0.61	5.939	1.06	0.3505	0.79	0.74	1998	22	1937	26	1967	18	3.07	Ventuari-Tapajós mobile belt
017-ZR12	3	0.0031	0.449	180516	13.00	0.12727	0.45	6.869	0.96	0.3914	0.76	0.79	2061	16	2129	28	2095	17	-3.34	2.0 - 1.82 Ga
009-ZR06	3	0.0052	0.354	271236	14.81	0.12876	0.49	7.138	0.84	0.4020	0.57	0.68	2081	17	2178	21	2129	15	-4.67	Maroni - Itacaiúnas Province 2.2 - 2.0 Ga
030-ZR22-COMP	2	0.0053	0.517	294340	11.37	0.13167	0.61	6.758	3.22	0.3722	3.14	0.97	2120	21	2040	109	2080	56	3.80	
027-ZR19-COMP	2	0.0015	0.399	83400	8.11	0.16120	1.01	10.296	2.30	0.4632	2.03	0.88	2468	34	2454	83	2462	42	0.59	Central Amazonian province >2.2Ga
048-ZR35	4	0.0020	0.403	108860	11.94	0.16637	0.51	11.047	1.07	0.4816	0.86	0.81	2521	17	2534	36	2527	20	-0.50	
019-ZR14-COMP	2	0.0056	0.229	316597	9.19	0.18674	0.49	13.087	1.33	0.5082	1.18	0.89	2714	16	2649	51	2686	25	2.38	

026-ZR18-COMP	1	0.0035	0.204	216700	7.46	0.19149	2.35	13.763	3.97	0.5212	3.19	0.80	2755	76	2704	140	2734	74	1.84	
013-ZR08	2	0.0023	0.186	127318	5.99	0.27308	0.40	25.197	0.87	0.6692	0.68	0.78	3324	12	3303	35	3316	17	0.64	

Tabela 8. Sumário dos dados de LA-ICPMS da amostra ARE-17.

Spot	^{204}Pb cps	^{206}Pb mV ¹	Th/U	$^{206}\text{Pb}/^{204}\text{Pb}$	1s %	$^{207}\text{Pb}/^{206}\text{Pb}$	1s %	$^{207}\text{Pb}/^{235}\text{U}$	1s %	$^{206}\text{Pb}/^{238}\text{U}$	1s %	Rho	$^{207}\text{Pb}/^{206}\text{Pb}$	2s abs	$^{206}\text{Pb}/^{238}\text{U}$	2s abs	$^{207}\text{Pb}/^{235}\text{U}$	2s abs	% U-Pb disc ⁴	Events
016-ZR11	1	0.0004	0.284	24123	5.20	0.05038	1.26	0.165	1.82	0.0238	1.26	0.69	213	58	151	4	155	5	28.78	
020-ZR15	5	0.0003	0.201	92067	56.94	0.04922	1.30	0.162	1.58	0.0239	0.81	0.51	159	60	152	2	153	4	4.02	Jurassic Arc 216-130 Ma
020-ZR15	1	0.0005	0.127	31042	5.40	0.05369	1.49	0.184	2.39	0.0249	1.83	0.77	358	67	158	6	172	8	55.75	
074-ZR54	4	0.0004	0.334	19196	10.30	0.05030	1.33	0.179	1.61	0.0258	0.84	0.52	209	61	164	3	167	5	21.24	
015-ZR10	1	0.0003	0.475	21590	3.99	0.05442	1.40	0.283	1.96	0.0378	1.32	0.67	389	62	239	6	253	9	38.52	
070-ZR52	1	0.0009	0.268	73532	19.58	0.05197	1.25	0.278	2.76	0.0388	2.43	0.88	284	57	245	12	249	12	13.61	Triassic rift 250 - 216 Ma
026-ZR18	1	0.0009	0.416	57399	7.78	0.05198	0.91	0.282	2.14	0.0393	1.90	0.89	284	41	249	9	252	10	12.56	
014-ZR9	2	0.0006	0.695	35174	8.78	0.05401	1.14	0.296	1.86	0.0397	1.43	0.77	371	51	251	7	263	9	32.46	
030-ZR22	1	0.0015	1.563	88122	7.48	0.05141	0.61	0.287	1.92	0.0406	1.79	0.93	259	28	256	9	257	9	1.08	Permian magmatism 0.3-0.25 Ga
046-ZR33	4	0.0012	0.339	58689	12.47	0.05217	0.68	0.294	1.11	0.0408	0.80	0.72	293	31	258	4	261	5	11.99	
006-ZR3	4	0.0010	0.432	49460	10.17	0.05189	0.63	0.297	0.97	0.0415	0.64	0.66	281	29	262	3	264	5	6.63	
028-ZR20	2	0.0015	0.391	75893	8.33	0.05263	0.78	0.308	1.98	0.0424	1.78	0.90	313	35	268	9	272	9	14.46	Permian magmatism 0.3-0.25 Ga
037-ZR27	1	0.0005	0.446	31387	7.37	0.05342	1.01	0.319	1.64	0.0433	1.23	0.75	347	45	273	7	281	8	21.24	
056-ZR41	5	0.0002	0.409	9666	10.45	0.05511	1.50	0.418	1.83	0.0550	0.99	0.54	417	66	345	7	354	11	17.16	
029-ZR21	2	0.0003	0.337	16211	6.77	0.05774	1.39	0.507	2.28	0.0637	1.76	0.77	520	61	398	14	416	16	23.48	
050-ZR37	4	0.0009	0.285	45325	13.99	0.05803	1.04	0.632	1.29	0.0790	0.67	0.52	531	45	490	6	498	10	7.61	
034-ZR24	1	0.0009	0.517	56775	7.30	0.05701	0.75	0.625	2.07	0.0795	1.89	0.92	492	33	493	18	493	16	-0.26	
034-ZR24	4	0.0005	1.202	22861	10.11	0.05979	1.62	0.660	1.92	0.0800	0.96	0.50	596	69	496	9	514	15	16.76	Famatinian 0.5 - 0.4 Ga
008-ZR5	5	0.0005	0.417	24660	13.84	0.05673	1.09	0.626	1.41	0.0801	0.82	0.58	481	48	497	8	494	11	-3.26	
058-ZR43	3	0.0002	0.504	12523	8.10	0.05911	1.25	0.664	1.62	0.0815	0.96	0.59	571	54	505	9	517	13	11.56	
013-ZR8	3	0.0018	0.311	92529	9.76	0.05811	0.60	0.714	0.89	0.0891	0.55	0.61	534	26	550	6	547	8	-3.07	
018-ZR13	2	0.0007	0.300	39005	8.39	0.06016	1.33	0.740	2.05	0.0892	1.51	0.74	609	57	551	16	562	18	9.56	
039-ZR29	1	0.0007	0.334	45889	4.94	0.05968	0.86	0.735	2.17	0.0893	1.96	0.90	592	37	552	21	560	19	6.85	
046-ZR33	1	0.0012	0.325	75773	4.21	0.05974	0.70	0.742	1.31	0.0901	1.05	0.80	594	30	556	11	564	11	6.41	
056-ZR41	1	0.0005	0.394	31254	3.24	0.06237	1.05	0.780	2.32	0.0907	2.03	0.88	687	44	560	22	585	21	18.52	
018-ZR13	5	0.0003	0.728	13332	10.50	0.06019	1.14	0.777	1.43	0.0937	0.77	0.54	611	49	577	8	584	13	5.45	

048-ZR35	2	0.0014	0.436	76430	9.88	0.06023	1.04	0.781	1.80	0.0940	1.43	0.79	612	44	579	16	586	16	5.32	
069-ZR51	7	0.0004	0.006	15077	13.62	0.06094	1.14	0.809	1.41	0.0963	0.74	0.53	637	49	593	8	602	13	6.95	
061-ZR46	1	0.0006	0.317	35679	8.55	0.06037	1.69	0.807	4.24	0.0969	3.88	0.91	617	72	596	44	600	38	3.33	
037-ZR27	4	0.0004	0.203	20264	9.77	0.06061	0.93	0.811	1.29	0.0970	0.82	0.63	626	40	597	9	603	12	4.60	
017-ZR12	2	0.0012	0.421	69058	8.91	0.06136	0.88	0.832	1.66	0.0984	1.36	0.82	652	38	605	16	615	15	7.22	
026-ZR18	2	0.0003	0.548	16178	9.56	0.06143	1.14	0.834	1.49	0.0984	0.89	0.60	654	48	605	10	616	14	7.53	Brazilian/Pampean 0.7 - 0.5 Ga
055-ZR40	5	0.0005	0.200	22445	9.83	0.06168	1.12	0.842	1.37	0.0990	0.68	0.50	663	48	608	8	620	13	8.24	
007-ZR4	5	0.0002	0.730	7823	9.81	0.06289	1.47	0.860	1.99	0.0992	1.29	0.65	705	62	610	15	630	19	13.45	
036-ZR26	3	0.0003	0.878	16953	8.23	0.06145	1.11	0.849	2.00	0.1003	1.62	0.81	655	47	616	19	624	19	5.98	
064-ZR46	9	0.0016	0.660	58094	15.07	0.06074	0.78	0.846	1.16	0.1010	0.78	0.67	630	34	620	9	622	11	1.61	
060-ZR45	1	0.0008	0.372	46384	7.76	0.06072	1.54	0.848	4.30	0.1013	3.99	0.93	629	66	622	47	624	40	1.18	
035-ZR25	5	0.0011	0.238	55257	11.72	0.06088	0.71	0.852	1.11	0.1014	0.76	0.69	635	31	623	9	625	10	1.91	
043-ZR31	2	0.0009	0.395	55193	6.58	0.06285	0.75	0.889	1.24	0.1026	0.91	0.74	703	32	630	11	646	12	10.47	
005-ZR2	4	0.0012	0.136	60966	14.20	0.06083	0.65	0.868	1.07	0.1034	0.76	0.71	633	28	634	9	634	10	-0.17	
049-ZR36	4	0.0016	0.383	81211	12.33	0.06137	0.75	0.878	1.07	0.1038	0.66	0.62	652	32	637	8	640	10	2.41	
009-ZR6	4	0.0001	1.189	3646	11.30	0.06326	1.88	0.909	3.12	0.1042	2.46	0.79	717	79	639	30	657	30	10.84	
055-ZR40	2	0.0026	0.214	148815	7.36	0.06085	0.60	0.875	1.90	0.1043	1.76	0.93	634	26	639	21	638	18	-0.90	Brazilian/Pampean 0.7 - 0.5 Ga
038-ZR28	3	0.0011	0.235	64072	7.38	0.06186	0.66	0.893	1.41	0.1046	1.19	0.84	669	28	642	14	648	13	4.14	
077-ZR57	5	0.0004	0.281	21117	12.18	0.06272	0.65	0.923	1.18	0.1067	0.91	0.77	699	28	654	11	664	11	6.46	
040-ZR30	4	0.0010	0.701	53140	17.77	0.06123	1.16	0.905	1.55	0.1072	0.96	0.62	647	49	657	12	655	15	-1.46	
035-ZR25	1	0.0015	0.275	88752	4.99	0.06193	0.84	0.924	4.43	0.1082	4.33	0.98	672	36	662	54	665	43	1.39	
051-ZR38	2	0.0018	0.123	105271	7.60	0.06098	0.69	0.916	1.81	0.1090	1.63	0.90	639	29	667	21	660	17	-4.39	
040-ZR30	1	0.0005	0.239	27429	6.17	0.06447	1.28	1.032	1.75	0.1161	1.14	0.65	757	54	708	15	720	18	6.50	
036-ZR26	4	0.0032	0.297	171520	8.88	0.06358	0.46	1.022	1.54	0.1166	1.43	0.92	728	19	711	19	715	16	2.30	
067-ZR49	6	0.0007	0.641	30952	10.29	0.06521	1.43	1.174	2.33	0.1306	1.80	0.77	781	60	791	27	789	25	-1.30	0.7 - 0.9 Ga
045-ZR32	2	0.0018	0.246	105009	6.56	0.06738	0.64	1.267	1.18	0.1364	0.91	0.78	850	26	824	14	831	13	2.99	
076-ZR56	3	0.0003	0.383	18633	9.61	0.07073	1.41	1.428	1.77	0.1465	1.00	0.57	949	57	881	16	901	21	7.20	
066-ZR48	3	0.0013	0.254	66844	10.80	0.07214	0.63	1.562	1.07	0.1570	0.78	0.73	990	25	940	14	955	13	5.02	
044-ZR31	4	0.0015	0.440	77022	12.61	0.07140	0.64	1.579	1.20	0.1604	0.94	0.79	969	26	959	17	962	15	1.01	
068-ZR50	7	0.0016	0.226	56347	11.80	0.07496	0.82	1.700	1.25	0.1645	0.87	0.70	1067	33	981	16	1008	16	8.06	
039-ZR29	4	0.0011	0.232	52506	11.75	0.07437	0.78	1.696	1.24	0.1654	0.89	0.72	1051	31	987	16	1007	16	6.17	
053-ZR38	3	0.0006	0.442	43427	32.29	0.07137	0.86	1.635	1.38	0.1661	1.01	0.74	968	35	991	19	984	17	-2.34	

059-ZR44	2	0.0009	0.731	49549	6.79	0.07485	0.95	1.718	1.25	0.1664	0.73	0.58	1065	38	992	13	1015	16	6.78	
075-ZR55	6	0.0008	0.168	41976	21.56	0.07280	0.68	1.689	1.15	0.1683	0.85	0.74	1008	27	1003	16	1004	15	0.58	
054-ZR39	2	0.0014	0.288	79752	8.19	0.07302	0.68	1.770	3.30	0.1758	3.20	0.97	1015	28	1044	62	1035	42	-2.91	
065-ZR47	1	0.0020	0.216	120407	7.19	0.07311	1.12	1.839	3.95	0.1824	3.78	0.95	1017	45	1080	75	1059	51	-6.19	
047-ZR34	8	0.0027	0.372	116467	16.75	0.07421	0.77	1.945	1.28	0.1901	0.95	0.74	1047	31	1122	20	1097	17	-7.15	
045-ZR32	5	0.0010	0.879	50783	11.57	0.07442	0.80	1.724	1.28	0.1680	0.93	0.73	1053	32	1001	17	1017	16	4.93	
014-ZR9	4	0.0002	0.591	14747	24.81	0.07467	1.39	1.795	2.20	0.1743	1.66	0.75	1060	56	1036	32	1044	28	2.23	
029-ZR21	4	0.0016	0.257	82702	11.19	0.07577	0.80	1.993	1.16	0.1908	0.75	0.65	1089	32	1126	16	1113	16	-3.37	
047-ZR34	2	0.0034	0.348	208195	6.43	0.07586	0.54	1.894	1.88	0.1811	1.77	0.94	1091	22	1073	35	1079	25	1.71	
054-ZR39	3	0.0011	0.598	61348	8.05	0.07604	0.69	1.894	1.01	0.1806	0.64	0.63	1096	28	1070	13	1079	13	2.36	
030-ZR22	5	0.0013	0.281	60705	12.56	0.07628	1.05	2.004	1.45	0.1906	0.93	0.64	1102	42	1124	19	1117	20	-1.99	
019-ZR14	3	0.0035	0.541	181656	9.56	0.09499	0.51	3.532	2.15	0.2697	2.05	0.96	1528	19	1539	56	1535	34	-0.74	Rondonia - San Ignacio mobile belt 1.54-1.3 Ga
073-ZR53	4	0.0007	0.249	44664	16.85	0.09609	0.74	3.342	1.23	0.2522	0.91	0.74	1550	28	1450	24	1491	19	6.42	
010-ZR7	4	0.0011	0.267	71994	22.39	0.09929	0.73	3.753	1.07	0.2741	0.70	0.65	1611	27	1562	19	1583	17	3.05	
016-ZR11	5	0.0019	0.235	89973	13.28	0.10180	0.53	4.141	0.85	0.2950	0.55	0.64	1657	20	1666	16	1662	14	-0.56	Rio Negro – Juruena mobile belt 1.82 - 1.54 Ga
057-ZR42	2	0.0078	0.319	427906	9.84	0.10463	0.73	4.406	3.20	0.3054	3.09	0.97	1708	27	1718	93	1714	52	-0.61	
059-ZR44	2	0.0038	0.343	229541	8.53	0.10811	1.32	5.033	4.35	0.3376	4.12	0.95	1768	48	1875	133	1825	72	-6.07	
068-ZR50	1	0.0053	0.392	322319	7.46	0.11062	0.91	4.866	4.62	0.3190	4.52	0.98	1810	33	1785	140	1796	76	1.37	
025-ZR16	9	0.0085	0.099	339172	17.53	0.11497	3.32	5.663	4.94	0.3572	3.64	0.74	1879	117	1969	123	1926	84	-4.76	
079-ZR59	2	0.0020	0.444	105671	12.48	0.11818	0.66	5.305	1.03	0.3255	0.70	0.68	1929	24	1817	22	1870	18	5.82	Ventuari-Tapajós (Trans-amazonian) mobile belt 2.0 - 1.82 Ga
033-ZR23	1	0.0045	0.959	279770	7.23	0.12071	0.50	5.991	2.00	0.3599	1.90	0.95	1967	18	1982	65	1975	34	-0.77	
060-ZR45	3	0.0011	0.315	56019	8.96	0.12138	0.85	5.761	1.26	0.3442	0.85	0.68	1977	30	1907	28	1941	22	3.54	
048-ZR35	5	0.0025	0.498	111983	13.71	0.12558	0.55	6.295	1.27	0.3635	1.08	0.85	2037	19	1999	37	2018	22	1.87	Maroni - Itacaiúnas Province 2.2 -2.0 Ga
065-ZR47	4	0.0045	0.437	298056	19.56	0.16300	0.51	10.889	1.06	0.4845	0.85	0.80	2487	17	2547	36	2514	20	-2.41	
033-ZR23	19	0.0052	0.627	175649	19.27	0.17421	0.60	10.863	1.12	0.4522	0.87	0.78	2599	20	2405	35	2511	21	7.45	Central Amazonian province >2.2Ga
057-ZR42	5	0.0008	0.458	37511	14.07	0.18214	1.16	13.380	2.37	0.5328	2.03	0.86	2672	38	2753	91	2707	44	-3.02	

Tabela 9. Sumário dos dados de LA-ICPMS da amostra ARE-339.

Spot	^{204}Pb cps	^{206}Pb mV ¹	Th/U	$^{206}\text{Pb}/^{204}\text{Pb}$	1s %	$^{207}\text{Pb}/^{206}\text{Pb}$	1s %	$^{207}\text{Pb}/^{235}\text{U}$	1s %	$^{206}\text{Pb}/^{238}\text{U}$	1s %	Rho	$^{207}\text{Pb}/^{206}\text{Pb}$	2s abs	$^{206}\text{Pb}/^{238}\text{U}$	2s abs	$^{207}\text{Pb}/^{235}\text{U}$	2s abs	% U-Pb disc ⁴	Events
115-ZR90	9	0.0005	0.431	14777	15.21	0.04878	2.50	0.145	3.65	0.0215	2.64	0.72	137	115	137	7	137	9	0.01	Jurassic Arc 216-130 Ma
070-ZR56	11	0.0005	0.467	19372	12.91	0.05174	2.89	0.160	4.59	0.0224	3.54	0.77	274	130	143	10	151	13	47.88	

016-ZR12	9	0.0008	0.859	41157	42.30	0.05292	1.74	0.299	2.65	0.0410	1.96	0.74	325	78	259	10	266	12	20.41	Permian magmatism 0.3 - 0.25 Ma
163-ZR130	13	0.0016	0.853	42557	17.79	0.05092	0.93	0.300	2.10	0.0428	1.84	0.88	237	43	270	10	267	10	-13.97	
067-ZR53	39	0.0010	0.531	20910	26.77	0.05332	9.18	0.325	9.25	0.0442	1.11	0.12	343	391	279	6	286	46	18.53	
033-ZR25	11	0.0010	0.496	37798	14.07	0.04949	2.96	0.339	3.70	0.0497	2.19	0.59	171	135	313	13	297	19	-82.80	0.4-0.3 Ga
117-ZR92	10	0.0010	0.188	40219	16.31	0.05375	1.42	0.395	2.03	0.0534	1.40	0.69	361	63	335	9	338	12	7.06	
057-ZR45	89	0.0009	0.759	6575	32.46	0.09374	3.99	0.791	4.40	0.0612	1.80	0.41	1503	147	383	13	592	39	74.52	
132-ZR105	18	0.0006	0.622	14719	17.03	0.07595	1.78	0.688	3.37	0.0657	2.84	0.84	1094	71	410	23	532	28	62.49	Famatinian 0.5 - 0.4 Ga
059-ZR47	17	0.0007	0.256	19658	18.74	0.05202	3.26	0.490	4.28	0.0684	2.74	0.64	286	146	426	23	405	28	-48.94	
007-ZR5	8	0.0033	0.056	116095	13.25	0.05626	0.60	0.580	1.06	0.0748	0.79	0.75	463	27	465	7	465	8	-0.54	
160-ZR127	10	0.0014	0.511	49151	14.86	0.05749	0.87	0.619	1.51	0.0781	1.17	0.78	510	38	485	11	489	12	5.07	
037-ZR29	13	0.0010	0.505	30348	17.57	0.05470	1.71	0.606	2.41	0.0803	1.66	0.69	400	76	498	16	481	18	-24.48	
135-ZR106	45	0.0015	0.420	48989	19.44	0.04925	7.78	0.548	7.86	0.0807	1.04	0.13	160	345	500	10	444	56	-213.21	Brazilian/Pampean 0.7 - 0.5 Ga
151-ZR120	12	0.0006	0.673	18760	18.83	0.05750	2.39	0.646	3.17	0.0815	2.05	0.65	511	103	505	20	506	25	1.14	
137-ZR108	13	0.0020	0.170	75801	13.86	0.05652	0.89	0.641	1.42	0.0823	1.04	0.74	473	39	510	10	503	11	-7.76	
170-ZR135	9	0.0005	1.748	22763	12.71	0.05489	2.24	0.626	3.24	0.0827	2.31	0.71	408	99	512	23	493	25	-25.55	
034-ZR26	12	0.0016	0.066	46896	16.67	0.05785	1.29	0.679	1.85	0.0852	1.28	0.69	524	56	527	13	526	15	-0.55	
118-ZR93	7	0.0020	0.547	100004	24.97	0.05855	0.96	0.693	1.38	0.0859	0.92	0.67	551	41	531	9	535	11	3.52	
099-ZR78	11	0.0029	0.286	118425	24.84	0.05817	0.74	0.690	1.83	0.0860	1.63	0.89	536	32	532	17	533	15	0.86	
058-ZR46	4	0.0015	0.220	112028	33.24	0.05709	1.37	0.679	2.11	0.0862	1.57	0.74	495	60	533	16	526	17	-7.71	
028-ZR22	9	0.0042	0.599	147134	14.51	0.05818	0.56	0.693	0.99	0.0864	0.74	0.74	537	24	534	8	535	8	0.44	
090-ZR72N	10	0.0005	2.777	14521	16.08	0.06118	2.48	0.730	3.97	0.0865	3.08	0.78	646	105	535	32	556	34	17.17	
047-ZR37	10	0.0017	0.308	55033	14.67	0.05829	1.04	0.703	1.55	0.0875	1.09	0.70	541	45	541	11	541	13	0.02	
025-ZR19	8	0.0009	0.770	51170	36.72	0.05817	1.76	0.706	2.57	0.0880	1.83	0.71	536	76	543	19	542	21	-1.37	
122-ZR97	10	0.0007	1.456	21952	15.06	0.05944	2.17	0.727	3.34	0.0887	2.52	0.75	583	93	548	26	555	28	6.07	
004-ZR2	12	0.0006	0.965	21930	16.45	0.06179	1.95	0.766	2.94	0.0899	2.17	0.74	667	82	555	23	578	26	16.79	
159-ZR126	9	0.0024	0.223	92094	22.28	0.05715	0.86	0.711	1.52	0.0902	1.20	0.79	497	38	557	13	545	13	-11.93	
105-ZR82	7	0.0007	0.485	30906	12.96	0.05796	1.53	0.721	2.22	0.0902	1.57	0.71	528	66	557	17	551	19	-5.43	
087-ZR69	9	0.0015	0.078	62583	19.06	0.06278	1.13	0.782	1.84	0.0903	1.41	0.77	701	48	557	15	586	16	20.48	
019-ZR15	10	0.0017	0.506	87698	38.32	0.06000	0.90	0.749	1.67	0.0905	1.36	0.81	603	39	558	14	567	14	7.48	
179-ZR142	6	0.0007	0.986	39603	18.68	0.06191	1.61	0.783	2.53	0.0917	1.92	0.76	671	68	565	21	587	22	15.71	
091-ZR72B	13	0.0005	1.451	13297	18.16	0.05782	2.41	0.738	3.39	0.0926	2.35	0.69	523	104	571	26	561	29	-9.16	
116-ZR91	36	0.0022	0.464	26356	32.84	0.05663	2.09	0.725	2.32	0.0929	0.92	0.40	477	91	572	10	554	20	-20.00	

121-ZR96	12	0.0022	0.461	62628	17.02	0.05972	0.72	0.765	1.11	0.0929	0.76	0.69	593	31	573	8	577	10	3.48	
068-ZR54	13	0.0020	0.597	71543	14.75	0.06106	1.41	0.797	1.77	0.0946	1.01	0.57	641	60	583	11	595	16	9.14	
039-ZR31	14	0.0010	0.466	26748	18.82	0.05931	1.40	0.784	1.98	0.0959	1.36	0.68	578	60	590	15	588	18	-2.09	Brazilian/Pampean 0.7 - 0.5 Ga
182-ZR145	8	0.0012	0.558	51779	19.73	0.05940	1.95	0.789	2.48	0.0963	1.49	0.60	582	83	593	17	591	22	-1.85	
098-ZR77	12	0.0014	0.597	37924	15.94	0.05944	1.05	0.794	1.64	0.0969	1.20	0.73	583	45	596	14	593	15	-2.17	
005-ZR3	13	0.0049	0.269	140471	20.00	0.05945	0.57	0.794	1.27	0.0969	1.07	0.85	584	24	596	12	594	11	-2.18	
106-ZR83	11	0.0025	0.448	86129	13.99	0.05920	0.92	0.813	1.31	0.0997	0.86	0.66	574	40	612	10	604	12	-6.62	
074-ZR58	9	0.0007	0.249	23662	13.49	0.06171	2.51	0.868	4.03	0.1020	3.13	0.78	664	106	626	37	634	38	5.73	
026-ZR20	8	0.0054	0.207	193853	12.33	0.06083	0.47	0.856	0.92	0.1021	0.70	0.76	633	20	626	8	628	9	1.09	
048-ZR38	21	0.0024	0.411	57057	18.98	0.06326	1.00	0.892	1.44	0.1022	0.96	0.67	717	42	627	12	647	14	12.51	
095-ZR74	11	0.0038	0.069	113548	14.91	0.06059	0.59	0.872	1.13	0.1043	0.89	0.79	625	25	640	11	636	11	-2.41	
109-ZR86	9	0.0028	0.011	87099	16.12	0.06087	1.25	0.880	1.62	0.1048	0.96	0.59	635	53	643	12	641	15	-1.25	
138-ZR109	8	0.0012	0.744	47510	12.55	0.06110	1.51	0.883	2.30	0.1048	1.69	0.74	643	64	643	21	643	22	0.03	
189-ZR150	14	0.0011	0.497	31357	17.15	0.06235	1.82	0.907	2.53	0.1054	1.71	0.68	686	77	646	21	655	24	5.80	
056-ZR44	14	0.0031	0.108	76409	17.48	0.06190	0.83	0.902	2.31	0.1057	2.13	0.92	671	35	648	26	653	22	3.42	
085-ZR67	11	0.0041	0.592	277770	40.81	0.06023	0.53	0.888	1.97	0.1069	1.86	0.94	612	23	655	23	645	19	-7.08	
112-ZR89	11	0.0016	0.950	59119	15.53	0.06216	2.14	0.928	2.37	0.1082	0.94	0.40	680	90	662	12	666	23	2.55	
141-ZR112	4	0.0019	0.426	91128	8.98	0.06106	0.91	0.915	1.51	0.1086	1.14	0.76	641	39	665	14	660	15	-3.68	
130-ZR103	8	0.0046	0.264	209474	12.33	0.06603	1.49	1.031	6.08	0.1133	5.88	0.97	807	62	692	77	720	62	14.32	
050-ZR40	12	0.0037	0.383	196234	38.45	0.06630	1.06	1.101	2.90	0.1204	2.68	0.92	816	44	733	37	754	31	10.16	
040-ZR32	7	0.0005	0.572	21214	14.19	0.06746	2.29	1.160	3.38	0.1247	2.46	0.73	852	94	757	35	782	37	11.09	
128-ZR101	6	0.0015	0.395	57080	12.34	0.06272	1.17	1.092	1.70	0.1262	1.17	0.69	699	50	766	17	749	18	-9.67	0.7 - 0.9 Ga
014-ZR10	19	0.0013	0.387	33987	19.97	0.06311	2.46	1.117	3.08	0.1283	1.82	0.59	712	103	778	27	761	33	-9.29	
013-ZR9	13	0.0018	0.263	54347	15.69	0.06502	1.03	1.156	1.76	0.1290	1.38	0.78	775	43	782	20	780	19	-0.91	
111-ZR88	14	0.0030	0.178	90159	18.85	0.07264	1.93	1.311	2.23	0.1309	1.05	0.47	1004	77	793	16	851	25	21.00	0.7 - 0.9 Ga
079-ZR63	10	0.0013	0.619	48015	13.19	0.06461	1.46	1.245	2.08	0.1398	1.44	0.69	762	61	843	23	821	23	-10.74	
150-ZR119	10	0.0007	0.318	26428	13.53	0.07432	1.85	1.561	3.91	0.1523	3.42	0.87	1050	74	914	58	955	48	12.96	
029-ZR23	10	0.0014	0.239	45146	15.82	0.07226	1.17	1.599	1.82	0.1605	1.35	0.74	993	47	959	24	970	23	3.41	
020-ZR16	12	0.0027	0.371	92689	14.31	0.06991	1.32	1.568	1.89	0.1626	1.31	0.69	926	54	971	24	958	23	-4.93	
086-ZR70	9	0.0017	0.532	183414	57.48	0.07204	0.90	1.627	1.54	0.1638	1.20	0.78	987	36	978	22	981	19	0.95	
055-ZR43	12	0.0017	0.297	36758	18.76	0.07324	1.24	1.661	2.07	0.1644	1.62	0.78	1021	50	981	29	994	26	3.86	
166-ZR131	12	0.0032	0.395	95709	17.75	0.06863	0.48	1.566	0.92	0.1654	0.69	0.75	888	20	987	13	957	11	-11.17	

077-ZR61	8	0.0016	0.229	60747	12.36	0.07100	1.00	1.649	1.62	0.1685	1.21	0.75	957	41	1004	23	989	20	-4.86	
146-ZR115	8	0.0006	0.501	22377	13.61	0.07147	2.23	1.697	3.53	0.1722	2.72	0.77	971	89	1024	51	1007	45	-5.50	
172-ZR137	9	0.0064	0.367	225222	12.53	0.07179	0.66	1.700	1.17	0.1717	0.89	0.76	980	27	1021	17	1008	15	-4.24	
086-ZR68	7	0.0030	0.597	129222	19.04	0.07278	0.85	1.844	1.69	0.1838	1.41	0.84	1008	34	1088	28	1061	22	-7.91	
044-ZR34	16	0.0032	0.581	74744	22.89	0.07309	0.96	1.791	1.28	0.1777	0.76	0.59	1017	39	1055	15	1042	17	-3.74	
100-ZR79	13	0.0028	0.237	84864	16.38	0.07333	0.66	1.776	1.08	0.1757	0.78	0.72	1023	26	1043	15	1037	14	-1.99	
017-ZR13	23	0.0019	0.422	46890	20.98	0.07341	1.83	1.880	2.27	0.1858	1.29	0.57	1025	73	1098	26	1074	30	-7.13	
181-ZR144	7	0.0029	0.350	128634	9.84	0.07346	1.28	1.826	1.67	0.1802	1.01	0.60	1027	51	1068	20	1055	22	-4.05	
096-ZR75	12	0.0049	0.423	240046	38.20	0.07348	0.55	1.741	1.16	0.1718	0.95	0.82	1027	22	1022	18	1024	15	0.49	Grenville - Sunsás 1.3 - 0.9 Ga
180-ZR143	5	0.0038	0.269	182761	8.42	0.07353	0.98	1.781	1.43	0.1756	0.97	0.68	1029	39	1043	19	1038	18	-1.38	
142-ZR113	8	0.0020	0.261	73553	13.24	0.07415	0.81	1.853	1.46	0.1812	1.16	0.79	1045	33	1074	23	1064	19	-2.70	
153-ZR122	9	0.0008	0.717	54203	33.74	0.07416	1.53	1.749	2.34	0.1711	1.73	0.74	1046	61	1018	33	1027	30	2.66	
125-ZR98	8	0.0036	0.527	132442	12.93	0.07477	0.71	1.827	1.28	0.1772	1.00	0.78	1062	29	1052	19	1055	17	1.01	
049-ZR39	17	0.0014	0.969	51470	16.03	0.07514	2.85	2.200	3.11	0.2123	1.18	0.38	1072	113	1241	27	1181	43	-15.74	
065-ZR51	10	0.0026	0.459	94755	15.02	0.07517	0.90	1.742	1.87	0.1681	1.60	0.85	1073	36	1001	30	1024	24	6.68	
024-ZR18	8	0.0032	0.284	108981	13.97	0.07530	0.69	1.905	1.28	0.1835	1.01	0.79	1076	27	1086	20	1083	17	-0.88	
136-ZR107	5	0.0039	0.530	168910	9.50	0.07540	0.67	2.047	1.18	0.1969	0.90	0.76	1079	27	1159	19	1131	16	-7.39	
081-ZR65	4	0.0021	0.278	100828	12.36	0.07564	0.87	1.932	1.36	0.1853	0.97	0.72	1085	35	1096	20	1092	18	-0.94	
161-ZR128	13	0.0125	0.045	504403	15.43	0.07571	0.43	2.037	0.90	0.1951	0.70	0.77	1087	17	1149	15	1128	12	-5.65	
006-ZR4	13	0.0055	0.497	163759	15.63	0.07603	0.46	1.913	0.90	0.1824	0.68	0.76	1096	18	1080	14	1085	12	1.41	
107-ZR84	8	0.0009	0.424	47754	20.98	0.07678	1.68	2.177	2.33	0.2057	1.57	0.67	1115	66	1206	35	1174	32	-8.11	
158-ZR125	12	0.0022	0.451	60579	18.20	0.07701	0.70	2.015	1.19	0.1898	0.88	0.75	1121	28	1120	18	1121	16	0.11	
157-ZR124	7	0.0049	0.297	167485	16.66	0.07739	0.51	2.091	1.10	0.1959	0.91	0.82	1131	20	1153	19	1146	15	-1.96	
069-ZR55	35	0.0032	0.444	39422	31.60	0.07853	1.01	1.849	1.67	0.1707	1.27	0.76	1160	40	1016	24	1063	22	12.44	
043-ZR33	11	0.0024	0.398	94255	15.55	0.07861	0.89	2.281	1.35	0.2104	0.95	0.70	1162	35	1231	21	1206	19	-5.92	
046-ZR36	5	0.0032	0.414	121424	11.24	0.07915	0.90	2.164	1.26	0.1983	0.80	0.63	1176	35	1166	17	1170	17	0.84	
147-ZR116	9	0.0050	0.438	170385	13.54	0.07923	0.62	2.127	1.61	0.1947	1.45	0.90	1178	24	1147	30	1158	22	2.66	
171-ZR136	5	0.0025	0.705	112525	11.33	0.07939	0.83	2.212	1.61	0.2021	1.32	0.82	1182	33	1186	29	1185	22	-0.38	
053-ZR41	12	0.0014	0.380	34573	16.66	0.07969	1.08	2.132	1.76	0.1940	1.34	0.76	1189	43	1143	28	1159	24	3.87	
127-ZR100	9	0.0050	0.697	182141	12.31	0.08030	0.47	2.370	1.16	0.2141	0.99	0.85	1204	19	1250	22	1234	16	-3.81	
149-ZR118	9	0.0014	1.468	83269	41.11	0.08034	1.57	2.272	2.32	0.2051	1.66	0.72	1205	61	1202	36	1204	32	0.23	Grenville - Sunsás 1.3 - 0.9 Ga
156-ZR123	8	0.0026	0.468	90367	13.63	0.08080	0.73	2.431	1.24	0.2182	0.93	0.75	1217	28	1272	21	1252	18	-4.59	

187-ZR148	9	0.0020	0.282	92858	21.60	0.08115	1.74	2.270	2.35	0.2029	1.54	0.66	1225	67	1191	33	1203	33	2.81	
078-ZR62	10	0.0027	0.375	93104	14.37	0.08138	0.72	2.446	1.29	0.2180	1.01	0.78	1231	28	1271	23	1256	19	-3.31	
152-ZR121	8	0.0040	0.311	160791	21.46	0.08145	0.73	2.509	1.18	0.2234	0.85	0.72	1232	28	1300	20	1275	17	-5.47	
110-ZR87	13	0.0036	0.426	99714	24.43	0.08192	1.81	2.503	2.19	0.2216	1.17	0.54	1243	70	1290	27	1273	31	-3.76	
075-ZR59	7	0.0010	0.444	38974	11.47	0.08291	1.26	2.469	1.92	0.2159	1.39	0.73	1267	49	1260	32	1263	28	0.53	
177-ZR140	16	0.0028	0.664	86687	17.78	0.08384	0.73	2.403	1.64	0.2079	1.42	0.87	1289	28	1217	31	1243	23	5.54	
027-ZR21	10	0.0018	0.539	65320	13.25	0.08517	1.11	2.679	1.61	0.2282	1.10	0.68	1319	43	1325	26	1323	24	-0.41	
045-ZR35	8	0.0037	0.278	217006	30.61	0.08835	0.61	2.885	1.05	0.2368	0.77	0.73	1390	23	1370	19	1378	16	1.42	
097-ZR76	13	0.0028	0.641	82554	16.20	0.08995	0.68	2.830	1.23	0.2281	0.95	0.77	1424	26	1325	23	1363	18	7.00	Rondonia - San Ignacio mobile belt 1.54-1.3 Ga
036-ZR28	26	0.0038	0.477	87995	21.70	0.09002	1.37	2.679	2.03	0.2158	1.45	0.71	1426	52	1260	33	1323	30	11.67	
192-ZR153B	15	0.0011	0.485	26962	17.90	0.09011	1.30	3.030	2.00	0.2439	1.48	0.74	1428	49	1407	37	1415	30	1.48	
193-ZR153N	13	0.0013	0.593	29321	18.31	0.09052	1.12	3.056	1.77	0.2448	1.32	0.75	1436	42	1412	34	1422	27	1.72	
190-ZR151	16	0.0012	0.273	32621	19.04	0.09096	1.55	3.093	2.12	0.2466	1.41	0.66	1446	58	1421	36	1431	32	1.71	
101-ZR80	12	0.0012	0.826	41068	18.23	0.09607	1.68	3.935	2.31	0.2970	1.55	0.67	1549	62	1676	46	1621	37	-8.22	
184-ZR147	15	0.0020	0.376	62351	17.22	0.10097	1.96	3.714	2.51	0.2668	1.52	0.60	1642	72	1524	41	1574	40	7.17	
089-ZR71	14	0.0040	0.521	127129	30.21	0.10371	0.71	4.246	1.44	0.2969	1.19	0.83	1692	26	1676	35	1683	23	0.92	Rio Negro - Juruena mobile belt 1.82 - 1.54 Ga
066-ZR52	17	0.0024	0.667	73713	16.99	0.10607	1.12	4.467	1.52	0.3054	0.97	0.64	1733	41	1718	29	1725	25	0.86	
119-ZR94	36	0.0105	0.225	182121	24.04	0.10734	0.52	4.727	0.89	0.3194	0.62	0.70	1755	19	1787	19	1772	15	-1.83	
169-ZR134	93	0.0048	0.445	42574	41.98	0.10899	0.98	4.274	1.56	0.2844	1.16	0.74	1783	35	1614	33	1688	26	9.48	
178-ZR141	193	0.0057	0.680	17775	60.48	0.10935	3.09	4.408	3.39	0.2923	1.34	0.40	1789	110	1653	39	1714	55	7.58	
008-ZR6	12	0.0127	0.522	575936	38.12	0.11341	0.43	4.885	1.10	0.3124	0.95	0.86	1855	15	1752	29	1800	19	5.51	Ventuari-Tapajós (Trans-amazonian) mobile belt 2.0 - 1.82 Ga
060-ZR48	14	0.0083	0.212	212915	21.58	0.11921	0.55	5.438	0.91	0.3308	0.62	0.69	1944	20	1842	20	1891	16	5.25	
168-ZR133	6	0.0068	0.853	320350	11.09	0.12086	0.40	6.163	0.95	0.3698	0.78	0.82	1969	14	2028	27	1999	17	-3.03	
173-ZR138	11	0.0056	0.686	217854	15.01	0.12261	0.60	6.269	1.12	0.3708	0.87	0.78	1995	21	2033	30	2014	20	-1.94	
035-ZR27	10	0.0111	0.591	440703	17.37	0.12504	0.32	6.396	0.98	0.3710	0.85	0.86	2029	11	2034	30	2032	17	-0.22	Marconi - Icataiúnas Province 2.2 -2.0 Ga
140-ZR111	14	0.0055	0.274	219175	16.24	0.13153	0.63	7.317	1.10	0.4034	0.83	0.75	2119	22	2185	31	2151	20	-3.13	
143-ZR114	4	0.0106	0.263	493029	8.81	0.13208	0.62	7.283	1.05	0.3999	0.76	0.72	2126	22	2169	28	2147	19	-2.02	
076-ZR60	6	0.0029	0.886	142835	13.71	0.13559	0.41	8.022	0.91	0.4290	0.73	0.80	2172	14	2301	28	2233	16	-5.98	
148-ZR117	9	0.0026	0.367	84240	14.37	0.13840	0.62	7.846	1.34	0.4111	1.12	0.84	2207	22	2220	42	2213	24	-0.58	Central Amazonian province >2.2Ga
174-ZR139	15	0.0145	0.414	411471	16.71	0.18230	0.45	13.907	1.06	0.5532	0.88	0.83	2674	15	2839	40	2743	20	-6.16	
162-ZR129	9	0.0086	0.264	311556	18.08	0.19029	0.50	13.739	1.99	0.5236	1.89	0.95	2745	16	2714	84	2732	37	1.10	
102-ZR81	18	0.0075	0.676	261015	51.80	0.21709	0.76	15.320	1.56	0.5118	1.31	0.84	2959	24	2664	57	2835	30	9.97	

126-ZR99	8	0.0043	0.510	144378	12.72	0.22071	0.64	17.139	1.29	0.5631	1.06	0.82	2986	21	2880	49	2943	25	3.56	
----------	---	--------	-------	--------	-------	---------	------	--------	------	--------	------	------	------	----	------	----	------	----	------	--

Tabela 10. Sumário dos dados de LA-ICPMS da amostra ARE-332.

Spot	^{204}Pb cps	^{206}Pb mV ¹	Th/U	$^{206}\text{Pb}/^{204}\text{Pb}$	1s %	$^{207}\text{Pb}/^{206}\text{Pb}$	1s %	$^{207}\text{Pb}/^{235}\text{U}$	1s %	$^{206}\text{Pb}/^{238}\text{U}$	1s %	Rho	$^{207}\text{Pb}/^{206}\text{Pb}$	2s abs	$^{206}\text{Pb}/^{238}\text{U}$	2s abs	$^{207}\text{Pb}/^{235}\text{U}$	2s abs	% U-Pb disc ⁴	Events
100-ZR80	6	0.0005	0.530	23094	10.55	0.04780	2.64	0.103	3.90	0.0156	2.85	0.73	89	123	100	6	100	7	-11.74	
003-ZR01-COMP	22	0.0008	0.355	22933	21.37	0.04638	2.36	0.102	3.46	0.0160	2.50	0.72	17	112	102	5	99	7	-489.08	
083-ZR65	9	0.0007	0.360	25563	13.48	0.04999	1.96	0.110	3.36	0.0160	2.70	0.80	195	90	102	5	106	7	47.38	
100-ZR80-COMP	10	0.0009	0.384	43527	25.87	0.04912	1.84	0.109	2.67	0.0161	1.90	0.71	154	85	103	4	105	5	32.86	
044-ZR34-COMP	12	0.0011	0.290	28384	17.92	0.04779	2.09	0.107	2.92	0.0162	2.00	0.69	89	98	104	4	103	6	-16.85	Andean arc <130 Ma
049-ZR39-COMP	12	0.0005	0.446	16722	17.53	0.04696	3.02	0.105	4.16	0.0162	2.84	0.68	47	141	104	6	101	8	-120.09	
110-ZR88-COMP	16	0.0005	0.395	12412	17.28	0.04725	2.53	0.107	3.55	0.0164	2.47	0.69	62	119	105	5	103	7	-69.64	
088-ZR70	8	0.0009	0.358	34191	13.83	0.04898	2.15	0.111	3.84	0.0164	3.16	0.82	147	99	105	7	107	8	28.41	
077-ZR61-COMP	12	0.0006	0.469	17839	15.82	0.05037	2.46	0.115	3.39	0.0165	2.30	0.68	212	112	106	5	110	7	50.19	
084-ZR66-COMP	12	0.0011	0.276	42318	12.79	0.05120	1.60	0.135	2.11	0.0191	1.33	0.63	250	73	122	3	129	5	51.07	
137-ZR109-COMP	13	0.0009	0.255	282387	89.19	0.04830	1.97	0.150	2.91	0.0225	2.11	0.72	114	92	144	6	142	8	-25.99	
057-ZR45-COMP	17	0.0010	0.263	29113	17.49	0.05220	1.83	0.165	2.35	0.0230	1.44	0.61	294	82	146	4	155	7	50.27	
066-ZR52-COMP	8	0.0007	0.281	25890	13.50	0.04985	2.68	0.160	3.65	0.0233	2.46	0.67	188	122	148	7	151	10	21.24	
013-ZR09-COMP	18	0.0006	0.294	14435	19.34	0.05463	2.99	0.175	4.49	0.0233	3.33	0.74	397	131	148	10	164	14	62.66	Jurassic Arc 216-130 Ma
135-ZR107-COMP	13	0.0007	0.322	20252	15.89	0.05031	2.51	0.165	3.38	0.0238	2.22	0.66	209	115	152	7	155	10	27.56	
129-ZR101	9	0.0007	0.308	26272	12.69	0.04955	2.26	0.168	3.34	0.0245	2.43	0.73	174	104	156	7	157	10	10.24	
087-ZR69	8	0.0011	0.302	47223	12.58	0.05000	2.00	0.170	3.58	0.0247	2.95	0.82	195	92	157	9	160	11	19.42	
024-ZR18	13	0.0007	0.364	26090	13.31	0.05117	2.24	0.175	3.06	0.0248	2.06	0.67	248	101	158	6	164	9	36.42	
117-ZR93-COMP	14	0.0006	0.598	25534	15.13	0.04888	2.68	0.171	3.77	0.0253	2.62	0.69	142	124	161	8	160	11	-13.34	
045-ZR35-COMP	25	0.0029	0.135	68342	20.59	0.05264	0.87	0.272	1.37	0.0375	0.99	0.73	314	39	237	5	244	6	24.33	Triassic rift 250 - 220 Ma
028-ZR22-COMP	13	0.0010	0.959	38530	12.14	0.05182	1.59	0.291	2.45	0.0407	1.83	0.75	278	72	257	9	259	11	7.43	Permian magmatism 290 - 252 Ma
138-ZR110-COMP	15	0.0008	0.380	22158	16.49	0.05379	2.44	0.308	3.07	0.0416	1.83	0.60	362	108	263	9	273	15	27.52	
125-ZR99-COMP	13	0.0021	0.416	78831	24.67	0.05189	0.93	0.329	1.37	0.0460	0.94	0.69	281	42	290	5	289	7	-3.37	
068-ZR54-COMP	14	0.0021	0.486	53199	17.57	0.05359	0.95	0.342	1.33	0.0463	0.85	0.64	354	43	292	5	299	7	17.59	
046-ZR36-COMP	17	0.0016	0.487	40486	17.89	0.05300	1.09	0.400	1.61	0.0547	1.13	0.70	329	49	343	8	341	9	-4.33	0.4 - 0.3 Ga
027-ZR21	14	0.0005	0.490	17419	14.48	0.05469	3.32	0.418	4.71	0.0555	3.33	0.71	399	145	348	23	355	28	12.90	
048-ZR38-COMP	15	0.0037	0.399	278136	64.84	0.05695	0.56	0.543	1.13	0.0692	0.92	0.81	490	24	431	8	441	8	11.90	Famatinian

107-ZR85	19	0.0028	0.416	63838	18.11	0.05934	0.78	0.615	1.59	0.0752	1.34	0.84	580	34	467	12	487	12	19.36	0.5 - 0.4 Ga
058-ZR46-COMP	12	0.0014	0.424	40314	15.36	0.05569	1.25	0.582	1.88	0.0758	1.36	0.72	440	55	471	12	466	14	-7.08	
047-ZR37-COMP	61	0.0043	0.309	38089	61.58	0.06256	0.54	0.656	1.79	0.0760	1.66	0.93	693	23	472	15	512	14	31.89	
034-ZR26-COMP	8	0.0028	0.140	120493	12.01	0.05604	0.72	0.607	1.19	0.0785	0.87	0.73	454	32	487	8	481	9	-7.33	
050-ZR40-COMP	14	0.0038	0.162	87393	18.12	0.05671	0.54	0.617	1.09	0.0789	0.87	0.80	480	24	489	8	488	8	-1.88	
040-ZR32-COMP	9	0.0035	0.145	129430	13.99	0.05819	0.65	0.641	1.94	0.0799	1.79	0.92	537	28	495	17	503	15	7.77	
054-ZR42-COMP	8	0.0015	0.347	50707	13.61	0.05714	1.19	0.639	1.85	0.0812	1.36	0.74	497	52	503	13	502	15	-1.24	
087-ZR69-COMP	8	0.0032	0.176	129279	10.73	0.05754	0.72	0.656	1.24	0.0827	0.95	0.76	512	31	512	9	512	10	0.06	
065-ZR51	13	0.0015	0.456	50428	14.61	0.05801	1.50	0.688	2.05	0.0860	1.35	0.66	530	65	532	14	531	17	-0.27	
105-ZR83	4	0.0015	0.566	60863	11.24	0.05774	1.23	0.692	2.24	0.0869	1.83	0.82	520	54	537	19	534	19	-3.24	
134-ZR106-COMP	27	0.0041	0.316	67530	27.76	0.05832	0.61	0.706	1.08	0.0877	0.80	0.75	542	27	542	8	542	9	-0.09	
060-ZR48-COMP	13	0.0031	0.415	90143	15.70	0.05746	0.64	0.701	1.13	0.0885	0.86	0.76	509	28	547	9	540	9	-7.40	
115-ZR91-COMP	12	0.0007	0.537	22541	15.21	0.05892	2.83	0.723	3.96	0.0890	2.75	0.69	564	121	550	29	552	34	2.55	
143-ZR113-COMP	9	0.0056	0.047	201485	13.03	0.05843	0.55	0.718	1.02	0.0891	0.78	0.76	546	24	550	8	550	9	-0.80	
037-ZR29	9	0.0014	0.503	65763	14.45	0.05674	1.34	0.713	2.67	0.0912	2.29	0.85	482	59	562	25	547	22	-16.79	Brazilian/Pampean 0.7 - 0.5 Ga
119-ZR95-COMP	15	0.0010	0.195	25320	17.32	0.05960	1.32	0.754	2.08	0.0917	1.56	0.75	589	57	566	17	570	18	3.97	
128-ZR100	44	0.0034	0.303	33743	28.99	0.06538	1.51	0.828	3.43	0.0919	3.05	0.89	787	63	567	33	613	31	27.97	
079-ZR63	10	0.0022	0.417	78699	16.81	0.05812	0.68	0.743	2.47	0.0927	2.35	0.95	534	30	572	26	564	21	-7.00	
127-ZR99	13	0.0029	0.381	86354	19.12	0.05804	1.31	0.749	2.17	0.0936	1.69	0.78	531	57	577	19	568	19	-8.63	
107-ZR85-COMP	11	0.0020	0.464	72834	14.18	0.05684	1.23	0.739	4.11	0.0943	3.90	0.95	485	54	581	43	562	35	-19.71	
120-ZR94	5	0.0019	0.317	106646	14.93	0.05947	0.89	0.791	1.57	0.0965	1.24	0.79	584	39	594	14	592	14	-1.61	
047-ZR37	16	0.0031	0.116	68430	17.62	0.06505	0.85	0.884	1.49	0.0986	1.17	0.78	776	36	606	14	643	14	21.88	
133-ZR103	9	0.0018	0.190	66726	18.95	0.05914	2.08	0.829	3.83	0.1017	3.20	0.83	572	89	624	38	613	35	-9.13	
017-ZR13	14	0.0026	0.222	79534	16.32	0.05965	0.96	0.949	1.90	0.1153	1.60	0.84	591	41	704	21	677	19	-19.06	
020-ZR16	11	0.0013	0.885	53559	17.80	0.06222	2.26	1.002	3.80	0.1167	3.03	0.80	682	95	712	41	705	38	-4.41	
067-ZR53	41	0.0066	0.087	38630	39.64	0.06911	1.53	1.152	2.15	0.1209	1.46	0.68	902	62	735	20	778	23	18.46	0.7 - 0.9 Ga
024-ZR18-COMP	36	0.0096	0.129	51706	26.21	0.06996	1.03	1.309	4.92	0.1357	4.80	0.97	927	42	820	74	850	56	11.56	
019-ZR15-COMP	10	0.0065	0.064	327184	18.46	0.06580	1.95	1.265	4.57	0.1394	4.12	0.90	800	81	841	65	830	51	-5.16	
085-ZR67-COMP	16	0.0081	0.269	269924	14.85	0.07081	0.91	1.441	3.07	0.1475	2.91	0.95	952	37	887	48	906	36	6.80	
090-ZR72	28	0.0098	0.037	212876	67.34	0.07777	1.29	1.644	3.92	0.1533	3.68	0.94	1141	51	919	63	987	49	19.42	Grenville - Sunsás 1.3 - 0.9 Ga
009-ZR07-COMP	15	0.0044	0.760	139301	16.72	0.07312	0.61	1.603	1.16	0.1590	0.91	0.79	1017	25	951	16	971	14	6.50	
078-ZR62-COMP	69	0.0105	0.292	42293	41.31	0.07603	0.90	1.675	3.64	0.1598	3.50	0.96	1096	36	956	62	999	46	12.80	

114-ZR90-COMP	18	0.0109	0.255	181967	22.09	0.07752	1.77	1.756	4.92	0.1643	4.58	0.93	1135	69	980	83	1029	63	13.59	
055-ZR43-COMP	42	0.0138	0.572	164424	27.60	0.07508	1.59	1.724	2.88	0.1665	2.37	0.82	1071	63	993	44	1017	37	7.28	
067-ZR53-COMP	17	0.0021	1.238	94680	58.39	0.07438	0.96	1.718	1.49	0.1675	1.07	0.72	1052	39	999	20	1015	19	5.06	
033-ZR25	12	0.0016	0.380	50481	16.02	0.07234	1.28	1.724	1.76	0.1728	1.15	0.65	996	52	1028	22	1018	23	-3.22	
109-ZR87	7	0.0098	0.048	407309	11.74	0.07254	0.56	1.742	0.98	0.1742	0.71	0.73	1001	23	1035	14	1024	13	-3.38	
073-ZR57-COMP	12	0.0036	0.094	129865	13.63	0.07255	0.62	1.679	1.10	0.1678	0.82	0.75	1001	25	1000	15	1000	14	0.15	
136-ZR106	7	0.0054	0.107	210689	14.18	0.07360	0.52	1.750	0.96	0.1724	0.71	0.74	1031	21	1025	13	1027	12	0.51	
049-ZR39	10	0.0050	0.216	153554	14.95	0.07398	0.71	1.874	2.10	0.1837	1.94	0.92	1041	28	1087	39	1072	28	-4.44	
026-ZR20-COMP	9	0.0019	0.654	81185	14.99	0.07411	0.92	1.743	1.41	0.1706	1.01	0.71	1044	37	1015	19	1025	18	2.79	
048-ZR38	147	0.0072	0.148	6715	21.89	0.07427	2.13	1.747	3.02	0.1706	2.12	0.70	1049	85	1015	40	1026	39	3.19	
084-ZR66	11	0.0024	0.912	66032	18.15	0.07473	0.95	1.836	2.38	0.1781	2.14	0.90	1061	38	1057	42	1058	31	0.42	Grenville - Sunsás 1.3 - 0.9 Ga
057-ZR45	29	0.0043	0.097	93491	30.30	0.07540	2.55	1.925	4.45	0.1851	3.63	0.82	1079	101	1095	73	1090	59	-1.45	
076-ZR60-COMP	26	0.0090	0.121	816935	72.21	0.07598	1.21	1.968	1.50	0.1879	0.81	0.54	1095	48	1110	16	1105	20	-1.39	
148-ZR118-COMP	21	0.0081	0.323	196654	19.25	0.07612	0.46	1.839	0.95	0.1752	0.75	0.78	1098	18	1041	14	1060	13	5.22	
050-ZR40	73	0.0093	0.221	151129	30.27	0.07648	0.93	1.966	2.68	0.1864	2.49	0.93	1108	37	1102	50	1104	36	0.50	
129-ZR103-COMP	13	0.0066	0.432	178851	17.03	0.07832	0.48	2.192	0.95	0.2029	0.73	0.77	1155	19	1191	16	1178	13	-3.13	
096-ZR76	20	0.0051	0.363	69162	16.77	0.07916	0.72	1.990	2.42	0.1823	2.28	0.94	1176	28	1080	45	1112	32	8.22	
128-ZR102-COMP	15	0.0074	0.285	208345	17.94	0.07939	0.51	2.344	2.52	0.2141	2.44	0.97	1182	20	1251	55	1226	36	-5.83	
124-ZR98-COMP	45	0.0102	1.339	87005	34.28	0.08003	0.33	2.012	2.42	0.1823	2.37	0.98	1198	13	1080	47	1120	33	9.87	
116-ZR90	11	0.0041	0.454	183280	37.37	0.08012	0.78	2.461	2.72	0.2227	2.58	0.95	1200	31	1296	60	1261	39	-8.02	
006-ZR4	10	0.0017	0.728	69635	12.23	0.08016	0.93	2.182	1.90	0.1974	1.62	0.85	1201	36	1161	34	1175	26	3.31	
116-ZR92-COMP	31	0.0071	0.952	78455	32.83	0.08062	0.57	2.098	3.14	0.1888	3.07	0.98	1212	22	1115	63	1148	43	8.04	
008-ZR6	7	0.0023	1.622	100202	10.72	0.08092	0.87	2.389	1.44	0.2141	1.09	0.76	1219	34	1251	25	1239	20	-2.56	
123-ZR97-COMP	14	0.0023	0.551	62566	17.19	0.08187	0.84	2.345	1.36	0.2078	1.00	0.74	1242	33	1217	22	1226	19	2.05	
065-ZR51-COMP	58	0.0107	0.682	85864	44.92	0.08308	0.40	2.265	0.87	0.1977	0.67	0.77	1271	16	1163	14	1201	12	8.52	
103-ZR81-COMP	12	0.0106	0.336	329329	16.08	0.08356	0.47	2.640	1.65	0.2291	1.54	0.93	1282	18	1330	37	1312	24	-3.71	
099-ZR79-COMP	9	0.0048	0.826	510999	74.12	0.08609	1.42	2.714	4.35	0.2286	4.09	0.94	1340	55	1327	98	1332	64	0.96	Rondonia - San Ignacio mobile belt 1.54-1.3 Ga
137-ZR107	18	0.0059	0.267	141524	23.60	0.08859	2.93	3.221	3.47	0.2637	1.81	0.52	1395	110	1509	49	1462	53	-8.12	
076-ZR60	6	0.0056	0.367	239701	10.77	0.09168	1.54	3.205	1.86	0.2535	0.97	0.52	1461	58	1457	25	1458	29	0.28	
014-ZR10	7	0.0038	0.320	163335	22.62	0.09199	1.69	2.971	2.54	0.2343	1.87	0.73	1467	63	1357	46	1400	38	7.52	
068-ZR54	24	0.0100	0.035	297810	26.16	0.09513	1.53	3.912	3.15	0.2982	2.72	0.87	1531	57	1683	80	1616	50	-9.93	
118-ZR94-COMP	28	0.0145	0.581	219794	23.84	0.09778	1.83	3.354	2.37	0.2488	1.47	0.62	1582	68	1432	38	1494	37	9.47	

036-ZR28-COMP	19	0.0097	0.202	341489	12.76	0.09930	0.50	3.743	1.28	0.2734	1.11	0.87	1611	19	1558	31	1581	20	3.30	
006-ZR04-COMP	24	0.0090	0.362	97614	28.39	0.10210	0.86	3.754	2.08	0.2666	1.86	0.89	1663	32	1524	50	1583	33	8.36	
090-ZR72-COMP	44	0.0170	0.766	212684	30.99	0.10464	2.83	4.375	3.37	0.3032	1.80	0.53	1708	102	1707	54	1708	55	0.06	Rio Negro - Juruena mobile belt
018-ZR14-COMP	13	0.0053	0.509	284285	37.15	0.10558	0.84	4.155	1.99	0.2854	1.76	0.89	1724	31	1618	50	1665	32	6.15	1.82 - 1.54 Ga
059-ZR47-COMP	12	0.0103	0.233	281255	17.91	0.10682	0.77	4.537	2.49	0.3080	2.34	0.94	1746	28	1731	71	1738	41	0.85	
125-ZR97	12	0.0056	0.597	195477	24.26	0.10693	0.48	4.918	1.71	0.3335	1.60	0.94	1748	17	1855	52	1805	29	-6.15	
135-ZR105	41	0.0044	0.518	110287	20.77	0.10861	2.13	4.337	2.51	0.2896	1.27	0.51	1776	77	1640	37	1701	41	7.70	
098-ZR78	11	0.0060	0.207	218547	23.23	0.10867	1.15	4.782	2.09	0.3191	1.71	0.82	1777	42	1785	53	1782	35	-0.46	
098-ZR78-COMP	12	0.0087	0.133	274999	14.65	0.10871	0.50	4.498	1.14	0.3000	0.96	0.84	1778	18	1692	29	1731	19	4.86	
015-ZR11-COMP	75	0.0120	0.176	195264	25.91	0.10939	0.53	4.584	1.03	0.3039	0.81	0.78	1789	19	1711	24	1746	17	4.39	Rio Negro - Juruena mobile belt
094-ZR74-COMP	19	0.0164	0.626	347632	20.40	0.10955	0.44	4.606	0.93	0.3049	0.73	0.79	1792	16	1715	22	1750	15	4.26	1.82 - 1.54 Ga
115-ZR89	10	0.0049	0.164	157317	18.18	0.11015	2.05	5.270	2.79	0.3470	1.85	0.66	1802	74	1920	61	1864	47	-6.58	
124-ZR96	10	0.0102	0.057	327790	14.65	0.11032	1.01	4.986	2.94	0.3278	2.73	0.93	1805	37	1828	87	1817	49	-1.27	
016-ZR12-COMP	30	0.0155	0.345	234357	21.73	0.11059	0.36	4.541	1.92	0.2978	1.85	0.96	1809	13	1680	55	1738	32	7.12	
069-ZR55-COMP	28	0.0088	0.296	252814	16.58	0.11113	1.86	5.093	2.43	0.3324	1.52	0.62	1818	67	1850	49	1835	41	-1.75	
004-ZR02-COMP	18	0.0096	0.264	240612	19.10	0.11123	0.41	5.172	2.29	0.3372	2.22	0.97	1820	15	1873	72	1848	39	-2.95	
009-ZR7	5	0.0023	0.433	105589	13.31	0.11144	2.90	5.593	3.64	0.3639	2.17	0.60	1823	103	2001	74	1915	62	-9.75	
130-ZR102	10	0.0069	0.183	322437	22.36	0.11154	0.52	5.022	1.08	0.3265	0.87	0.80	1825	19	1822	27	1823	18	0.17	
010-ZR08-COMP	18	0.0128	1.198	306016	19.24	0.11164	0.45	5.447	2.69	0.3538	2.63	0.98	1826	16	1953	88	1892	46	-6.93	
126-ZR100-COMP	26	0.0098	1.098	179368	21.32	0.11193	0.40	5.148	0.85	0.3335	0.65	0.77	1831	14	1856	21	1844	14	-1.34	
089-ZR71-COMP	11	0.0077	0.543	371227	22.26	0.11213	0.66	5.309	1.33	0.3433	1.10	0.82	1834	24	1903	36	1870	23	-3.74	
039-ZR31	14	0.0085	0.423	210562	19.48	0.11238	1.03	5.579	3.21	0.3600	3.02	0.94	1838	37	1982	103	1913	55	-7.83	
145-ZR115-COMP	10	0.0047	0.502	219176	28.34	0.11261	0.49	4.983	0.96	0.3209	0.73	0.77	1842	18	1794	23	1816	16	2.59	Ventuari-Tapajós (Trans-amazonian) mobile belt
027-ZR21-COMP	14	0.0129	0.533	370998	16.39	0.11267	1.19	4.711	1.62	0.3032	1.04	0.64	1843	43	1707	31	1769	27	7.35	2.0 - 1.82 Ga
064-ZR50-COMP	17	0.0092	0.174	309689	20.10	0.11276	1.35	5.160	2.65	0.3319	2.25	0.85	1844	48	1847	72	1846	45	-0.16	
056-ZR44	20	0.0069	0.670	136641	21.68	0.11301	2.66	5.528	3.49	0.3547	2.24	0.64	1848	95	1957	75	1905	59	-5.88	
127-ZR101-COMP	17	0.0044	0.565	150664	16.78	0.11322	0.52	5.141	0.92	0.3293	0.67	0.72	1852	19	1835	21	1843	16	0.92	
105-ZR83-COMP	16	0.0156	0.727	488871	21.07	0.11388	0.52	5.204	1.76	0.3314	1.64	0.93	1862	19	1845	53	1853	30	0.91	
130-ZR104-COMP	16	0.0119	0.289	464401	37.32	0.11424	0.71	5.261	1.26	0.3340	0.97	0.77	1868	26	1858	31	1863	21	0.55	
120-ZR96-COMP	16	0.0089	0.282	205048	19.72	0.11644	0.48	5.423	1.19	0.3378	1.03	0.86	1902	17	1876	33	1888	20	1.38	
017-ZR13-COMP	61	0.0304	0.425	43750	18.14	0.11645	0.32	5.183	1.98	0.3228	1.92	0.97	1902	11	1803	60	1850	33	5.21	
056-ZR44-COMP	202	0.0141	0.699	155103	34.40	0.11675	2.01	5.633	3.56	0.3499	2.92	0.82	1907	71	1934	97	1921	61	-1.41	

083-ZR65-COMP	29	0.0107	0.335	280071	18.50	0.11991	0.62	5.635	1.00	0.3408	0.68	0.69	1955	22	1891	22	1922	17	3.29	
106-ZR84-COMP	12	0.0051	0.173	180582	25.06	0.12000	0.93	5.900	1.58	0.3566	1.22	0.77	1956	33	1966	41	1961	27	-0.51	
133-ZR105-COMP	21	0.0157	0.527	435567	24.16	0.12020	0.44	6.018	1.26	0.3631	1.12	0.89	1959	16	1997	38	1978	22	-1.93	
023-ZR17-COMP	12	0.0105	0.599	401326	14.36	0.12551	0.84	6.226	1.53	0.3598	1.22	0.80	2036	30	1981	42	2008	27	2.70	Marconi - Icataiúnas Province 2.2 -2.0 Ga
053-ZR41-COMP	26	0.0158	0.451	219501	25.50	0.12575	1.01	6.362	1.37	0.3669	0.85	0.62	2039	35	2015	29	2027	24	1.21	
035-ZR27-COMP	14	0.0054	0.340	141101	15.69	0.13250	1.22	7.364	4.47	0.4031	4.29	0.96	2131	42	2183	158	2157	78	-2.43	
029-ZR23-COMP	16	0.0047	0.804	129305	16.57	0.18829	0.55	13.381	1.56	0.5154	1.41	0.90	2727	18	2680	62	2707	29	1.75	Central Amazonian province >2.2Ga